Characterization of the roles of neuropeptide-activated GPCR20 and two decarboxylases for pairing-dependent developmental processes in female *Schistosoma mansoni*

INAUGURAL-DISSERTATION

zur Erlangung des Grades eines

Dr. med. vet.

beim Fachbereich Veterinärmedizin

der Justus-Liebig-Universität Gießen

vorgelegt von

Xuesong Li

Juni 2023

Aus dem Institut für Parasitologie, Justus-Liebig-Universität Gießen

Betreuer: Prof. Dr. Christoph G.Grevelding

Characterization of the roles of neuropeptide-activated GPCR20 and two decarboxylases for pairing-dependent developmental processes in female *Schistosoma mansoni*

INAUGURAL-DISSERTATION

zur Erlangung des Grades eines

Dr. med. vet.

beim Fachbereich Veterinärmedizin der

Justus-Liebig-Universität Gießen

eingereicht von

Xuesong Li

aus Henan, V. R. China

Gießen 2023

Mit Genehmigung des Fachbereichs Veterinärmedizin

der Justus-Liebig-Universität Gießen

Dekan: Prof. Dr. Dr. Stefan Arnhold

Gutachter:

Prof. Dr. Christoph G.Grevelding

Prof. Dr. Martin Diener

Prüfer:

Prof. Dr. Franco Falcone

Tag der Disputation: 16.08.2023

To my parents who gave me my life and strength,

to my friends who accompanied me through the last 30 years,

and to Yongle, who completed my soul.

Contributions

Publications

Li, X., Weth, O., Haeberlein, S., and Grevelding, C.G. (**2023**). Molecular characterization of *Smtdc-1* and *Smddc-1* discloses roles as male-competence factors for the sexual maturation of *Schistosoma mansoni* females. *Frontiers in Cellular and Infection Microbiology* 13, 1173557. https://doi.org/10.3389/fcimb.2023.1173557.

Li, X., Weth, O., Haimann, M., Möscheid, M.F., Huber, T.S., and Grevelding, C.G. (**2023**). Rhodopsin orphan GPCR20 interacts with neuropeptides and directs growth, sexual differentiation, and egg production in female *Schistosoma mansoni*. Manuscript under review.

Conferences

30th Annual meeting of the German Society for Parasitology 2023, 15-17 March 2023, Giessen, Germany.

Talk: Li X., Weth O., Haimann M., Grevelding C.G. (**2023**). Identification of GPCR-neuropeptide interaction and their functional analysis in *Schistosoma mansoni*.

15th Annual GGL Conference 2022, 29-30 September 2022, Giessen, Germany.

Poster: Li X., Weth O., Haimann M., Grevelding C.G. (**2022**). Identification of GPCR-neuropeptide interaction and their functional analysis in *Schistosoma mansoni*.

15th International Conference of Parasitology (ICOPA) 2022, 21-26 August 2022, Copenhagen, Denmark.

Poster: Li X., Weth O., Haeberlein S., Grevelding C.G. (**2022**). Male-mediated roles of biogenic amines in the reproductive development of female *Schistosoma mansoni*.

14th Annual GGL Conference 2021, 29-30 September 2021, Giessen, Germany.

Talk: Li X., Weth O., Haimann M., Grevelding C.G. (**2021**). Identification of GPCR-neuropeptide interaction and their functional analysis in *Schistosoma mansoni*.

13th Annual GGL Conference 2020, 29-30 September 2020, Giessen, Germany.

Talk: Li X., Grevelding C.G., Weth O., Haimann M. (**2020**). Identification of GPCR-neuropeptide interaction and their functional analysis in *Schistosoma mansoni*.

LIST OF ABBREVIATIONS

Abbreviations	Full name
aa	Amino acid
ABAM	Antibiotic-Antimycotic
AC	Adenylyl cyclase
ACh	Acetylcholine
AFA	Acidified formaldehyde alcohol
AP	Alkaline phosphatase
ATP	Adenosine triphosphate
BAs	Biogenic amines
BATT	β-alanyl-tryptamine
BCIP	4-toluidine salt
BLAST	Basic Local Alignment Search Tool
BMP	Bone morphogenic protein
bF	Female worms from couples obtained from mixed-sex infections
bM	Male worms from couples obtained from mixed-sex infections
bO	Ovaries isolated from bF
bp	Base pairs
bT	Testes isolated from bM
Ca^{2+}	Calcium
cAMP	Cyclic adenosine 3′,5′-monophosphate
cDNA	Complementary DNA
CLSM	Confocal laser scanning microscope
CO_2	Carbon dioxide
d	Day
DA	Dopamine
DAG	Diacylglycerol
DDC	DOPA decarboxylase
ddH_2O	Double distilled water
DEPC	Diethylpyrocarbonate
dH_2O	Distilled water
DIG	Digoxygenin

DIG-AP	Digoxigenin-alkaline phosphatase
DIG-dUTP	Digoxygenin-uridinetriphosphate
DIG-POD	Digoxigenin-horse-radish peroxidase
DNA	Desoxyribonucleic acid
dsDNA	Double-stranded DNA
dsRNA	Double-stranded RNA
EdU	5-ethynyl-2'-deoxyuridine
EtOH	Ethanol
FISH	Fluorescence *in situ* hybridization
FITC	Fluorescein isothiocyanate
FITC-POD	Fluorescein isothiocyanate-orse-radish peroxidase
FLPRs	FMRFamide-like peptide GPCR
FLPs	FMRFamide (Phe-Met-Arg-Phe-NH2)-related peptides
gDNA	Genomic DNA
GDP	Guanosine diphosphate
GIRK1	G protein gated inward rectifier potassium channels subunit 1
Glu	Glutamate
G proteins	GTP-binding proteins
GPCRs	G protein-coupled receptors
GRKs	G protein-coupled receptor kinases
GSC	Germline stem cells
GST	Glutathione S-transferase
GTP	Guanosine triphosphate
HA	Histamine
HEPES	2-4-(2-hydroxyethyl)-1-piperazinyl ethane sulfonic acid
HCl	Hydrochloric acid
Hoechst 33342	2'-[4-ethoxyphenyl]-5-[4-methyl-1-piperazinyl]-2,5'-bi-1H-benzimidazole trihydrochloride trihydrate
HSP-70	Heat shock protein 70
ILPs	Insulin-like peptides
IP3	Inositol triphosphate
KCl	Potassium chloride
KD	Knock-down

KH_2PO_4	Monopotassium phosphate
Letm1	Leucine zipper-EF-hand-containing transmembrane protein 1
LDL	Low density lipoprotein
LiCl	Lithium chloride
M	Molar
mA	Milliampere
MALAR-Y2H	Membrane Anchored Ligand and Receptor Yeast-two-Hybrid system
MeOH	Methanol
Mg^{2+}	Magnesium
min	Minute
mL	Milliliter
mm	Millimeter
mRNA	Messenger ribonucleic acid
Na_2HPO_4	Disodium phosphate
$Na_3C_6H_5O_7$	Trisodium citrate
NaN_3	Sodium azide
NaClO	Sodium hypochlorite
$NaHCO_3$	Sodium bicarbonate
NBT	Nitro blue tetrazolium
NCS	Newborn cattle serum
NE	Noradrenaline
NLPs	Neuropeptide-like proteins
NPF	Neuropeptide F
NPFF	Neuropeptide FF
NPP	Neuropeptide precursor
NPY	Neuropeptide Y
NRPs	Non-ribosomal peptide synthetase
NTD	Neglected tropical diseases
OA	Octopamine
PBS	Phosphate-buffered saline
PBSTx	PBS/Triton X-100
PCR	Polymerase chain reaction
PKA	Protein kinase A

PKC	Protein kinase C
PLCβ	Phospholipase Cβ
PPC	Possible prohormone convertase
PROF	Platyhelminth-Specific Rhodopsin-like Orphan-Family
PZQ	Praziquantel
RT-qPCR	Quantitative real-time polymerase chain reaction
Rho	Rat sarcoma homolog
RhoGEFs	Rho guanine nucleotide exchange factors
RNA	Ribonucleic acid
RNAi	RNA interference
RNA-Seq	RNA sequencing
RT	Room temperature
sec	Second
sF	Females obtained from single-sex infections
sM	Male worms obtained from single-sex infections
*Sm*TRPM$_{PZQ}$	*S. mansoni* transient receptor potential melastatin channel
sO	Ovaries isolated from sF
SOD	Superoxide dismutase
SSC	Saline-sodium citrate
sT	Testes isolated from sM
SMART	Simple Modular Architecture Research Tool
SOD	Superoxide dismutase
TA	Tyramine
TM	Transmembrane
TSP-1	Tetraspanin 1
TSP-2	Tetraspanin 2
TDC	L-tyrosine decarboxylase
TGFβ	Transforming growth factor β
TNT	Tris/NaCl/Tween
TPI	Triose phosphate isomerase
Tricaine	Ethyl 3-aminobenzoate methanesulfonate
Tris	Tris(hydroxymethyl)aminomethane
Tyr1	Tyrosinase 1

Tyr2	Tyrosinase 2
TTP	Thymine triphosphate
UTP	Uridine triphosphate
WHO	World-Health Organization
WISH	Whole mount *in situ* hybridization
5-HT	Serotonin

LIST OF CONTENTS

1. Introduction

1.1. Schistosomiasis

1.1.1. Epidemiology

Schistosomiasis is one of the most prevalent and serious diseases caused by parasitic trematodes in the genus *Schistosoma*, and it ranks close to malaria with respect to the burden of tropical infectious diseases. Accordingly, schistosomiasis has been classified by the world health organization (WHO) as a neglected tropic disease (NTD). As a disease with zoonotic potential, it affects humans and animals. In human, the species *Schistosoma mansoni*, *S. japonicum*, *S. mekongi*, *S. guineensis*, and *S. intercalatum* cause intestinal schistosomiasis, whereas *S. haematobium* triggers urogenital schistosomiasis (WHO, 2023). Schistosomiasis cases have been recorded in 78 countries around the world (LoVerde, 2019), particularly in poor and rural regions of Africa, Asia, and South America. The WHO reported that at least 251.4 million people are infected with schistosomes and required preventive treatment for schistosomiasis in 2021 (WHO, 2023). Schistosomiasis occurrence is not limited to endemic areas in the global south, a total of more than 100 cases have been reported in Europe from 2013 to 2017. Travellers returning from Korsika and farmers in southern Spain got infected from urogential schistosomiasis (Holtfreter et al., 2014; Boissier et al., 2016; Ramalli et al., 2018; Oleaga et al., 2019; Salas-Coronas et al., 2021), which indicates the risk of disease spreading also in non-endemic areas.

Schistosomiasis also affects wild and domestic animals, and a wide range of mammals are susceptible to schistosome infection, including buffaloes, camels, cattle, goats, horses, pigs, and sheep (Modena et al., 2008; Standley et al., 2012; Catalano et al., 2018; Kouadio et al., 2020). Prevalence studies indicated about 530 million cattle in endemic areas (De Bont and Vercruysse, 1997; Quack et al., 2006), which poses a significant socio-economic threat to local farming and livestock industry.

1.1.2. Schistosome life cycle

Schistosomes are the only trematodes that are dioecious. They have a complex life cycle including two free-living larval stages (miracidium, cercaria), an intermediate snail host, and a vertebrate final host (**Figure 1.1**). Schistosome eggs are released together with the feces (*S. mansoni*, *S. japonicum* and others) or urine (*S. haematobium*) of infected final hosts into the

freshwater. The first free-living larval stage, the miracidia, hatch from the eggs and infect intermediate snail hosts, which differ according to the schistosome species (LoVerde, 2019). Within the intermediate snail host, the miracidia undergo mother- and daughter-sporocyst development by asexual reproduction. This finally leads to the development of the second free-living larval stage, the cercaria. Infected snails release cercariae into freshwater. Following contact with a final host, cercariae penetrate the skin of their final host to reach blood vessels for transformation into a juvenile stage, the schistosomula.

During their migration through the blood circulatory system, schistosomes reach the portal venous system as adults. Here, males and females pair, and as couples they move to their final destination, the mesenteric veins of the gut (*S. mansoni* and *S. japonicum*) or the bladder (*S. haematobium*) (LoVerde, 2019). For pairing, the male forms a ventral groove, the gynaecophoric canal, to enclose the female for a pairing contact that can be maintained for many years. Pairing is a prerequisite for egg production. Eggs pass through the wall of the gut (*S. mansoni* and *S. japonicum*) or the bladder wall (*S. haematobium*) to reach the feces or urine, respectively, to be secreted to the environment for continuing the life cycle (Sibomana et al., 2020).

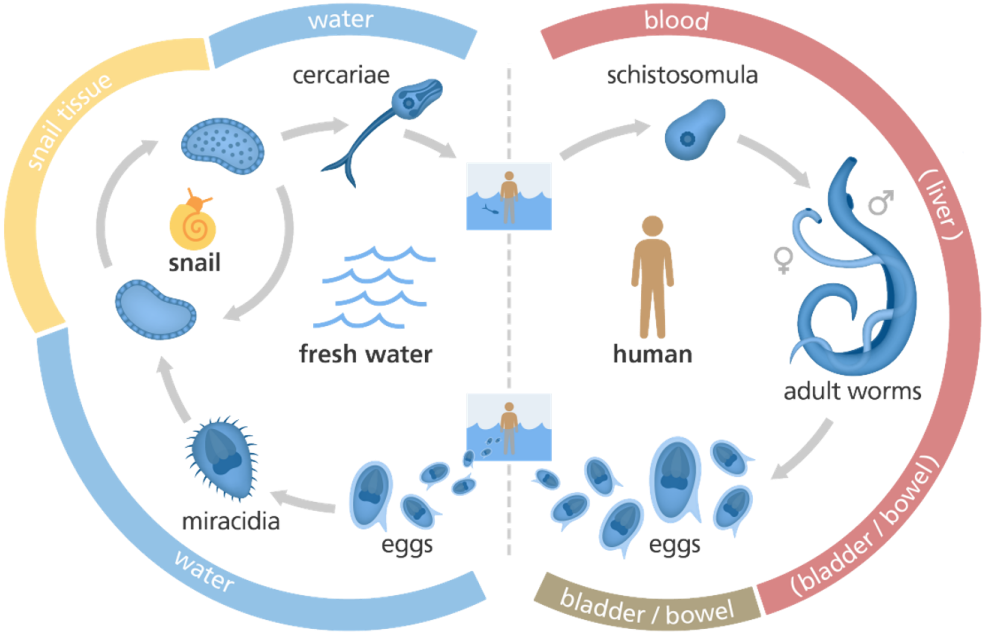

Figure 1.1: Schistosomes life cycle.

The different developmental stages are presented. Picture source: **www.yourgenome.org/**.

However, not all eggs reach the environment. Instead, remaining eggs become lodged in the blood vessels near liver and spleen, invade the tissue and cause the main pathogenicity of

schistosomiasis, e.g the inflammatory reaction and granuloma formation, which are induced by the egg secrets proteins. This finally causes liver fibrosis and hepatosplenomegaly (Da Silva et al., 2005; Olveda et al., 2014; McManus et al., 2018; WHO, 2023). Furthermore, an association to bladder cancer was shown for infections with *S. haematobium,* while an elevated risk for liver cancer development has been discussed for infections with *S. mansoni* (Da Silva et al., 2005; Sibomana et al., 2020; von Bülow et al., 2021).

1.1.3. Current control and treatment of schistosomiasis

The drug of choice to control schistosomiasis is praziquantel (PZQ), which was developed by Bayer & Merck in 1970s and shown to be active against parasitic flatworms (Seubert et al., 1977; Vale et al., 2017). PZQ is highly efficient against adult worms of all schistosome species, however, it is less active against juvenile worms and larval stages (McManus et al., 2020). Despite many years of use and the treatment of millions of people, the mechanism of PZQ has not finally been solved yet. In the past, several studies have shown that PZQ might be associated with the intracellular Ca^{2+} and muscular contractions in schistosomes (Cioli et al., 1995; Pica-Mattoccia et al., 2008; Cioli et al., 2014), resulting in the worms' death. Recently, a first target of PZQ was validated in *S. mansoni*, the transient receptor potential melastatin channel (*Sm*TRPM$_{PZQ}$) (Park et al., 2019; Park and Marchant, 2020), which appears to be associated with Ca^{2+} transport. Due to its long lasting use worldwide, there is increasing fear of resistance development against PZQ. Evidence for the possibility of resistance development has been obtained in the laboratory as early as the 1970s and have continued until today (Katz et al., 1973; Campos et al., 1976; Dias and Olivier, 1986; Vale et al., 2017). In mass drug administration programs, low drug efficacy has been reported in different countries (Raso et al., 2004; Barakat and El Morshedy, 2011). For *S. japonicum* infection, a study has reported PZQ resistance in different developmental stages (adult worms, miracidia, and cercariae) *in vitro* (Li et al., 2011).

Besides the lack of alternatives for drug treatment, there is no schistosomiasis vaccine available. This indicates the urgent need for continued efforts towards alternative treatment options (Bergquist et al., 2017). An early investigation of mice vaccinated with *S. mansoni*-irradiated cercariae has identified five molecules, including triose phosphate isomerase (TPI), glutathione S-transferase (GST), heat shock protein 70 (HSP-70), paramyosin and a 23-kDa integral membrane protein (Richter et al., 1993; McManus et al., 2020) as vaccination candidates. In addition, transmission-blocking vaccine candidates have been identified in

S. japonicum, including *Sj*-GST26, *Sj*-GST28, *Sj*-97 (paramyosin), and *Sj*-TPI (McManus and Loukas, 2008; You and McManus, 2015; Bergquist and McManus, 2017; Vale et al., 2017; You et al., 2018; McManus et al., 2020), which can reduce egg excretion from buffalo and cattle, thereby interrupting transmission from bovines to snails. Some human schistosomiasis vaccine candidates, *Sh*28GST, *Sm*-p14 (*S. mansoni* 14 kDa fatty acid-binding protein), *Sm*-p80 (large subunit of calpain), and *Sm*-TSP-2 (Tetraspanin-2), are under investigation and clinical development (Tran et al., 2006; Riveau et al., 2012; Santini-Oliveira et al., 2016; Riveau et al., 2018; Zhang et al., 2018; McManus et al., 2020). However, none of these candidates has fulfilled adequate protective efficacy in experimental animal models yet.

In summary, the potential emergence of PZQ resistance is a continuous concern, and no schistosomiasis vaccine has been approved yet for use in humans and animals. Both facts motivate research activities for the discovery of new targets and the development of alternative treatment options (Gray et al., 2010; Adekiya et al., 2019; McManus et al., 2020).

1.2. Reproductive biology of schistosomes

1.2.1. Pairing and male-dependent maturation of the female

One nearly unique feature of schistosome reproductive biology is that the female has to pair with a male partner to fully mature sexually. In the biological sense, females without pairing experience have a virgin character, which is characterized by an underdeveloped ovary with undifferentiated, stem cell-like oogonia and precursor vitelline cells of an otherwise completely undeveloped vitellarium (**Figure 1.2A**) (Clough, 1981). Pairing leads to the complete differentiation of the female gonads, the ovary, represented by a typical oval structure containing small part stem cell-like oogonia and immature oocytes as well as large mature oocytes in its larger posterior part, and the vitellarium containing stem-cell like S1 cells, differentiating S2 and S3 cells, and terminally differentiated S4 calls. Both cell types, mature oocytes and S4 vitelline cells are required for egg production (Kunz, 2001; LoVerde et al., 2004) (**Figure 1.2A**). Interestingly, this pairing effect is reversible. Separation of couples leads to the loss of the reproductive capacity of the female. This coincides with a loss of egg production and dedifferentiation processes of the female gonads, which after separation from a male partner are similar to females without pairing experience. However, after re-pairing of separated females, the ovary and vitellarium re-differentiate, and egg production is resumed (Popiel and Basch, 1984; Honeycutt et al., 2014; Wang et al., 2019).

The male stimulus that induces female maturation is not restricted to a specific body region. Immature females, which were partly paired with segments of transected males without insemination, can produce haploid embryos as offspring (Popiel and Basch, 1984; Wang et al., 2019). However, unlike the diploid karyotype of embryos from eggs laid by paired schistosomes, which have 2n=16 chromosomes, mitotic cells from eggs laid by females paired with emasculated schistosome males were haploid, containing only 8 chromosomes (Wang et al., 2019). To date, several studies have tried to explain the mechanism(s), by which male worms stimulate female development in *S. mansoni*. Some studies have been conducted to identify "molecular components" transported from male to female during an initial pairing contact, thereby induce female sexual maturation (Lu et al., 2016; Wang et al., 2017; Lu et al., 2019; Chen et al., 2022; Li et al., 2023). But only recently, a first factor β-alanyl-tryptamine (BATT) dipeptide has been identified, which is generated by a non-ribosomal peptide synthetase (Smp_158480, *Sm*NRPs), and released by ciliated sensory neurons into the gynaecophoric canal. Independent of a pairing contact with a male, a synthetic form of this dipeptide partly induced the sexual maturation of immature females (Chen et al., 2022).

1.2.2. Schistosome reproductive organs

In the ovary of a paired schistosome female, oocytes are produced that leave the ovary at its posterior part to be fertilized by sperm stored in a sperm reservoir (receptaculum seminis), a dilated region close to the ovary in the oviduct. The fertilized oocyte moves along the oviduct, which joins the vitelline duct (**Figure 1.2B**). Additionally, S4 vitelline cells, originating from the vitellarium, migrate via the vitelloduct to the ootype, the egg-forming organ of trematodes. Here, the fertilized oocyte reaches the zygote stage and is surrounded by 30-40 S4 cells that provide energy resources and egg-shell precursor proteins (Smyth and Clegg, 1959; Kunz, 2001; Grevelding, 2004). This process is supported by excretion products of the Mehlis´ gland that surrounds the ootype (**Figure 1.2B**). In the ootype, vitelline cells release their granules contents, which are needed for egg-shell formation and embryogenesis (Bobek et al., 1986; Reis et al., 1989; Chen et al., 1992). The egg-shell is finally formed by biochemical cross-linking processes of these precursor proteins, and two developmentally regulated tyrosinases (*Sm*TYR1 and *Sm*TYR2) were demonstrated to contribute to this process (Fitzpatrick et al., 2007; deWalick et al., 2012). The synthesized egg, finally, passes the uterus to be released through a pore near the ventral sucker into the environment. Here, the miracidium develops inside the egg (deWalick et al., 2012). Induced by an aqueous surrounding and by light, the miracidium hatches from the

egg to actively search for the intermediate host, in case of *S. mansoni* the freshwater snail *Biomphalaria glabrata*.

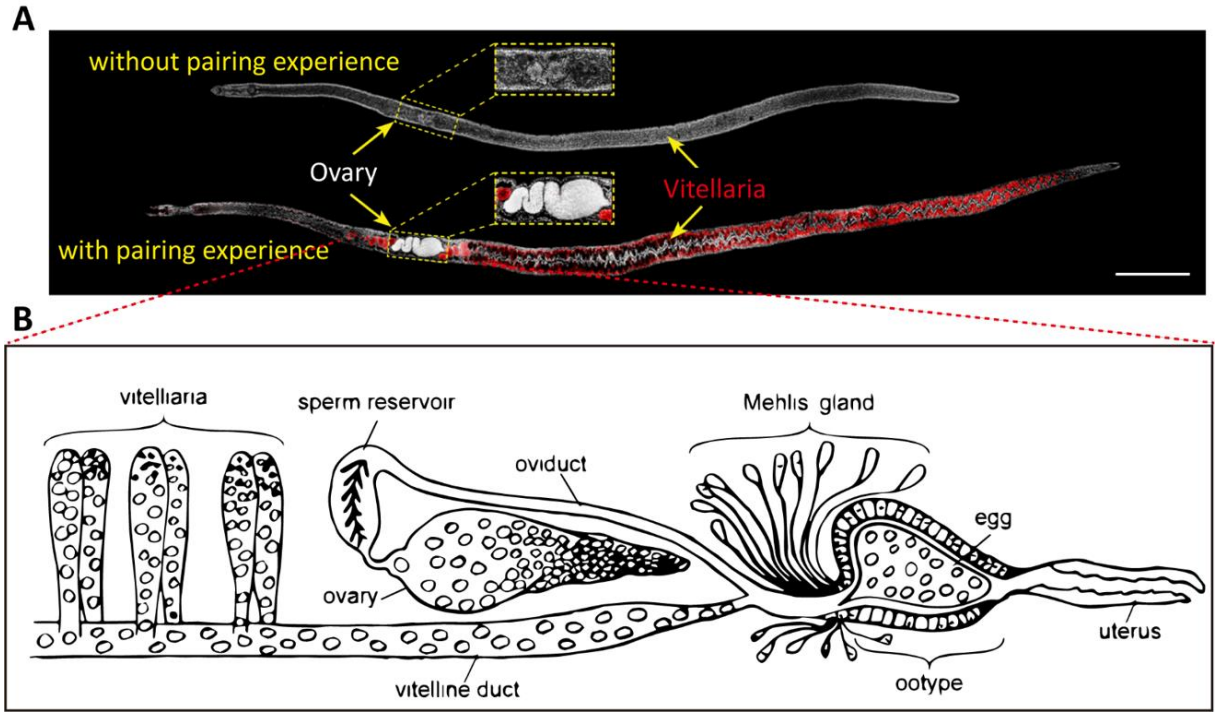

Figure 1.2: Schistosome female reproductive organs.

(**A**) Shown are an unpaired, sexually immature "virgin" and a paired, sexually mature *S. mansoni* female; modified from (Chen et al., 2022). (**B**) Diagram of the reproductive organs of a *S. mansoni* female; modified version of earlier studies (Gonnert, 1955a, b; deWalick et al., 2012).

1.3. G protein-coupled receptor (GPCRs) signaling in *S. mansoni*

Parasitic flatworms (cestodes, trematodes, and monogeneans) represent a diverse group of parasites, many of which are causative agents of diseases in humans and domestic animals (Hotez, 2008; Budke et al., 2009). The nervous system plays important roles for flatworm biology since it is not only transducing sensory and neuromuscular signals, but it is also responsible for the systemic transmission of developmental and hormonal cues. Research of the nervous systems of flatworms has increased during the last ten years. One motivation is the druggability of GPCRs (Overington et al., 2006; Miao et al., 2016), which are the main target of many anthelmintic drugs currently in use (McKellar and Jackson, 2004; Holden-Dye and Walker, 2007; Lecová et al., 2014).

1.3.1. G protein-coupled receptors (GPCRs)

G protein-coupled receptors (GPCRs) are the largest superfamily of integral transmembrane receptors. GPCRs are classified into five families, Glutamate, Rhodopsin, Adhesion, Frizzled/Taste2, and Secretin (Schiöth and Fredriksson, 2005; Krishnan et al., 2012; Hofmann and Palczewski, 2015). These receptors are characterized by a conserved structure, which comprises seven transmembrane (TM) domains (**Figure 1.3**) (Attwood and Findlay, 1994), consisting of α-helices that span the plasma membrane in a serpentine manner (Lefkowitz et al., 2000). Together with the extracellular parts of the TM domains, the N-terminus is involved in ligand binding (**Figure 1.3**) (Fredriksson et al., 2003). At the intracellular parts, which includes the C-terminus and intracellular regions of the TM domains, the receptor upon ligand binding can activate heterotrimeric GTP-binding proteins (G proteins) (**Figure 1.3**). Due to their structural diversity, GPCRs can interact with different ligands such as peptides, biogenic amines (BAs), hormones, neurotransmitters, gases, volatiles, nucleotides, and photons (Luttrell, 2008; Kenne et al., 2019). In the inactive state of the G protein, the Gα subunit binds a guanosine diphosphate (GDP). Upon ligand activation, the GPCR undergoes a conformational change (**Figure 1.3**), which enables the activation of a heterotrimeric G protein that consists of α, β and γ subunits (Gilman, 1987; van Biesen et al., 1996). The activated Gα subunit triggers the exchange of GDP for GTP (guanosine triphosphate) (**Figure 1.3**). This results in the dissociation of Gα-GTP from the βγ subunits (**Figure 1.4**). G protein-sensitive effectors are then directly regulated by free GTP-bound α subunits, βγ subunits, or both, regulating the activity of further molecules in downstream signaling responses such as the activation of intracellular second messengers or the opening of ion channels (**Figure 1.4**) (van Biesen et al., 1996).

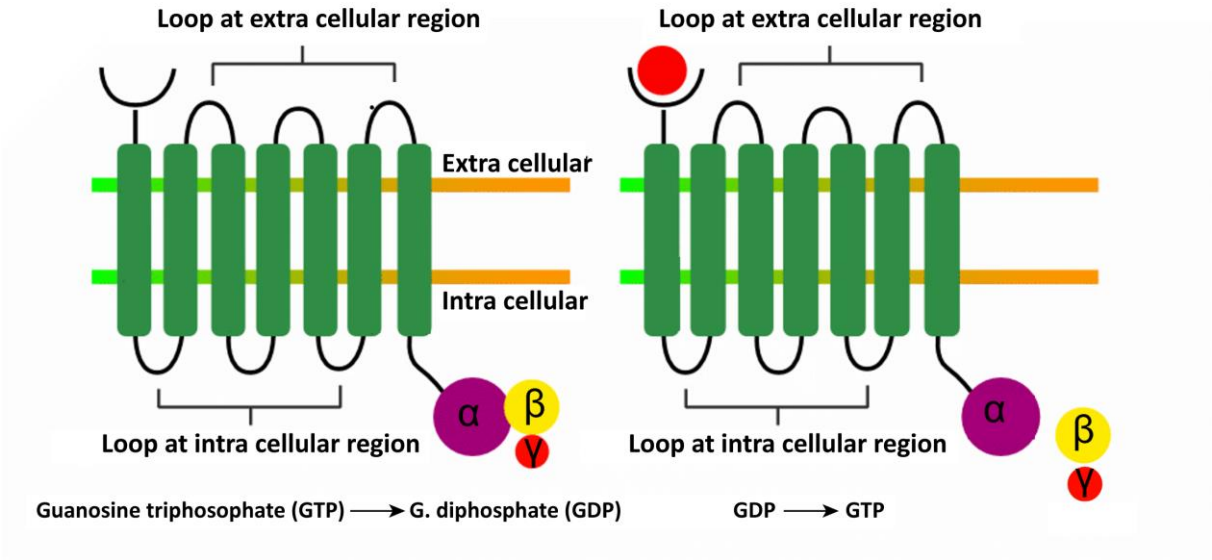

Figure 1.3: Schematic diagram of the G protein-coupled receptor (GPCR) structure in different activity states.

GPCRs are composed of seven transmembrane (TM) domains, which are connected by intracellular and extracellular loops. The Gα subunit also binds to either GTP (active protein) or GDP (inactive protein); this exchange is mediated by interaction with an activated GPCR. Picture source: https://www.geeksforgeeks.org/gpcr-pathway/.

There are four major subtypes of Gα subunit: $G\alpha_s$, $G\alpha_{i/o}$, $G\alpha_{q/11}$, and $G\alpha_{12/13}$ (**Figure 1.4**) (Milligan and Kostenis, 2006; Wang et al., 2020a). The Gα subunits perform a range of functions and interact with a variety of other proteins. $G\alpha_s$ proteins, for instance, stimulate adenylyl cyclase (AC) (Ross and Gilman, 1977a; b; Ross et al., 1978), and the intracellular cyclic adenosine 3′, 5′-monophosphate (cAMP) concentration is increased (McKnight, 1991). Furthermore, increased cAMP activates several effectors such as cAMP-dependent protein kinase A (PKA) (Pierce et al., 2002) or protein kinase C (PKC) (Naghshineh et al., 1986; Zimmermann et al., 1996). $G\alpha_i$ family proteins are able to inhibit certain types of AC (Meng et al., 1999; Zimmermann et al., 1999). In addition, $G\alpha_s$ and $G\alpha_i$ family proteins were demonstrated to modulate Ca^{2+} by either activating ($G\alpha_s$) or inhibiting ($G\alpha_i$) different subtypes of AC (Cooper et al., 1995; Bruce et al., 2003). $G\alpha_q$ proteins regulate activation of phosphatidylinositol (PI)-specific phospholipase Cβ (PLCβ) (Booden et al., 2002) by PLCβ1 ≥ PLCβ3 ≥ PLCβ2, transducing signals via the PI signaling pathway, active PLC hydrolyzes phosphatidylinositol-(4,5)-bisphosphate (PIP2) into inositol trisphosphate (IP3) and diacylglycerol (DAG). IP3 opens the IP3-sensitive Ca^{2+} channel, which results in a Ca^{2+} release from the endoplasmic reticulum (Foskett et al., 2007). $G\alpha_{12}$ and $G\alpha_{13}$ proteins form a separate

subfamily (**Figure 1.4**). Earlier studies demonstrated that Btk and a Ras-GTPase-activating-protein ($Gap1^m$) can be stimulated by $G\alpha_{12/}\alpha_{13}$ (Jiang et al., 1998). These proteins also activate Rho guanine nucleotide exchange factors (RhoGEFs) (Worzfeld et al., 2008), and they can be involved in communication between heterotrimeric G-protein-linked signaling pathways and cell responses. This includes processes organizing cellular shape and morphology as well as cell proliferation (Riobo and Manning, 2005).

Gβγ dimers regulate a wide range of downstream effectors, including phospholipases, AC, G protein-coupled receptor kinases (GRKs), and ion channels (Ford et al., 1998). Gβγ can regulate the activity of particular AC isoforms that generate the cAMP upon receptor activation (Tang and Gilman, 1991; Tennakoon et al., 2021). Further, Gβγ can transduce signals via the PI signaling pathway, promote activation of PLC (Boyer et al., 1992; Camps et al., 1992; Stephens et al., 1994) by PLCβ3 ≥ PLCβ2 ≥ PLCβ1 (Kakkar et al., 1999). Additionally, Gβγ also interacts with ion channel proteins such as G protein gated inward rectifier potassium channels subunit 1 (GIRK1) and directly binds to both the N-terminal hydrophilic and C-terminal domains of GIRK1, and voltage-gated Ca^{2+} channels (Zamponi et al., 1997) regulating neuronal and cardiovascular excitability (Huang et al., 1995; Berlin et al., 2010).

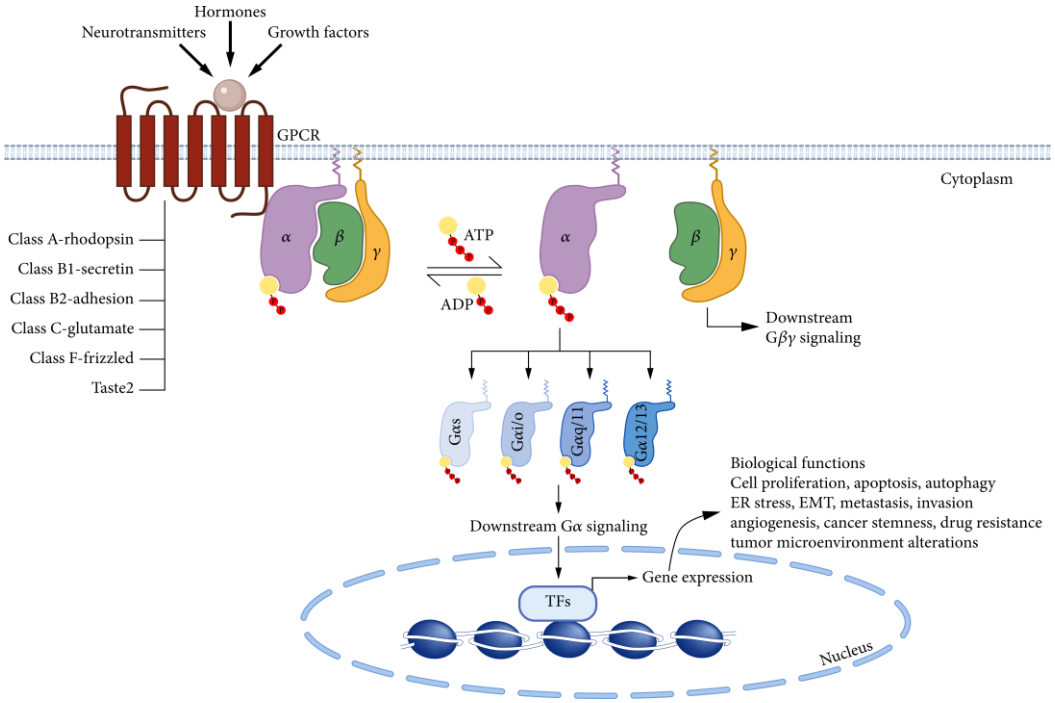

Figure 1.4: G protein-coupled receptor (GPCR) signaling pathway.

Ligands (such as hormones, neurotransmitters, or growth factors) bind to the extracellular domain of a GPCR. The binding of the ligand causes a conformational change in the GPCR, which activates the intracellular G protein. The activated G protein releases the α subunit, which then activates an effector

enzyme or ion channel. The activated effector enzyme or ion channel induces downstream signaling responses, such as the activation of intracellular second messengers or the opening of ion channels. Modified from (Kumari et al., 2021).

1.3.2. *S. mansoni* GPCRs

GPCRs are as diverse as G protein-mediated signal transduction processes, which can result in a multiplicity of downstream effects including growth, differentiation, neuronal signaling, olfaction, metabolism, and reproduction. In most cases, GPCR signaling is mediated by the binding of neuropeptides or neurotransmitters (eg. biogenic amines (BAs)). At present, GPCRs have not been widely investigated in platyhelminthes. Our knowledge of platyhelminthes GPCRs (including both flukes and tapeworms, as well as free-living species) is still fragmentary. In this scientific context, the genome data of *S. mansoni* (Berriman et al., 2009) has provided a valuable basis for *in silico* analyses of undiscovered and potentially novel receptors (Lu et al., 2016; Wendt et al., 2020; Buddenborg et al., 2021). Recently, an updated phylogenetic analysis of the *S. mansoni* GPCR complement confirmed the presence of 126 *S. mansoni* GPCRs (Kamara et al., 2023), up from 115 reported by Hahnel et al. (2018), representing all of the major families: 105 Rhodopsin, 2 Glutamate, 3 Adhesion, 2 Secretin and 5 Frizzled (Zamanian et al., 2011; Hahnel et al., 2018). Among the Rhodopsin family, a large and highly diverged, platyhelminthes-specific PROF subfamily was identified that comprised 19 *S. mansoni* receptors. In addition, receptors that respond to tyramine (TA), octopamine (OA), dopamine (DA), serotonin (5-HT), histamine (HA), glutamate (Glu), and acetylcholine (ACh) were identified. As putative peptidergic receptors, receptor potentially binding neuropeptide Y (NPY), neuropeptide F (NPF), and neuropeptide FF (NPFF), and one FMRFamide-like peptide GPCR (FLPRs) were identified (Zamanian et al., 2011; Hahnel et al., 2018; Kamara et al., 2023). These data demonstrate the diversity of GPCRs in *S. mansoni*, which allows speculations about their putative involvement in a multiplicity of biological processes.

1.4. Involvement of neuropeptidergic signaling in *S. mansoni*

Neuropeptides consist of short peptides (typically of 3-40 amino acid residues) that originate from post-translational endoproteolytic processing of longer precursors in the secretory pathway. Cleavage is performed by possible prohormone convertase (PPC) sites (K, R, KR, KK, or RR), which decompose neuropeptide precursors into smaller, active segments. After cleavage, the exposed basic residues in the carboxyterminus are removed by

carboxypeptidase E (Hook et al., 2008). Single basic residues can also be cleaved in some precursors (Amare et al., 2006; Southey et al., 2006). In invertebrates, it is common that one precursor contains similar copies (paracopies) of one neuropeptide, multiple distinct neuropeptides, multiple copies of a single neuropeptide, or any combination thereof (Li and Kim, 2008). The released neuropeptides may also undergo posttranslational modifications before they are secreted. This includes C-terminal amidation, which involves the conversion of a terminal glycine residue into an alpha-amide (Bradbury and Smyth, 1991).

1.4.1. Neuropeptidergic signaling in *S. mansoni*

As in mammalian systems, the neuropeptidergic signaling component of invertebrate nervous systems is complex. In *Caenorhabditis. elegans*, the number of predicted neuropeptides is > 100 (Li et al., 1999; Pierce et al., 2001). Most of the neuropeptides fall into two large families: the insulin-like peptides (ILPs) (Pierce et al., 2001; Li et al., 2003) and the FMRFamide (Phe-Met-Arg-Phe-NH2)-related peptides (FLPs) or FaRPs (Li, 2005). FLPs can induce different effects like excitation, relaxation, or a combination of both on somatic musculature, reproductive musculature, the pharynx and motor neurons (Li, 2005), and there is immunocytochemical evidence that FLPs have a regulatory role in the mechanism of egg assembly (Halton and Maule, 2004). ILPs play essential roles in nematode dauer formation and other developmental processes (Li, 2005). The remaining peptides are classified as neuropeptide-like proteins (NLPs), which are a diverse group of neuropeptides that have little similarity among each other (Nathoo et al., 2001). We only know little about the function of NLPs in invertebrates. A former study showed that DYRPLQFa induced a nerve cord-independent excitatory effect (reminiscent of bwRT3) on both dorsal and ventral muscle strips that appeared to be insensitive to external high K^+ and Ca^{2+}; the injection of DYRPLQFa induced ventral coiling but had no effect on cAMP levels (McVeigh et al., 2006; Reinitz et al., 2000). In Platyhelminthes, many of the physiological studies have been conducted in two parasite species, *Schistosoma* and *Fasciola.* A number of 34 putative NPP families were found in *S. mansoni* using a comparative approach (Koziol et al., 2016). Among these, neuropeptide F (NPF) (*Smnpp-20*, Smp_159950.1) (Koziol et al., 2016) and ILP (Smp_317800) (Wang et al., 2014) homologues were predicted. Further studies have described several novel flatworm NPFs with structural features characteristic of the NPY superfamily. The reported characteristics support the view of a common ancestry of flatworm NPFs with the NPY-superfamily (McVeigh

et al., 2009). In addition, another study showed that NPF potently inhibit cAMP accumulation in schistosome homogenates (Humphries et al., 2004).

1.5. Biogenic amines (BAs)

BAs are small cationic monoamines derived from the metabolism of amino acids, either aromatic amino acids or histidine (Schayer, 1960; Koslow and Butler, 1977; Sainio et al., 1996). BAs represent the largest subset of classical transmitters in the animal kingdom (Maule and Day, 2005). Among the most common BAs are 5-HT and HA, which are synthesized from tryptophan and histidine, respectively. The catecholamines (DA and noradrenaline (NE)) and phentolamines (TA and OA) are derived from tyrosine (**Figure 1.5**) (Lange, 2009). Interestingly, TA and OA are rare in the vertebrate nervous system, but they are major neuroactive substances among invertebrates. OA is considered to be the chemical "equivalent" of NE in phyla where adrenergic signaling is missing, NE and OA are synthesized by structurally related enzymes (DA- and TA-β-hydroxylase) that recognize both catechol and phenol substrates (Lange, 2009).

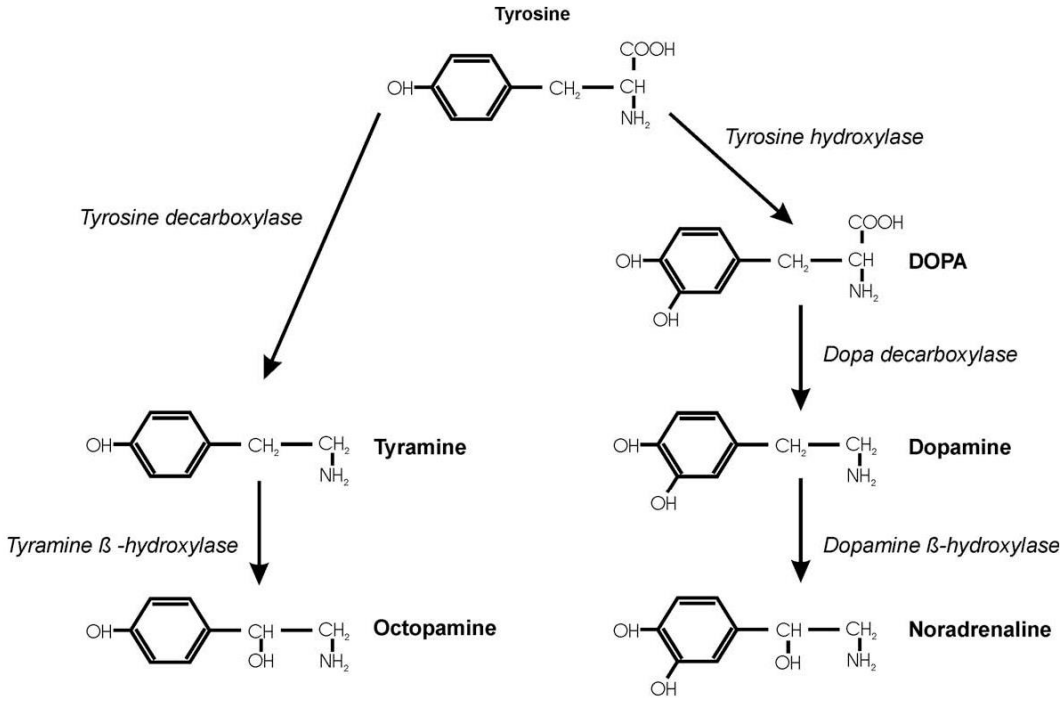

Figure 1.5: The biosynthetic pathway from tyrosine leads to the production of different BAs.
Tyrosine can be hydroxylated by tyrosine hydroxylase to produce DOPA. Both DOPA and tyrosine can be decarboxylated to produce DA and TA, respectively. These may then be further hydroxylated to produce NE and OA, respectively. Modified from (Lange, 2009).

1.5.1. BAs in *S. mansoni*

In invertebrates, BAs act through receptors and downstream signaling mechanisms similar to those that operate in the mammalian brain. Candidate BA receptors belong to the heptahelical family A GPCRs. In flatworms, neuronal signaling is mediated by the same variety of neuroactive substances that is seen in other animals. Some GPCRs of *S. mansoni* have been characterized as receptors responding to Glu as myoexcitatory neurotransmitters (El-Shehabi et al., 2009; Taman and Ribeiro, 2011), 5-HT (Patocka and Ribeiro, 2013; Patocka et al., 2014), and to ACh as a myoinhibitory neurotransmitter (MacDonald et al., 2015). Further studies indicated the presence of other neurotransmitters such as DA (Taman and Ribeiro, 2009; El-Shehabi et al., 2012), TA (Ribeiro et al., 2012), OA (Ribeiro et al., 2012; El-Sakkary et al., 2018), and HA (Hamdan et al., 2002; El-Shehabi and Ribeiro, 2010). *S. mansoni* appears to have all enzymes required for endogenous biosynthesis of the major BAs (Ribeiro et al., 2012). For instance, Smp_163900 shares the same level of sequence homology with dopamine-β-hydroxylase (DBH) as with tyramine-β-hydroxylase (TBH) and could function in either (or both) pathways. Smp_171580 is distantly related to aromatic amino acid decarboxylase (AADC), while Smp_135230 is an amino acid decarboxylase whose amino acid sequence resembles *C. elegans* TDC-1 (Chase and Koelle, 2007). In addition, schistosomes can take up exogenously supplied serotonin *in vitro* via a dose-dependent, saturable mechanism (Catto and Ottesen, 1979; Boyle et al., 2000). BAs are of substantial interest in schistosomes because they are widely distributed in the nervous system, and they play key roles as modulators of neuromuscular function and movement, either stimulating movement or inhibiting, depending on the amine (Mellin et al., 1983; Pax et al., 1984; Boyle et al., 2000; El-Shehabi et al., 2012). Whereas locomotion is critical for parasite survival, the BA system is regarded as a potential target for anthelmintic drug discovery, not only against schistosomes but against other helminth parasites as well (Smith et al., 2007).

1.6. Schistosome transcriptomic studies

Transcriptomics data obtained from various studies have uncovered transcriptomic profiles of *Schistosoma* across different time points throughout the whole life cycle (egg, miracidium, sporocyst, cercaria, schistosomulum, juvenile (21-28d), and adult), and also the pairing effect was investigated (with pairing-experienced (bM) and -unexperienced (sM) males, as well as the pairing-experienced (bF) and -unexperienced (sF) females) (Fitzpatrick and

Hoffmann, 2006; Cai et al., 2016; Lu et al., 2016; Wang et al., 2017). With respect to transcript profiling of genes in different life stages and upon pairing, some of the pairing-dependently transcribed genes such as follistatin have been showed to play important roles in the TGFβ pathway (Leutner et al., 2013). By yeast-two-hybrid analysis, a TGFβ-receptor orthologue from *S. mansoni* was found to interact with the TGFβ-receptor agonists inhibin/activin (*Sm*InAct) and bone morphogenic protein (*Sm*BMP) (Leutner et al., 2013). This study highlighted a yet unknown role of neurotransmitters in male development. Recently, it was demonstrated that one stimulus for female sexual development is the activity of *Sm*NRPs expressed in paired males (Chen et al., 2022). Of note, the expression of *Smnrps* was found to be higher in bM and bF versus sM and sF (Lu et al., 2016; Chen et al., 2022). *Sm*NRPs generates a BATT dipeptide that is released by ciliated sensory neurons into the gynaecophoric canal. Independent of a pairing contact with a male, a synthetic form of this dipeptide partly induced the sexual maturation of immature females. In these females, however, egg number and quality as well as ovary differentiation were inferior compared to naturally paired females (Chen et al., 2022). This indicates the need and contribution of further molecules, which in concert with this dipeptide govern female sexual development in *S. mansoni*. As hypothesized in former RNA-seq studies of the Grevelding lab comparing paired and unpaired *S. mansoni*, during male-female interaction the contribution of the male seems not to be limited to nutritional care and muscular strength to transport the paired female, but also to deliver a variety of (probably signaling) molecules that fulfill roles as male competence factors for female sexual maturation (Lu et al., 2019).

1.6.1. GPCR and NPP expression in *S. mansoni*

Among the genes that were found to be differentially expressed in paired versus unpaired *S. mansoni* were GPCRs that exhibited a male-dominated transcript profile (Lu et al., 2016; Hahnel et al., 2018). These GPCRs represented a so-called bM-sM-sF subgroup, in which a pairing-influenced transcript occurrence was discovered with high transcript levels in bM, sM, and sF, whereas comparably low or no transcripts of these GPCRs were found in bF. Transcripts of the majority of these bM-sM-sF subgroup GPCRs were not found in the gonads (**Figure 1.6A**) (Lu et al., 2016; Hahnel et al., 2018). Based on the same RNA-seq data, a comparative analysis revealed transcriptional patterns for neuropeptides of *S. mansoni*, *Sm*_NPPs, whose transcript profiles resembled the patterns observed for the bM-sM-sF subgroup GPCRs: compared to bF, transcripts of these *Sm*_NPPs occurred in higher abundance in sM, bM, and

sF. Furthermore, the majority of *Sm*_NPPs seemed not to be expressed in the gonads (**Figure 1.6B**) (Lu et al., 2019). Thus, it was speculated that the (bM-sM-sF subgroup) GPCRs and *Sm*_NPPs with the highest transcript levels in sF may contribute to processes in male attraction and/or repressing female maturation until pairing (Hahnel et al., 2018; Lu et al., 2019). High transcript levels of these genes in sM may suggest functions in locomotion and female attraction (Hahnel et al., 2018; Lu et al., 2019). In turn, highest transcript levels in bM may indicate a higher need for neuronal processes associated with pairing and increase muscular strength to transport the paired female (Hahnel et al., 2018; Lu et al., 2019). Even before the expression patterns of these genes were known, previous studies aimed at the molecular characterization of some of these genes without addressing their pairing-dependent role(s) (Hoffmann et al., 2001; Taman and Ribeiro, 2009; 2011; Patocka et al., 2014; MacDonald et al., 2015). As GPCRs and *Sm*_NPPs exhibited similar pairing-dependent expressions pattern in the RNA-seq studies (Lu et al., 2016; Hahnel et al., 2018; Lu et al., 2019), new research activities in the Grevelding lab were initiated to unravel potential interactions between GPCRs and *Sm*_NPPs. To this end, candidate GPCRs and *Sm*_NPPs were recombinantly expressed in a heterologous system, the Membrane Anchored Ligand and Receptor Yeast-two-Hybrid system (MALAR-Y2H), which allows to identify potential interactions of binding partners as a kind of GPCR deorphanization approach for *S. mansoni* (Weth et al., 2019).

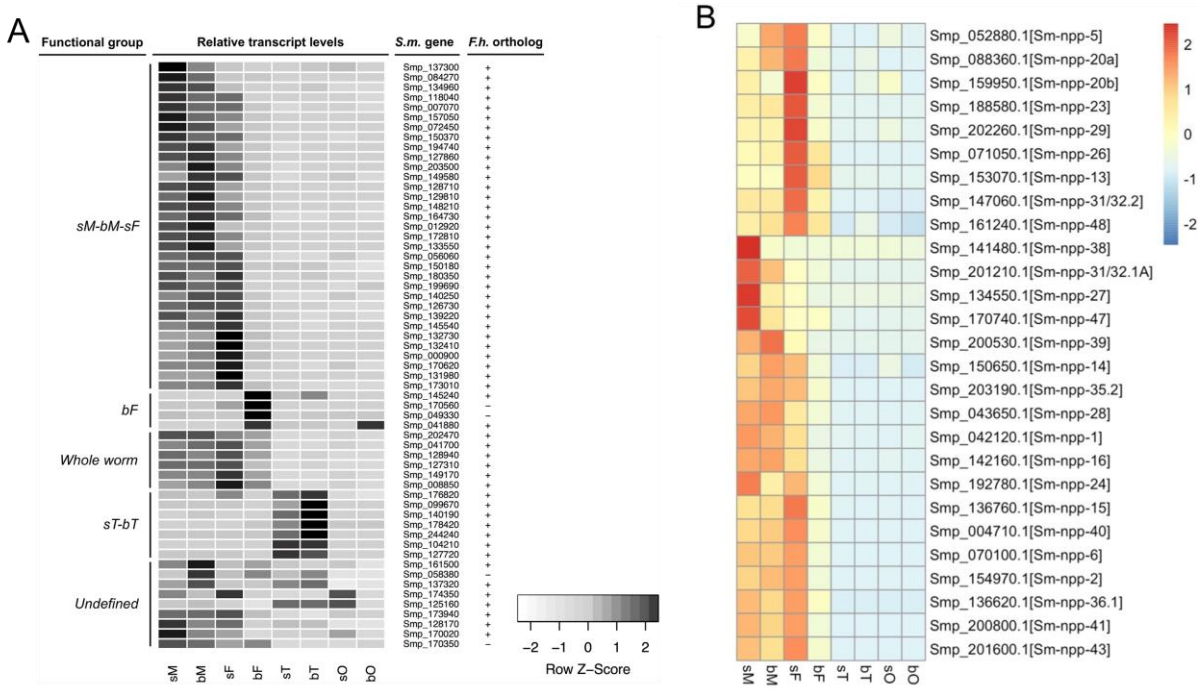

Figure 1.6: Heatmaps showing the relative expression levels of GPCRs and *Sm*_NPPs at the transcript level.

(**A**) Heatmaps showing the relative expression levels of GPCR genes transcribed in adult *S. mansoni* and their gonads (Hahnel et al., 2018). Indicated are different subgroups (starting with the bM-sM-sF subgroup; see text), which had been defined according to the transcript profiles of the appropriate GPCRs. (**B**) Heatmaps showing the relative expression levels of *Sm*_NPPs (Lu et al., 2019) in *S. mansoni* adults and gonads. Black (**A**) and red (**B**): transcript up-regulation; white (**A**) and blue (**B**): down-regulation. sM = pairing-unexperienced male; bM = pairing-experienced male; sF = pairing-unexperienced female; bF = pairing-experienced female; sT = testes of sM; bT = testes of bM; sO = ovaries of sF; bO = ovaries of bF.

1.6.2. Transcript profiles of genes involved in dopaminergic signaling

Furthermore, the mentioned RNA-seq data revealed many genes putatively involved in DOPA neurotransmitter synthesis and transport to be transcribed in a male-biased manner, some of which additionally in pairing-influenced mode. Among these were genes with enzymatic functions such as Smp_135230.1 (*Smtdc-1*) and Smp_171580.1 (*Smddc-1*), which exhibited high similarity to L-tyrosine decarboxylase (TDC) and DOPA decarboxylase (DDC), respectively (see also **Chapter 1.5.1**). Both enzymes catalyze decarboxylation reactions of neurotransmitters and neuromodulators (De Luca et al., 2003; Bertoldi, 2014). Transcript levels of these genes were remarkably high in bM compared to sM, whereas they were low or absent in female worms. These remarkable transcript patterns suggested functions for *Smtdc-1* and *Smddc-1* in male-female interaction and their superior role for males after pairing. In this scenario, *Smtdc-1* and *Smddc-1* may be rate-limiting elements of dopaminergic signaling and, with respect to its pairing-induced "turn-on/stay-on" status, *Smtdc-1* and *Smddc-1* were hypothesized to represent male competence factors. Recently, Wendt generated single-cell RNA-seq libraries from bM, bF, and sF, and after clustering identified 68 molecularly distinct clusters composed of 43,642 cells. Among these, 31 neuronal clusters were uncovered (Wendt et al., 2020). According to this first single-cell atlas for *S. mansoni*, transcripts of *Smtdc-1* and *Smddc-1* dominated in neurons cluster 2. Interestingly, these expression patterns are similar to the *Smnrps* expression, which leads the synthesis of the BATT dipeptide involved in female sexual maturation (see **Chapter 1.6**).

1.7. Objectives of this study

Schistosomiasis is a NTD with a huge impact on animal and human health. PZQ is still used as the only drug of choice. Since the potential emergence of PZQ drug resistance is a justified concern, and no schistosomiasis vaccine exists, there is an urgent need to find alternative treatment options. Previous transcriptomic studies have consistently pointed to neuronal genes being differentially expressed in bM, sM, bF, and sF. These genes included one putative Rhodopsin orphan GPCR gene (Smp_084270, *Sm*GPCR20), as well as Smp_135230 and Smp_171580, both annotated as decarboxylases involved in synthesis of biogenic amines.. The aim of the project is to identify binding potential partners of *Sm*GPCR20, to understand the potential roles of *Sm*GPCR20 - *Sm*_NPPs interactions, and to unravel the functions of *Sm*TDC-1 and *Sm*DDC-1 for male-female interaction. In detail, objectives of my study were:

1) To identify interactions of *Sm*_NPPs partners with *Sm*GPCR20 for a first deorphanization approach using the MALAR-Y2H system.

2) To verify the annotations of *Sm*GPCR20, *Sm*_NPPs, *Sm*TDC-1, and *Sm*DDC-1 in *S. mansoni* using *in silico* analyses.

3) To confirm the transcript profiles of *Smgpcrs*, *Sm_npps*, *Smtdc-1*, and *Smddc-1* by RT-qPCR.

4) To localize transcript occurrence by whole-mount *in situ* hybridization of *Smgpcrs*, *Sm_npps*, *Smtdc-1*, and *Smddc-1*.

5) To improve the *in vitro*-culture conditions for re-pairing experiments of *S. mansoni in vitro*.

6) To investigate the effect of knock-down (KD) of *Smgpcrs*, *Sm_npps*, *Smtdc-1*, and *Smddc-1* transcripts by RNA-interference (RNAi). Phenotype analysis should include worm viability-, pairing stability-, and egg production-assays as well as EdU assay to determine potential stem-cell effects and morphological analyses with a focus on female and male gonads using bright-field and confocal microscopy.

2. Materials and Methods

2.1. Materials

2.1.1. Chemicals

Table 2.1: List of liquid chemicals

Chemicals	Supplier	Batch / Cat# – Number	Application
Agarose NEEO	Carl Roth	2267.3	Gel electrophoresis
Anti-Digoxigenin-AP, Fab-Fragment	Roche	11093274910	WISH
Anti-Digoxigenin-POD, Fab-Fragments	Roche	11207733910	FISH
Anti-Fluorescein-POD, Fab-Fragments	Roche	11426346910	FISH
Antibiotic-Antimycotic	c.c pro	Z-18-M	Supplement for *in vitro* culture
BCIP [50 g/L]	Roche	13513022	WISH
Betaine solution [5 M]	Sigma Aldrich	SLCD3837	PCR
Blocking Reagent	Roche	11096176001	FISH
Canada balsam solution	Sigma Aldrich	#BCBZ8227	Staining of *S. mansoni*
Certistain® Carmine (C.I.75470)	Merck	FN1464533031	Staining of *S. mansoni*
CutSmart® Buffer [10x]	New England Biolabs	10091458	Cloning
Deionized Formamide	Fisher	#BP228-100	WISH, FISH
Diethylpyrocarbonate (DEPC) ≥ 97%	Carl Roth	026238397	*In vitro* transcription,

			dsRNA synthesis, WISH, FISH
Dextran Sulfate	Sigma Aldrich	#D8906	WISH, FISH
di-Sodium hydrogen phosphate	Carl Roth	499291235	Buffer preparation
EtOH Rotipuran® ≥ 99.8%	Carl Roth	9065.4	*In vitro* transcription, dsRNA synthesis, WISH, FISH
Ethylenediamine tetraacetic acid disodium salt dihydrate	Carl Roth	035223917	Buffer preparation
Ethyl 3-aminobenzoate methanesulfonate (Tricaine) [13 mg/mL]	Sigma Aldrich	E10521	Narcotization of worms
Formaldehyde solution 37%	Carl Roth	4979.1	WISH, FISH, EdU staining
Formamide deionized	Genaxis Biotechnology	024732	WISH, FISH
Gel loading dye purple [6x]	New England Biolabs	B7024S	Gel electrophoresis
GelRed Nucleic Acid Stain [10,000X in water]	Biotium	41003	Gel electrophoresis
Glycerol ≥ 98%	Carl Roth	260297353	WISH, FISH
Heat inactivated Horse Serum	Sigma Aldrich	#H1138	Buffer preparation
Hydrochloric acid 37%	Carl Roth	128268146	WISH, FISH, AFA fixation

Hydrogen peroxide Rotipuran® [30%]	Carl Roth	320299217	WISH, FISH
Magnesium chloride, waterfree ≥ 98.5%	Carl Roth	435235264	WISH, FISH, EdU staining
MeOH Rotipuran® ≥ 99.9%	Carl Roth	4627	WISH, FISH, EdU staining
NBT [100 g/l]	Roche	14799526	WISH
Newborn Calf Serum (NCS)	Sigma Aldrich	N4637	Supplement for *in vitro* culture
Poly (vinyl alcohol)	Sigma Aldrich	P8136	WISH
RNase Away	Thermo Scientific	7002	RNA isolation
Sodium Azid	Sigma Aldrich	S8032-25G	FISH
Sodium chloride ≥ 99.5%	Carl Roth	3957.1	Buffer preparation
Sodium hydrogen carbonate	Carl Roth	6885.1	Buffer preparation
ssRNA Ladder Loading Buffer [2x]	New England Biolabs	0011005	dsRNA synthesis, *in vitro* transcription
Potassium chloride	Carl Roth	034204130	Buffer preparation
Potassium dihydrogen phosphate	Carl Roth	11785870	Buffer preparation
TSA Plus Cyanine 3	AKOYA BIOSCIENCES	NEL744001KT	FISH
TSA Plus Cyanine 5	AKOYA BIOSCIENCES	NEL745001KT	FISH

Transcription Buffer [10x]	Roche	11465384001	dsRNA synthesis, *in vitro* transcription
Tris ≥ 99.9%	Carl Roth	4855.2	Buffer preparation
tri-Sodium Citrate 2-hydrate	Carl Roth	3580.3	Buffer preparation
Triton™ X-100	Sigma Aldrich	T8787	Buffer preparation
Tween® 20	Carl Roth	9127.2	WISH, FISH
Type F Immersion liquid	Leica Microsystems	11513859	CLSM, FISH
Western Blocking Reagent	Roche	11096176001	FISH

2.1.2. Buffers and Solutions

Table 2.2: Buffers and solutions

Solution / buffer	Composition	Application
AFA	2% acetic acid; 1.1% formaldehyde; 66.7% EtOH	CLSM
Antibody solution	1:2000 Anti-Digoxigenin-AP (Roche) in Colorimetric blocking solution	WISH
Antibody solution	1:1000 Anti-Digoxigenin-POD (Roche) in FISH blocking solution	FISH
Antibody solution	1:1000 Anti-FITC-POD (Roche) in FISH blocking solution	FISH
AP buffer	100 mM Tris pH 9.5; 100 mM NaCl; 50 mg $MgCl_2$; 0.1% Tween-20; 10% PVA	WISH
Bleaching solution	9 mL DEPC H_2O; 500 µL Formamide; 250 µL 20x SSC (pH 7.0); 400 µL H_2O_2 [30%]	WISH, FISH

Carmine red solution	1 g carmine (Certistain, Merck); 1 mL conc. HCL [37%]; 1 mL dH_2O, EtOH [90%] ad 40 mL	CLSM
Colorimetric blocking Solution	7.5% Heat inactivated Horse Serum (Sigma Aldrich) in TNT	WISH
DEPC H_2O	0.1% diethylpyrocarbonate filtered in dH_2O and autoclaved	*In vitro* transcription, WISH, FISH
DIG-NTP mix	10 mM ATP; 10 mM CTP; 10 mM GTP; 7 mM UTP; 3.5 mM DIG-UTP in DEPC H_2O	WISH, FISH
dNTP mix	10 mM dATP; 10 mM dCTP; 10 mM dGTP; 10 mM dTTP	PCR
FISH blocking solution	5% Heat inactivated Horse Serum (Sigma Aldrich) and 0.5% Western Blocking Reagent in TNT	FISH
Fixation solution	3.7% Formaldehyde in PBSTx	EdU staining, WISH, FISH
Hybridization solution	50% deionized formamide (Fisher); 10% (w/v) dextran sulfate (Sigma Aldrich); 5x SSC; 1 mg/mL Yeast RNA in formamide; 1% Tween 20	WISH, FISH
PBS [10x]	1.37 M NaCl; 27 mM KCl; 65 mM $NaHPO_4$; 15 mM KH_2PO_4; dH_2O ad 1 L (pH 7.0 - 7.2); autoclaved	Wash buffer
PBSTx	1x PBS; 0.3% Triton X-100	WISH, FISH, EdU staining
PerfeCTa SYBR Green SuperMix	Composition from the manufacturer Quanta (95054)	Real-time quantitative PCR
Prehybridization solution	50% deionized formamide; 5x SSC; 1 mg/mL Yeast RNA; 1% Tween-20; DEPC H_2O	WISH, FISH

Snail water	0.3% solution I (1 M $CaCl_2$; 0.35 M $MgCl_2$), 0.2% solution II (21.71 M K_2CO_3; 273.78 M $NaHCO_3$); 0.04% solution III (0.6 M NaOH); dH_2O ad 1 L	Culture of intermediate host *Biomphalaria glabrata*
SSC [20x]	3 M NaCl; 0.3 M Tri-sodium citrate; dH_2O ad 1 L pH 7.0	WISH
TAE buffer [50x]	2 M Tris; 50 mM EDTA; 5.71% glacial acetic acid; dH_2O ad 1 L pH 8.0	Gel electrophoresis
TFB1	100 mM RbCl; 50 mM MnCl; 10 mM $CaCl_2$; 30 mM Potassium acetate; 15% Glycerol; dH_2O ad 0.3 L; pH 5.8; filtered sterile; store at 4°C	Production of competent *E. coli* cells
TFB2	10 mM MOPS; 10 mM RbCl; 75 mM $CaCl_2$; 15% Glycerol; dH_2O ad 0.3 L; pH 6.8; filtered sterile; store at 4°C	Production of competent *E. coli* cells
TNT	0.1 M Tris pH 7,5; 150 mM NaCl; 0.1% Tween-20	WISH, FISH
Wash Hybridization Solution	25% formamide; 3.5x SSC; 0.5% Tween-20; 0.05% TritonX-100; dH_2O ad 0.5 L	WISH, FISH

2.1.3. Media and supplements

Table 2.3: Media and supplements

Media / supplement	Composition	Application
ABAM	Antibiotic / antimycotic solution (Sigma)	Supplement for *in vitro* culture
ABC 169 media	BM169, 200 µM ascorbic acid (Sigma-Aldrich), 0.2% V/V human washed RBCs (10% suspension), 2.5% human low-	*In vitro* culture of *S. mansoni*

	density lipoprotein (LDL) (TRINA, Switzerland)	
Agar-Agar Kobe I	Carl Roth (480302481)	Supplement of LB agar plates
Ampicillin	Ampicillin trihydrate [D (-)-α-aminobenzylpenicillin]; stock conc. 100 mg/mL in dH2O; final conc. 100 µg/mL	Supplement of LB medium and LB agar plates
Basal Medium Eagle	Sigma Aldrich (B9638-10X1L)	*In vitro* culture of *S. mansoni*
BM169	Basal Medium Eagle, 1 g Glucose, 2.4 g HEPES, 1 g Lactalbumin, 2.2 g Sodium bicarbonate, 5 mL hypoxanthine, 1 mL hydrocortisone, 1 mL triiodothronin, 1 mL insulin, 50 mL Schneider's medium, 5mL 100x MEM in 1L dH_2O (PH 7.3-7.4)	*In vitro* culture of *S. mansoni*
Glucose	Sigma Aldrich (G8270)	Supplement of BM169 medium
HEPES	1 M 2-[4-(2-hydroxyethyl)-1-piperazinyl-ethane-sulfonic acid; pH 7.4; filtered sterile	Supplement for *in vitro* culture
Human low-density lipoprotein (LDL)	TRINA (CD1111-N)	Supplement of ABC169 medium
Hypoxanthine	Sigma Aldrich (H9377)	Supplement of BM169 medium
Hydrocortisone	Sigma Aldrich (H0888)	Supplement of BM169 medium
lnsulin	Sigma Aldrich (I1882)	Supplement of BM169 medium
LB medium (Lennox)	Carl Roth (270298190)	*E. coli* medium (fluid)
L-ascorbic acid	Sigma Aldrich (A92902)	Supplement of ABC169 medium

M199	10.43 g M199; 1 g glucose; 2.2 g $NaHCO_3$; 20 mL Tris (1 M; pH 7.4); dH2O add 1 l (pH 7.0); filtered sterile	*In vitro* culture of *S. mansoni*
M199 3+	M199; 1% HEPES; 1% ABAM; 10% NCS	*In vitro* culture of *S. mansoni*
Perfusion medium	1% (w/v) M199 (powder medium); 2% (v/v) 0.5 M Tris (pH 7.4); 0.1% glucose; heparin (final conc. 10 mg/L)	Perfusion of the hamsters (final hosts)
Schneider's medium	Gibco (21720024)	Supplement of BM169 medium
Triiodothyronin	Sigma Aldrich (709719)	Supplement of BM169 medium

2.1.4. Enzymes

Table 2.4: Enzymes

Enzymes	Supplier	Batch - / Lot Number	Application
Acc65I	New England Biolabs	R0599S	Cloning
Accu Prime *Taq* DNA Polymerase High Fidelity	Invitrogen	2248310	PCR
AhdI	New England Biolabs	10030388	Cloning
BamHI-HF	New England Biolabs	R3552S	Cloning
DNase I (RNase-free)	New England Biolabs	M0303L	*In vitro* transcription
FIREPol DNA Polymerase	Solis Biodyne	01011240.3	PCR
KpnI	New England Biolabs	R3142S	Cloning

MluI	New Biolabs	England	R3198S	Cloning
NcoI	New Biolabs	England	R0193S	Cloning
NotI	New Biolabs	England	R0189S	Cloning
Proteinase K	Ambion		MW19K20003	WISH, FISH, EdU staining
Pyrophosphatase, Inorganic (*E. coli*)	New Biolabs	England	M0361S	*In vitro* transcription
Q5 High-Fidelity DNA Polymerase	New Biolabs	England	M0591S	PCR
RNase Inhibitor, Murine	New Biolabs	England	M0314L	WISH
SmaI	New Biolabs	England	R0141S	Cloning
SP6 RNA Polymerase	Roche		11487671001	WISH
T3 RNA Polymerase	Roche		11031163001	WISH
T4 DNA Ligase	New Biolabs	England	M0202S	Cloning
T7 RNA Polymerase	New Biolabs	England	E2050S	Synthesis of dsRNA
T7 RNA Polymerase	Self-made			Synthesis of dsRNA

2.1.5. Kits

Table 2.5: Kits

Name	Supplier	Application
Agilent RNA 6000 Nano /Pico Kit	Agilent Technologies	RNA analysis

GeneJET Plasmid Midiprep Kit	Thermo Scientific	Plasmid purification
Monarch DNA Cleanup and Gel Extraction Kit	New England Biolabs	DNA extraction
Monarch Plasmid Miniprep Kit	New England Biolabs	Extraction of plasmid-DNA from bacteria
Monarch total RNA Miniprep Kit	New England Biolabs	RNA isolation
PerfeCTa SYBR Green Super Mix	Quanta	Real-time qPCR
QuantiTect Reverse Transcription Kit	Qiagen	cDNA synthesis

2.1.6. Online databases and software tools

Table 2.6: Online databases and softwares

Database / software	Hyperlink address	Application
NCBI – national center for biotechnology information	https://pubmed.ncbi.nlm.nih.gov/	Literature search, Homology search
WormBase ParaSite	https://parasite.wormbase.org/index.html	Homology search, protein or nucleotide blast
SMART	http://smart.embl-heidelberg.de/	Protein domain analyses
Reverse Complement	https://www.bioinformatics.org/sms/rev_comp.html	Reverse complement
Clustal Omega	https://www.ebi.ac.uk/Tools/msa/clustalo/	Multiple sequence alignment
DeepTMHMM	https://dtu.biolib.com/DeepTMHMM	Transmembrane domain prediction
interpro	https://www.ebi.ac.uk/interpro	Protein family identification

Meta RNA-seq in *S. mansoni*	https://v7test.schisto.xyz/	Gene transcripts of *S. mansoni*
SACS HMMTOP	https://www.sacs.ucsf.edu/cgi-bin/hmmtop.py	Transmembrane domain prediction
SchistoCyte Atlas	http://collinslab.org/schistocyte/	Single-cell transcriptomic of *S. mansoni*
Snapgene	https://www.snapgene.com/	Cloning
Primer3Plus	https://www.bioinformatics.nl/cgi-bin/primer3plus/primer3plus.cgi	Primer design
Oligo Calc - Oligonucleotide Properties Calculator	http://biotools.nubic.northwestern.edu/OligoCalc.html	Melting temperature adjustment
Oligo Analyzer Tool	https://eu.idtdna.com/pages/tools/oligoanalyzer	Primer analyses
ImageJ	https://imagej.nih.gov/ij/	Worm length measurement
Prism (Version 8.0)	https://www.graphpad.com/features	Statistical analyses
MEGA11	https://www.megasoftware.net/	Phylogenetic tree constrution
Uniprot	https://www.uniprot.org/	Protein database
interpro	https://www.ebi.ac.uk/interpro	Protein family identification

2.1.7. Primers

Primers designed for RT-qPCR (see 2.1.6, Primer3Plus) were 18-25 nt in size, and a salt-adjusted melting temperature of 60±0.5°C. When possible, primers were designed binding to different exons of a gene to distinguish amplification products derived from (contaminating) gDNA versus cDNA by size. To analyze these properties, the online tool OligoCalc (**Table 2.6**) was used. For analyses of primer dimerization and hairpin formation, IDT's online tool OligoAnalyzer (**Table 2.6**) was used. In addition, primers were designed to amplify specific DNA fragments with a length between 140-200 bp, respectively. All used primers were synthesized by Integrated DNA Technologies (IDT) (Leuven, Belgium) and listed in the following tables.

Table 2.7: Primers used for cloning and RT-qPCR

Primer name	Application	Sequence (5'-3')
Smp_084270 (*Smgpcr20*) _ pJC 53.2_s	Cloning	ATACGGCTTGCAATGTTGGG
Smp_084270 (*Smgpcr20*) _ pJC 53.2_as	Cloning	TGTGGCCTGATACAACGCTT
Smp_084270 (*Smgpcr20*) _ qPCR_For	RT-qPCR	CCGTATACGACAAATGGAACC
Smp_084270 (*Smgpcr20*) _ qPCR_Rev	RT-qPCR	TCGGATGAAGCACATACAC
Smp_084270 (*Smgpcr20*) _T7_For	dsRNA	cctaatacgactcactatagggagCGATTACTGCATGCCGCTTT
Smp_084270 (*Smgpcr20*) _T7_Rev	dsRNA	cctaatacgactcactatagggagTGTTGGGTTCAGAGTGCCAA
Smp_084270 (*Smgpcr20*) _ qPCR_For	RT-qPCR (RNAi)	CCGTATACGACAAATGGAACC
Smp_084270 (*Smgpcr20*) _qPCR_Rev	RT-qPCR (RNAi)	TCGGATGAAGCACATACACG
Smp_071050 (*Smnpp26*) _ pJC 53.2_s	Cloning	TCGTCAATGCTATACCTGTGC
Smp_071050 (*Smnpp26*) _ pJC 53.2_as	Cloning	TTCATTGATTACATTGTGCGTCT
Smp_071050 (*Smnpp26*) _ qPCR_For	RT-qPCR	TGGGTTTTCATGGGTTGCAAG
Smp_071050 (*Smnpp26*) _ qPCR_Rev	RT-qPCR	TACACCTCCACCAATTCCGC
Smp_004710 (*Smnpp40*) _ pJC 53.2_s	Cloning	GTTTATTACTTACCCCTCCTCCA
Smp_004710 (*Smnpp40*) _ pJC 53.2_as	Cloning	GTTCAACTTTAGGCGGTAGACC
Smp_004710 (*Smnpp40*) _ qPCR_For	RT-qPCR	GGTCTACCGCCTAAAGTTGAAC
Smp_004710 (*Smnpp40*) _ qPCR_Rev	RT-qPCR	TGAAATCTAGTTGGTGCTGGT
Smp_335630 (*Smtsp-2*) _ pJC 53.2 _s	Cloning	CTCTTGGTTGTGGGTATAAG
Smp_335630 (*Smtsp-2*) _ pJC 53.2_as	Cloning	CATGTTCGTCATTACGGTAC
Smp_065110 (*Smletm1*) _qPCR_For	RT-qPCR	CGTGGAATGCGTTCAGTTGG
Smp_065110 (*Smletm1*) _qPCR_ Rev	RT-qPCR	GAAGCTGATGGAGGTAATTGAG
Smp_055740 (*Smnanos-1*) _qPCR_For	RT-qPCR	ACTTGTCCATTATGCGGTGCT
Smp_055740 (*Smnanos-1*) _qPCR_Rev	RT-qPCR	GGTTCCAACAAACCAGCTTCA
Smp_051920 (*Smnanos-2*) _qPCR_For	RT-qPCR	GCCGTGTTATGACCTCTGG
Smp_051920 (*Smnanos-2*) _qPCR_Rev	RT-qPCR	GACGATCTGGAGACTCTGG
Smp_000270 (*Smfs800*) _qPCR_For	RT-qPCR	CAGCCGAAAAAGTCAAACA

Smp_000270 (*Smfs800*) _qPCR_Rev	RT-qPCR	CCCTTTTGCATCGTAAGCT
Smp_333540 (*Smmeiob*) _ qPCR_For	RT-qPCR	TGCTGGATATGCCTGTACATTCGCC
Smp_333540 (*Smmeiob*) _ qPCR_Rev	RT-qPCR	ACCTGGAGTAGCGCACATTGCAAAC
Smp_050270 (*Sm*TYR1) _qPCR_For	RT-qPCR	AGTATGCGGTGGACCAAAAC
Smp_050270 (*Sm*TYR1) _qPCR_Rev	RT-qPCR	ATCGTCCTTTCCATCCAAAC
Smp_013540 (*Sm*TYR2) _ qPCR_For	RT-qPCR	ACAGCATTCCCAACAACTCA
Smp_013540 (*Sm*TYR2) _ qPCR_Rev	RT-qPCR	CACCGGGAAAAGAACAAAAT
Smp_165360 (*Smmyst4*) _qPCR_For	RT-qPCR	GAAATTCGTTTCCCAAGCAG
Smp_165360 (*Smmyst4*) _qPCR_Rev	RT-qPCR	GCCCCTTCGTAGCCATTTA
Smp_165360 (*Smmyst4*) _ pJC 53.2_s	Cloning	CCACATATCAAGCAAAGTCAACTGCTGAA
Smp_165360 (*Smmyst4*) _ pJC 53.2_as	Cloning	CAGTTGGTTGACTTGATGAAATAAGCTCATC
Smp_131110 (*Smp14*) _qPCR_For	RT-qPCR	CCTATGGCGGTGATTATGG
Smp_131110 (*Smp14*) _qPCR_Rev	RT-qPCR	GGCTGGGTTTGTAAGTGC
Smp_095980 (*Smsod*)_ qPCR_For	RT-qPCR	TTTGATCCGGCTATTGCTTC
Smp_095980 (*Smsod*)_ qPCR_Rev	RT-qPCR	TCATGGTGCACGAAATCCTA
Smp_171580 (*Smddc-1*)_ pJC 53.2_s	Cloning	ATCCAGCTTGCACAGAACTTGA
Smp_171580 (*Smddc-1*)_ pJC 53.2_as	Cloning	AGTTCCCAAAGTTGCACAGC
Smp_171580 (*Smddc-1*)_ qPCR_For	RT-qPCR	AGTCGCTCTATTGGCTGCAC
Smp_171580 (*Smddc-1*)_qPCR_Rev	RT-qPCR	CTGAACTATGTGCCTGATCCGA
Smp_135230 (*Smtdc-1*)_ pJC 53.2_s	Cloning	AGCGGAATTGGTGGAGGTGTA
Smp_135230 (*Smtdc-1*)_ pJC 53.2_as	Cloning	GCAGCGTCCACATGTAACCA
Smp_135230 (*Smtdc-1*)_ qPCR_For	RT-qPCR	TGGGTTTTCATGGGTTGCAAG
Smp_135230 (*Smtdc-1*)_ qPCR_Rev	RT-qPCR	TACACCTCCACCAATTCCGC
Smp_158480 (*Smnrps*)_pJC 53.2_s	Cloning	TGCCTCCAGGAATAGATCGT
Smp_158480 (*Smnrps*)_pJC 53.2_as	Cloning	GATCCACCAGGAACAACCAC
pJC 53.2_sequence_s	Cloning	TTCTGCGGACTGGCTTTCTAC
pJC 53.2_T7_extended primer	Riboprobe synthesis	CCTAATACGACTCACTATAGGGAG

*The sequence of the T7 promoter is in lower case.

Table 2.8: Primers used for GPCR gene amplification

GPCR	5'-3' sequence (forward and reverse)	Length(bp)
Smp_084270	CCGCCCAATACGAGCCCATGATAAGTATGAACTCAAGTGAATT	43
(*Sm*GPCR20)	GTTGATCCACCTTCTAGGATCCCGTAATTGTGGCCTGATACAACG	45

Table 2.9: Primers used to generate neuropeptide CDS

NPP	5'3' sequence (forward and reverse)		Length(bp)
1a	Fw	GTACCCAAACCGCTTTTGTACGTCTGGGG	29
	Re	CCCCAGACGTACAAAAGCGGTTTGG	25
1b	Fw	GTACCCAAACCGGATTTGTTCGGATCGGT	29
	Re	ACCGATCCGAACAAATCCGGTTTGG	25
2a	Fw	GTACCCAAACCCGAGGAATGATTGGC	26
	Re	GCCAATCATTCCTCGGGTTTGG	22

2b	Fw	GTACCCAAACCCGAGGTTTTATGGGT	26
	Re	ACCCATAAAACCTCGGGTTTGG	22
5a	Fw	GTACCCAAACCGCTGCTTACATGGATTTACCATGGGGT	38
	Re	ACCCCATGGTAAATCCATGTAAGCAGCGGTTTGG	34
5b	Fw	GTACCCAAACCGCAGCTTATATTGATTTACCATGGGGT	38
	Re	ACCCCATGGTAAATCAATATAAGCTGCGGTTTGG	34
6	Fw	GTACCCAAACCGCTGTCCGATTAATGAGACTTGGT	35
	Re	ACCAAGTCTCATTAATCGGACAGCGGTTTGG	31
13	Fw	GTACCCAAACCCATTTTATGCCTCAACGATTTGGA	35
	Re	TCCAAATCGTTGAGGCATAAAATGGGTTTGG	31
14	Fw	GTACCCAAACCGGATTACGTAATATGCGTATGGGT	35
	Re	ACCCATACGCATATTACGTAATCCGGTTTGG	31
15a	Fw	GTACCCAAACCGTTCAATTTCTACGTCTTGGT	32
	Re	ACCAAGACGTAGAAATTGAACGGTTTGG	28
15b	Fw	GTACCCAAACCTCTGCTTATCCTTATGTTGGT	32
	Re	ACCAACATAAGGATAAGCAGAGGTTTGG	28
16	Fw	GTACCCAAACCAATTATTTATGGGATACACGTTTGGGT	38
	Re	ACCCAAACGTGTATCCCATAAATAATTGGTTTGG	34
20a	Fw1	GTACCCAAACCGCACAAGCATTAGCTAAACTTATGTCATTATTTTATA CTAGTGATGCAT	60
	Fw2	TTAATAAATATATGGAAAATCTTGATGCATATTATATGCTTAGAGGTA GACCAAGATTTGGT	62
	Re1	TTAAATGCATCACTAGTATAAAATAATGACATAAGTTTAGCTAATGCT TGTGCGGTTTGG	60
	Re2	ACCAAATCTTGGTCTACCTCTAAGCATATAATATGCATCAAGATTTTC CATATATTTA	58
20b	Fw1	GTACCCAAACCGCAGTTGAAATTGTTCCACCAGAAAGACCATTTATA TTTGAAACACCTG	60
	Fw2	AAGCTCTTAGAACATATTTACATAAATTAAATGAATATTTTGCTATTA TAGGTCGTCCTAGATTTGGT	68
	Re1	GCTTCAGGTGTTTCAAATATAAATGGTCTTTCTGGTGGAACAATTTCA ACTGCGGTTTGG	60
	Re2	ACCAAATCTAGGACGACCTATAATAGCAAAATATTCATTTAATTTATG TAAATATGTTCTAAGA	64
23	Fw	GTACCCAAACCTATATTAGATTTGGA	26
	Re	TCCAAATCTAATATAGGTTTGG	22
24	Fw	GTACCCAAACCGGTGGAATGTATGGTGGTCTATTAGGA	38
	Re	TCCTAATAGACCACCATACATTCCACCGGTTTGG	34
26a	Fw	GTACCCAAACCAATTTTGATCCAATTCTGTTT	32
	Re	AAACAGAATTGGATCAAAATTGGTTTGG	28
26b	Fw	GTACCCAAACCTCATACTTTGATCCAATTATTTAT	35
	Re	ATAAATAATTGGATCAAAGTATGAGGTTTGG	31
26c	Fw	GTACCCAAACCTCATACTTTGATCCTATATTATTT	35

	Re	AAATAATATAGGATCAAAGTATGAGGTTTGG	31
26d	Fw	GTACCCAAACCAATGAGGATCGTCAGTTTGAA	32
	Re	TTCAAACTGACGATCCTCATTGGTTTGG	28
26e	Fw	GTACCCAAACCGAACATTTTGATCCGATAATTTAT	35
	Re	ATAAATTATCGGATCAAAATGTTCGGTTTGG	31
27	Fw	GTACCCAAACCGTTCCACCTTATATAACCGGTGGAATTCGGTAT	44
	Re	ATACCGAATTCCACCGGTTATATAAGGTGGAACGGTTTGG	40
28	Fw	GTACCCAAACCGCTTATCATTTCTTTCGATTG	32
	Re	CAATCGAAAGAAATGATAAGCGGTTTGG	28
29	Fw	GTACCCAAACCATGGTGTATTGG	29
	Re	CCAATACACCATGGTTTGG	19
32.1A	Fw	GTACCCAAACCGGTCCAGAAACACTTTGGGAACTGGAC	38
	Re	GTCCAGTTCCCAAAGTGTTTCTGGACCGGTTTGG	34
32.1B	Fw	GTACCCAAACCGGTCCAGAACCATTATGGGTAGTAGAAACT	41
	Re	AGTTTCTACTACCCATAATGGTTCTGGACCGGTTTGG	37
32.2	Fw	GTACCCAAACCGGTCCAGAATTAATTATTCCATTTATAAGTGGCGGTG TTCCAGCA	56
	Re	TGCTGGAACACCGCCACTTATAAATGGAATAATTAATTCTGGACCGG TTTGG	52
35.1	Fw	GTACCCAAACCTATGGACATTATTCACAACGTTTAGGA	38
	Re	TCCTAAACGTTGTGAATAATGTCCATAGGTTTGG	34
35.2	Fw	GTACCCAAACCTATTATATATCACAAAGACTTGGT	35
	Re	ACCAAGTCTTTGTGATATATAATAGGTTTGG	31
36.1	Fw	GTACCCAAACCTGGTTTCCTATAAAAGAATATCGTGGTGGATTAATG GAAGTT	53
	Re	AACTTCCATTAATCCACCACGATATTCTTTTATAGGAAACCAGGTTTG G	49
36.2a	Fw	GTACCCAAACCTGGTATCCTGTGAAAGAATTTCATTATGATGAACCGT TAGAGATT	56
	Re	AATCTCTAACGGTTCATCATAATGAAATTCTTTCACAGGATACCAGGT TTGG	52
36.2b	Fw	GTACCCAAACCTGGTTTCCAGTGAAAGAATTCCATTATGATGGACCA CTTGAAGTG	56
	Re	CACTTCAAGTGGTCCATCATAATGGAATTCTTTCACTGGAAACCAGGT TTGG	52
36.2c	Fw	GTACCCAAACCTGGTCTCCTGTCAAAGAATTTCATTATGATGAACCAA TAGAAGTG	56
	Re	CACTTCTATTGGTTCATCATAATGAAATTCTTTGACAGGAGACCAGGT TTGG	52
37	Fw	GTACCCAAACCTGGACTGATTTT	23
	Re	AAAATCAGTCCAGGTTTGG	19
38a	Fw	GTACCCAAACCGTTTTAGCTGATTAT	26
	Re	ATAATCAGCTAAAACGGTTTGG	22

38b	Fw	GTACCCAAACCCAAGCTATATTAGCTGATTAC	32
	Re	GTAATCAGCTAATATAGCTTGGGTTTGG	28
39	Fw	GTACCCAAACCTTCACTCGTCCATATGGT	29
	Re	ACCATATGGACGAGTGAAGGTTTGG	25
40a	Fw	GTACCCAAACCTTTCTGTTAGCTTTACCGTCACCC	35
	Re	GGGTGACGGTAAAGCTAACAGAAAGGTTTGG	31
40b	Fw	GTACCCAAACCTTTCTACTTGGTCTACCGCCTAAAGTTGAACAT	44
	Re	ATGTTCAACTTTAGGCGGTAGACCAAGTAGAAAGGTTTGG	40
40c	Fw	GTACCCAAACCTTTCTACTTGGTTTACCACCATCACTTAGACAACAT	47
	Re	ATGTTGTCTAAGTGATGGTGGTAAACCAAGTAGAAAGGTTTGG	43
40d	Fw	GTACCCAAACCTTCATTTTAGGGCTACCAGCACCAACTAGATTTCATT CG	50
	Re	CGAATGAAATCTAGTTGGTGCTGGTAGCCCTAAAATGAAGGTTTGG	46
41	Fw	GTACCCAAACCTTCTTTTGTAATCCAATGGGATGCGTT	38
	Re	AACGCATCCCATTGGATTACAAAAGAAGGTTTGG	34
42	Fw	GTACCCAAACCCCTTGGACATTACGTGACCCACTGAATTGTTGCTTGG ATAATGCTAAATGTTGT	65
	Re	ACAACATTTAGCATTATCCAAGCAACAATTCAGTGGGTCACGTAATG TCCAAGGGGTTTGG	61
43a	Fw	GTACCCAAACCGCAAGTTTAGCATATTTT	29
	Re	AAAATATGCTAAACTTGCGGTTTGG	25
43b	Fw	GTACCCAAACCGCAAGTTTATCCTATTTT	29
	Re	AAAATAGGATAAACTTGCGGTTTGG	25
47	Fw	GTACCCAAACCGGCAAATTTTTCATGTTAGGA	32
	Re	TCCTAACATGAAAAATTTGCCGGTTTGG	28
48	Fw	CGTTGTGGGTACCCAAACCTATTATACAAATTTGAAAACAATTG	44
	Re	GGTCGTACCAGATCCCCCACCATATCTCATCACATTAGG	39

2.1.8. Bacterial strains used for cloning

Table 2.10: Bacterial strains

Bacterial Strain	Supplier	Batch/Cat#
NEB 10-beta competent *E. coli* (High Efficiency)	NEB	C3019H

2.2. Methods

2.2.1. Ethics Statement

All animal experiments have been performed in accordance with the European Convention for the Protection of Vertebrate Animals used for experimental and other scientific purposes

(ETS No 123; revised Appendix A) and have been approved by the Regional Council (Regierungspraesidium) Giessen (V54-19 c 20/15 c GI 18/10).

2.2.2. Laboratory cycle of *Schistosoma mansoni*

To obtain the parasite life cycle under laboratory conditions, the freshwater snail *Biomphalaria glabrata* (*B. glabrata*) was used as intermediate hosts, and Syrian golden hamsters (*Mesocricetus auratus*) were used as final hosts. Adult and larval schistosome stages originated from a Liberian isolate from Bayer AG, Monheim (Grevelding, 1995; Grevelding et al., 1997). Adult worms were obtained by hepatoportal perfusion at 42-49 days (d) p.i.. In case of infection with single sex (ss) worms, snails were infected by a single miracidium each (monomiracidial infection) to obtain clonal cercariae for infection. In this case, perfusion occurred 67 d p.i..

2.2.3. Maintenance and infection of snails

B. glabrata snails were kept in aquaria with commercially available spring water (Rossbacher 2:1) in a ventilated incubator at 26°C. The snails were exposed to a day-night rhythm of 16 hours (h) light and 8 h darkness. For infection, the snails were placed in 12-well microtiter plates filled with 2 mL of snail water in each well. The snails were incubated with 10-15 miracidia for 12 h for a bisex infection (polymiracidial) or with only one miracidium in case of a single-sex infection (monomiracidial) to ensure the development of only one sex (Grevelding et al., 1997). After infection, the snails were placed back into their aquaria.

2.2.4. Infection of hamsters

Syrian golden hamsters originated from in-house breeding (ZVTH Giessen), or they were purchased from Janvier Labs (France). Infection with cercariae was performed according to previous protocol (Dettman et al., 1989). To this end, eight to ten weeks old hamsters were bathed in 30°C snail-water (water level: 1.5 cm) for 45 to 60 min to soften their skin and facilitate skin penetration of cercariae. The water was replaced by new water containing about 1,750 cercariae for bisex infections and 2,500 cercariae for single-sex infections. For bisex infections, cercariae of both genders were used, whereas for single-sex infection, only cercariae of one gender were added. The sex of cercariae was determined by polymerase chain reaction (PCR) prior infection (Webster et al., 1989; Gasser et al., 1991; Grevelding, 1995). Incubation in cercariae-containing water occurred for 45 min. Afterwards, hamsters were placed back in

their cages and kept for 46 d in case of bisex infections, or 67 days in case of single-sex infections.

2.2.5. Worm perfusion

After the infection of hamsters, cercariae mature in the host's blood stream into schistosomula and subsequently to adult worms. To obtain worms after the infection period, hepatoportal perfusion was performed (Duvall and DeWitt, 1967). For this, infected hamsters were sedated by inhalation of the anesthetic isoflurane (Baxter, Germany). During sedation, hamsters obtained an overdose of the narcotic mixture xylazine and ketamine (cp-pharma, Germany) by intraperitoneal injection. Through its muscle relaxing effect, as an additional effect, this mixture resulted in a detachment of the adult worms from endothelia of the blood vessels. Afterwards, the hamsters' thorax was opened to expose inner organs. The portal vein was opened by incision and the left ventricle was punctured using a cannula. Next, prewarmed (37°C) perfusion medium (M199 3+ (Sigma-Aldrich; supplemented with 10% Newborn Calf Serum (NCS), 1% HEPES [1 M] and 1% ABAM-solution [10,000 units of penicillin, 10 mg of streptomycin and 25 mg of amphotericin B per mL]) was pumped into the blood stream through the cannula. This leads to a flush of adult worms out of the portal vein opening. The worms were collected on a gauze net and were transferred into a prewarmed medium using a fine brush. Depending on the purpose of later use, the worms were sorted into couples, single males or single females and transferred to 60 mm petri dishes. For maintenance, 20 couples were placed in a 5 mL dish as or 30 single males, or 50 single females. All worms were kept at 37°C and 5% CO_2 in an incubator (RS Biotech, France) until further usage.

2.2.6. *In vitro* culture and pairing experiments of *S. mansoni*

For regular maintenance *in vitro*, worms were cultured in M199 3+ medium supplemented with 10% NCS, 1% 1 M HEPES and 1% ABAM solution (10,000 units/mL penicillin, 10 mg/mL streptomycin and 25 mg/mL amphotericin B) at 37°C in a 5% CO_2 atmosphere (Grevelding et al., 1997). For pairing and re-pairing experiments, the recently developed ABC169 *in vitro*-culture medium (Wang et al., 2019) was used with modifications. ABC169 is a modified version of Basch medium (Basch, 1981) and was supplemented with 1% ABAM solution, 10% NCS, 200 µM ascorbic acid, and 0.2% V/V human washed red blood cells (10% suspension). Low density lipoprotein (LDL) of human was added instead of the original 0.2% V/V porcine cholesterol concentrate used in other studies (Wang et al., 2019). Firstly, groups

of each 5 males and 5 females were used to investigate the effects of different LDL concentrations (from 0% to 2%) on re-pairing and vitality over a three-day observation period *in vitro*. To find out the most suitable male:female ratio for re-pairing, different ratios of male and female worms (4:4, 3:9, 6:2, 15:10) per well were investigated, and standard M199 3+ medium was used as a medium control.

For the later re-pairing experiments, worms were kept in 6-well plates at 37°C in 5% CO_2 in 5 mL modified ABC169 medium. The medium was changed every 2 d, and worms were monitored over observation periods up to 21 d, depending on the experiments. Re-paired worms were transferred in AFA fixation buffer for CLSM analysis or collected for RNA isolation.

2.2.7. Soaking of *S. mansoni* with dsRNA

For RNAi analysis, 10 couples each were cultured in 3 mL M199 3+ medium at 37°C and 5% CO_2 in 6-well cell-culture plates. Amounts of 15-60 µg/mL dsRNA were used. As a negative control, worms were cultured in culture medium without dsRNA. All parasites were cultured for 15 d, the culture medium and dsRNA were replaced every 2 d. Monitoring RNAi effects included parameters like pairing stability, motility, and egg production, which were recorded by bright-field microscopy (Leica, Germany). Egg production was determined by counting egg every 2 d. After 15 d, 10 worms were harvested for RT-qPCR analysis to determine mRNA levels of *Smgpcr20*, *Smnpp26*, and *Smnpp40*, respectively, and for morphologic examination (5 technical replicates each). All experiments were performed in biological triplicates (n=3).

For re-pairing experiment in the context of the functional analyses of *Smgpcr20*, *Smnpp26*, and *Smnpp40*, single-sex females (sF) and pairing-experienced male worms (bM, separated from their previous female partners at the day of perfusion = sbM) were treated with 30 µg/mL dsRNA of each gene (60 µg/mL maximum) at d0 in BM169 medium for 8 d, respectively (Wang et al., 2019). Thereafter, opposite sex worms were added, the culture medium replaced by fresh ABC169, the worms kept for another 21 d in culture. During this time media change occurred every 2 d. All experiments were repeated three to four times (n = 3-4).

For *Smtdc-1* and *Smddc-1*, re-pairing experiments were done with bM and bF or pairing-unexperienced females (sF), respectively. Depending on the experiment, I separated bM from their female partners at the day of perfusion and kept them in culture with sF, or bF (because of the limitation in sF recovery, females were separated from their male partners at the day of perfusion, followed by a 7-14 days separation period for dedifferentiation to obtain a sF-like

status) for 21 d. The worms were incubated with 4 µg/mL dsRNA of each gene at d0 to d21. During this period, the medium was changed every 2 d. The experiments were performed in triplicate (n=3).

2.2.8. Confocal laser scanning microscopy (CLSM)

For morphological analyses by CLSM, worms were fixed in AFA (95% EtOH, 3% formaldehyde, and 2% glacial acetic acid) for at least 24 h at 4°C. After staining with Certistain carmine red for 30 min, as previously described (Neves et al., 2005; Beckmann and Grevelding, 2010), worms were de-stained in acidic 70% EtOH and dehydrated progressively in 90% and 100% EtOH. Worms were mounted on glass slides with Canada balsam. For EdU labelling and detection of proliferating cells, the Click-iT Plus EdU Alexa Fluor 488 Imaging Kit (Thermo Fisher Scientific) was used. After 24 h of incubation with EdU, couples were separated, fixed, and stained as described before (Hahnel et al., 2014). Worms were counter-stained with Hoechst 33342 in a final concentration of 8 µM. Stained worms were examined on an inverse CLSM (Leica TSC SP5; Leica, Germany). Hoechst was excited with a 405 nm laser, and Alexafluor488 with an argon-ion laser at 488 nm. A TSC SP5 inverse confocal laser scanning microscope (Leica, Germany) was used for imaging. Carmine red was excited using an argon laser excitation of 20% at 488 nm and a 470 nm long pass filter for detection. The background and thickness of optical sections were defined by setting the pinhole size to airy unit 1. For FISH, samples were imaged on an inverse CLSM, Cy3 and Cy5 were excited with 561 nm and 633 nm, respectively.

2.2.9. *In silico* analyses

The sequences of Smp_084270 (*Sm*GPCR20), Smp_071050 (*Sm*NPP26), and Smp_004710 (*Sm*NPP40) are available on the Uniprot website (https://www.uniprot.org/) under the accession numbers A0A3Q0KIK8, G4V7X3, and G4VD53, or in WormBase ParaSite (https://parasite.wormbase.org; version 9) (Howe et al., 2017). I used interpro (https://www.ebi.ac.uk/interpro) for protein family identification. The MEGA11 software (Tamura et al., 2021) was used to construct phylogenetic trees based on the maximum likelihood method, which was done using the Bootstrap method with 1000 bootstrap replications. As bioinformatic tools to predict TM domains for *Sm*GPCR20, Rhodopsin-like orphan GPCR in *S. japonicum* and *S. haematobium*, I used DeepTMHMM (https://dtu.biolib.com/DeepTMHMM) (Hallgren et al., 2022) and SACS HMMTOP

(https://www.sacs.ucsf.edu/cgi-bin/hmmtop.py) (Tusnády and Simon, 2001). Multiple sequence alignments were performed with Clustal Omega (https://www.ebi.ac.uk/Tools/msa/clustalo/) (Sievers et al., 2011).

For *Sm*NPP26 and *Sm*NPP40, all gene or protein sequences were obtained from Uniprot website or WormBase ParaSite. BLASTp searches were done on the NCBI server (https://www.ncbi.nlm.nih.gov/). NPP sequences were compiled from the literature (McVeigh et al., 2009; Koziol et al., 2016). After collecting all sequences, multiple sequence alignment was done using Clustal Omega. Cleavage-site prediction was investigated at the ProP1.0 server (http://www.cbs.dtu.dk/services/ProP/) (Duckert et al., 2004).

2.2.10. RNA extraction and reverse transcription

2.2.10.1. RNA extraction

For the RNA extraction, 20 male and female worms (either bs or ss) were collected into 1.5 mL tubes and washed three times with 1 mL PBS (1x), respectively. Total RNA was isolated according to the manufacturer's instructions (Monarch® Total RNA Miniprep kit; NEB), and finally eluted with 30-50 µL nuclease-free water. The RNA was stored on ice, when used for downstream analyses, or at -20°C for short-term storage (less than 1 week), or at -80°C for long-term storage.

2.2.10.2. RNA analyses

Quality and quantity of total RNA from schistosome whole worms were checked by electropherogram analysis (Agilent 2100 Bioanalyer; Agilent Technologies, USA) using the Agilent RNA 6000 Nano or Pico kit according to manufacturer's instruction. For this, 1 µL RNA was loaded onto the chip. A good RNA quality is characterized by the presence of two distinct RNA peaks, which correspond to 18S and 28S RNAs (**Figure 2.1**).

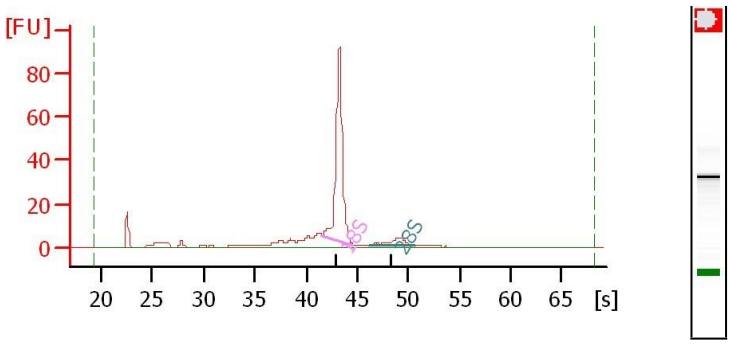

Figure 2.1: Quantity and quality of total RNA isolated from *S. mansoni* samples.

Electropherogram analysis was obtained using BioAnalyzer (Agilent technologies). There is no clear 28S peak because of the existence of a 28S rDNA region that creates an rRNA gap resulting in two smaller 28S rRNA subunits (28S*α* and 28S*β*) (van Keulen et al., 1991).

2.2.10.3. Reverse transcription/cDNA synthesis

For cDNA synthesis, 10-200 ng RNA was used as template and the procedure performed as recommended by the manufacturer (QuantiTect Reverse transcription kit). In this process, genomic DNA (gDNA) was first digested with 2 µL of gDNA wipeout mixture at 42°C for 2 min in a total volume of 14 µL. Next, 5x Quantiscript RT buffer, RT primer mix, and reverse transcriptase was added and a total volume of 20 µL obtained. The reaction mix was incubated at 42°C for 15 min. In a final step, the enzyme was heat-inactivated at 95°C for 3 min. The synthesized cDNA was stored at -20°C. The total volume of cDNA was diluted at 1:5-1:10 in RNase-free water for RT-qPCR or other experiments.

2.2.11. Polymerase chain reaction (PCR)

2.2.11.1. Quantitative real-time PCR

Transcript amounts were quantified by qPCR using the SYBR Green method. This method is based on the intercalation of a fluorescent dye into the dsDNA (Zipper et al., 2004). The fluorescence signal increases exponentially during amplification. A 10-fold dilution series was used, and a standard curve was generated by plotting the Ct-value against the amount of DNA, DNA fragments were amplified from 1:5-1:10 diluted cDNA by reverse transcription (**Chapter 2.2.11.2**). In my study, the efficiencies of amplification for all designed primer pairs for RT-qPCR ranged between 90-110% (Dorak et al., 2006). Only primers that exhibited single peak melt curves were used. The expression of the gene of interest was compared with a reference gene for relative quantification (Pfaffl, 2001). The reference gene *Smletm1* (Smp_310830) is a housekeeping gene and stably expressed in schistosomes kept in culture and independent of sex, mating status, and external or internal stimuli (Haeberlein et al., 2019). Each sample was analyzed for the expression of the gene of interest (GOI) and the reference gene. Fold change of gene expression levels between dsRNA treated worms and controls was calculated by the delta-delta-Ct-method (Livak and Schmittgen, 2001). First, the GOI was normalized to the reference gene *Smletm1* using the equation:

$$\Delta Ct = Ct_{\,target} - Ct_{\,reference}$$

The difference was formed to compare gene expression of a treated and an untreated sample:

$$\Delta\Delta Ct = \Delta Ct_{\,target} - \Delta Ct_{\,control}$$

The fold change was calculated with the formula (Livak and Schmittgen, 2001):

$$\text{Fold change} = 2^{-\Delta\Delta Ct}$$

Gene expression levels of bM, sM, bF, and sF were calculated using the formula: relative expression = $2^{-\Delta Ct} \times f$, with f = 1,000 as an arbitrary factor. First, the GOI was normalized to the reference gene *Smletm1* using the equation:

$$\Delta Ct = Ct_{\,target} - Ct_{\,reference}$$

The fold change was calculated with the formula (Houhou et al., 2019):

$$\text{Relative gene transcript levels} = 2^{-\Delta Ct} \times 1{,}000$$

For qPCRs, the PerfeCTa SYBR Green Super Mix of Quanta was used with the fluorophore included. The reaction mixture consisted of:

20 µL reactions:	**Volume (µL)**	**Ingredients**
	10	Quanta SYBR Green Super Mix (2×)
	1	5’ primer (10 µM)
	1	3’ primer (10 µM)
	8	cDNA template

The master mix was prepared in a PCR chamber, which was UV-irradiated for 20 min. All samples were pipetted as technical triplicates. qPCRs were performed in a Rotor Gene Q (Qiagen) with the program under the following conditions:

Cycle step	**Temp.**	**Time**	**Cycles**
Initial denaturation	95ºC	3 min	1x
Denaturation	95ºC	10 s	45x
Annealing	60ºC	5 s	
Elongation	72ºC	20 s	
Final elongation	60ºC	3 min	1x

2.2.11.2. Standard PCR

Standard PCRs were carried out with FirePol DNA polymerase.

PCRs were performed as follows:

25 µL reactions:	Volume (µL)	Ingredients
	2.5	Reaction-buffer (10×)
	2.5	$MgCl_2$ (25 mM)
	0.5	dNTP mix (10 mM)
	1	5' primer (10 µM)
	1	3' primer (10 µM)
	0.5	FirePol DNA polymerase (5 U/µL)
	10-100 ng	template-DNA
	up to 25	PCR H_2O

DNA fragments were amplified using the following PCR program:

Cycle step	Temp.	Time	Cycles
Initial denaturation	95ºC	3 min	1x
Denaturation	95ºC	30 s	32x
Annealing	60ºC	30 s	
Elongation	72ºC	1 min	
Final elongation	72ºC	5 min	1x

2.2.11.3. Amplification of a fragment of a GOI transcript by PCR

To determine transcript amounts of a GOI, cDNA fragments (500-800 bp) were amplified by specific primers, using AccuPrime™ *Taq* DNA Polymerase high fidelity Kit (Invitrogen, USA), from cDNA.

The following ingredients were used for PCR:

50 µL reactions:	Volume (µL)	Ingredients
	5	10×Buffer I
	0.2	Tag DNA-polymerase
	3	cDNA (Reverse transcription with oligo-dt and 1:5-1:10)

1	Forward primer (10 µM)
1	Reverse primer (10 µM)
39.8	PCR H_2O

cDNA fragment of GOIs were amplified using the following PCR program:

Cycle step	Temp.	Time	Cycles
Initial denaturation	94ºC	3 min	1x
Denaturation	94ºC	30 s	34x
Annealing	58ºC	20 s	
Elongation	68ºC	45 s	
Final elongation	68ºC	5 min	1x

Purification of the PCR products was done from 1% agarose gels, and the obtained PCR products were purified as describe above.

2.2.11.4. Amplification of GOI fragments from pJC53.2

PCRs were also performed to amplify 500-800 bp of GOIs cloned into the plasmid pJC53.2 (Addgene).

The following ingredients were used for PCR:

15 µL reactions:	Volume (µL)	Ingredients
	10	Q5 reaction buffer (5×)
	1	dNTPs (20 mM each)
	6	T7_extended primer (10 µM)
	0.5	Q5 polymerase
	1	Betaine solution (5 M)
	x	pJC53.2 based plasmid
	Up to 50	PCR-H_2O

The PCR was performed using the following PCR program:

Cycle step	Temp.	Time	Cycles
Initial denaturation	98ºC	2 min	1x
Denaturation	98ºC	15 s	

Annealing	64ºC	20 s	
Elongation	72ºC	40 s	34x
Final elongation	72ºC	3 min	1x

The products were confirmed by 1% agarose gel electrophoresis. The purified PCR products (eluted in 15 µL) were used as cDNA templates for *in vitro* transcription to synthesize RNA probes or dsRNA.

2.2.12. Cloning

2.2.12.1. Cloning with pJC53.2

All pJC53.2 constructs were cloned by digesting pJC 53.2 (**Figure 2.2**) with *AdhI*.

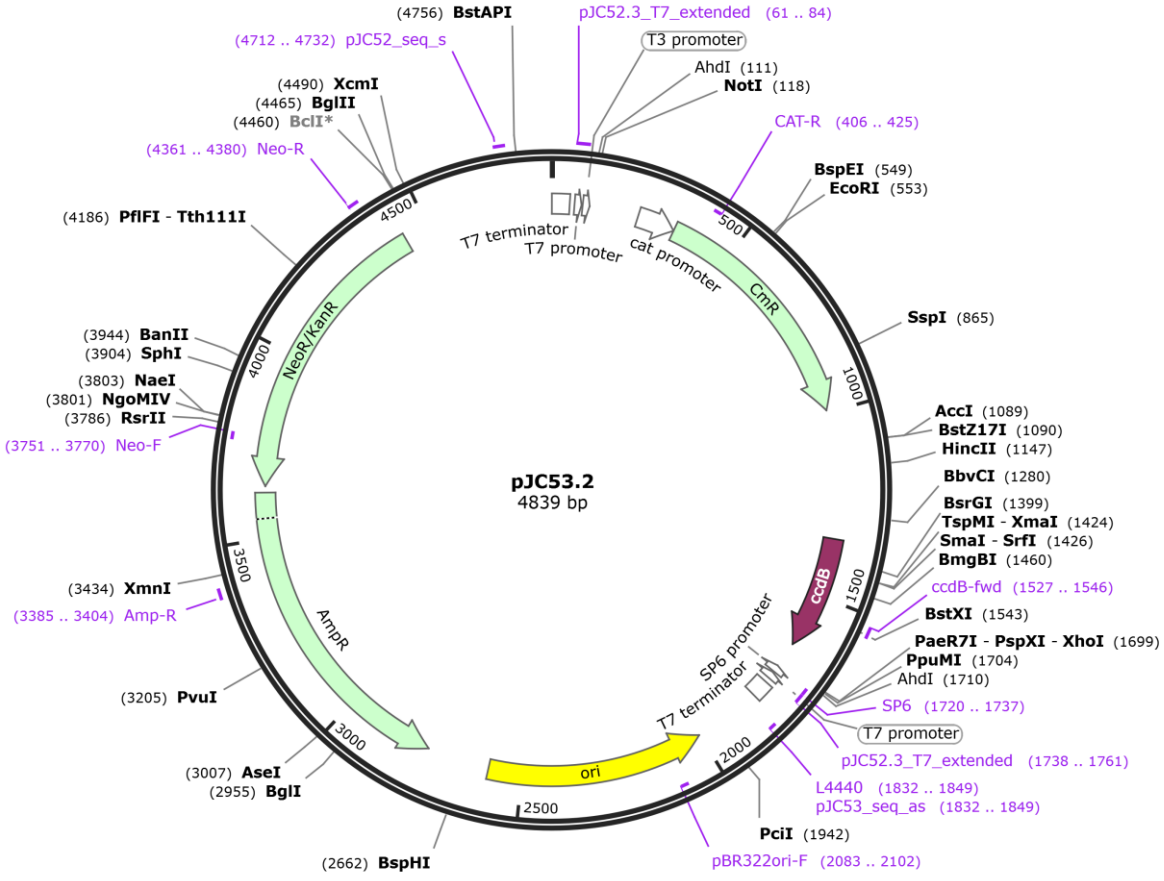

Figure 2.2: pJC53.2 cloning vector.

The following mix was prepared for vector digestion:

30 µL reactions:	**Volume (µL)**	**Ingredients**
	1 µg	vector (depending on vector concentration)

1	*AhdI*
3	Cut-smart buffer (10×)
x	PCR H_2O (depending on vector volume)

The digestion mix was incubated at 37°C for 60 min. Purification of the digestion products was done from 2% agarose gel, and the larger fragment was purified using the Monarch® Gel extraction kit following the manufacturer's protocol.

Subsequently, purified DNA products (**Chapter 2.2.11.3**) were ligated with 50 ng of *AdhI*-digested pJC53.2 using T4 DNA Ligase in a ratio of 3:1. The required amount of insert was calculated with the NEBio Calculator.

$$X\ g\ cDNA\ fragment\ (insert)\ = (insert\ \div vector\ molar\ ratio)\ \times$$
$$mass\ of\ vector\ (g)\ \times (insert \div vector\ lengths\ ratio)$$

The ligation reaction was done as follow:

20 µL reactions:	**Volume (µL)**	**Ingredients**
	2	T4 DNA ligase buffer (10×)
	50 ng	Vector (depending on vector concentration)
	X	cDNA fragment (depending on DNA concentration)
	2	T4 DNA ligase
	up to 20	Nuclease-free water

The ligation mixture was incubated overnight at 4°C.

Escherichia coli cells of strain 10β were used for transformation experiments. The transformation was performed using the heat shock method. The *E. coli* cells were stored at -80°C and thawed on ice. 2-10 µL of the ligation mixture was added to 100 µL aliquots of 10β cells and incubated on ice for 30 min. The heat shock was applied for 2 min at 42°C followed by incubation on ice for 5 min. 1 mL of LB (Luria broth) medium was added, and the cells were incubated for 1 h at 37°C and 300 rpm in a thermoblock (Eppendorf, Thermomixer comfort). The bacteria were centrifuged at 9,000 rpm for 1 min at room temperature (RT). The resulting pellet contained the transformed cells. The supernatant was discarded, and the pellet was resuspended in residual liquid. The remaining 50-100 µL of cell culture were plated on an LB agar plate containing 100 µg/mL ampicillin and were incubated overnight at 37°C.

For the multiplication of a bacterial clone, 5 mL of LB-medium was incubated with a single clone grown in LB liquid medium. Ampicillin [100 µg/mL] was added to the LB-medium to ensure the growth of only successfully transformed *E. coli* cells, which were incubated overnight at 37°C at 200 rpm. An amount of 3 mL of this culture were used for plasmid-DNA isolation. The Monarch® Plasmid Miniprep kit was used following the manufacturer's instructions. The cloned sequences were first checked digestion using the restriction enzyme *Bam*HI-HF.

The digestion using the restriction enzyme *Bam*HI-HF was done as follow:

15 µL reactions:	**Volume (µL)**	**Ingredients**
	1	Plasmid
	1.5	Cut-smart buffer (10×)
	0.5	*Bam*HI-HF
	12	PCR H_2O

The mixture was incubated for 15-30 min at 37°C and subsequently loaded on a 1% agarose gel. If cloning was successful, isolated plasmid-DNA was sent to Microsynth AG (Switzerland) for sequencing. Samples were prepared according to the company's directions.

2.2.12.2. Cloning of pGAD and pGBKT7 plasmids

The neuropeptide (NPP) library was generated by Oliver Weth as described previously (Weth et al., 2019). In short, bait plasmid pGAD SP-WBP1_cloning_linker_TMP_Cub_ GAL4 was generated by cutting pGAD WBP1-Cub-GAL4 (Li et al., 2016) with *KpnI* and *MluI* and assembled it with a gBlock® (IDT, Iowa, USA) to destroy *Acc65I* restriction site. The intermediate clone was digested with *NcoI*, and a second gBlock was introduced with the following modifications: (1) WBP1 amino acid (aa) 24-430 was deleted, (2) a flexible linker was introduced 5′ to TMP, and (3) new *Acc65I* and *SmaI* restriction sites were generated to insert NPPs in frame with the WBP1 signal-peptide aa 1-23. Prey plasmids were created by digesting pGBKT7 OST1-NubG with the restriction enzymes *NcoI* and *NotI* and assembly with a gBlock utilizing Gibson Assembly. The resulting vector pGBKT7_SP_OST1_cloning_NubG was modified as described previously. The CDS of the GPCR-coding gene was amplified using Q5® polymerase from cDNA obtained from total RNA preparation of *S. mansoni*. Primers were designed to assemble products into pGBKT7_SP_OST1_cloning_NubG digested with *NcoI* and *SmaI* (Weth et al., 2019).

2.2.13. Yeast two hybrid assays

Saccharomyces. cerevisiae strain Y187 was transformed with the prey plasmid expressing Smp_084270 (*Sm*GPCR20) and mated overnight with the AH109 strain transformed with bait plasmids expressing the NPP fusion proteins by Oliver Weth as described before (Weth et al., 2019). The chemokine CXCL12 and its known receptor CXCR4 were used as positive control (Li et al., 2016). OST1 is a transmembrane protein of *S. cerevisiae* and in combination with CXCL12 was used as the negative control (Li et al., 2016). After incubation, diploid yeasts cells were plated on selective medium lacking -Leu/-Trp to ensure co-expression of bait and prey in the cells, and then on selective medium lacking -Leu/-Trp/-His/-Ade to monitor protein-protein interactions of two mated yeast clones. The plates were incubated at 30°C in an incubator.

2.2.14. *In situ* hybridization

2.2.14.1. RNA probe synthesis, precipitation, and purification

About 300 ng cDNA (**Chapter 2.2.11.4**) was used to perform probe synthesis by *in vitro* transcription according to the following reaction procedure:

20 µL reactions:	**Volume (µL)**	**Ingredients**
	~300 ng	DNA template
	1	T3 or SP6 RNA polymerase
	2	Reaction buffer (10×)
	2	DIG-NTP mix / FITC-NTP mix
	0.6	Murine RNase inhibitor
	Up to 20	DEPC H_2O

The mixture was incubated at 27°C for 16 h. To remove the DNA template, 1 µL of DNaseI was added to the mixture, which was incubated at 37°C for 15 min. Precipitation of the generated probes was done by adding 3 µL of 4 M lithium chloride (LiCl), 50 µL of 96% EtOH and incubation at -80°C for 1 h. Next, the mixture was centrifuged at 16,000 rpm at 4°C for 0,5 - 1h. The supernatant was removed, and the RNA was resolved in 20 µL of DEPC H_2O and stored at -20°C until usage. The concentration of the probes was determined by photometric analysis.

2.2.14.2. Worm preparation and hybridization procedure

Whole mount colorimetric *in situ* hybridization (WISH) and fluorescence *in situ*

hybridization (FISH) were performed as previously described (Collins et al., 2010). Separated males and females were prepared by incubation in 0.6 M $MgCl_2$ for 1 min while shaking, and then fixed for 4 h in 4% formaldehyde dissolved in PBSTx (1X PBS, 0.3% Triton X-100) at RT. Fixed worms were dehydrated in 100% MeOH and stored at -20°C. After rehydration by incubation in 50% MeOH dissolved in PBSTx, the samples were bleached for 1 h in bleaching solution (9 mL DEPC H_2O, 500 µL formamide, 250 µL 20x SSC pH 7, 400 µL 30% H_2O_2) under direct light. After bleaching, the samples were rinsed with PBSTx and treated with proteinase K (20 mg/mL) solution (bM: 45 µg/mL; bF: 25 µg/mL; sF: 7.5 µg/mL dissolved in PBSTx for 45 min, respectively). Post fixation, the samples were incubated in 4% formaldehyde for 15 min, and washed in prehybridization solution in PBSTx (1:1) for 10 min. The parasites were placed in small baskets in a 48 well-plate in 300 µL prehybridization solution for 2 h at 55°C while shaking.

For hybridization, DIG-labelled riboprobes were used for WISH and DIG, and FITC riboprobes were used for FISH. For double-FISH, single-stranded RNA probes for *Smgpcr20* and *Smtdc-1* were labelled with FITC, and probes for *Smnpp26*, *Smnpp40*, and *Smddc-1* were labelled with DIG. The probes were heated in hybridization solution (10-50 ng probe/1 mL hybridization solution) for 5 min at 78°C to dissolve the secondary structures. Subsequently, hybridization was performed at 55°C for overnight (at least 16 h) while shaking. After incubation, a series of washing steps followed using preheated wash solution (2x SSC + 0.1 % TritonX-100, 0.2x SSC + 0.1 % TritonX-100) at 55°C to reduce unspecific binding of RNA probes.

2.2.14.3. Antibody incubation and signal detection

For WISH, an anti-DIG-AP (1:2000) antibody was incubated in colorimetric blocking solution (7.5% heat-inactivated horse serum in TNT) overnight at 4°C and developed with nitro-blue tetrazolium (NBT) and 5-bromo-4-chloro-3'-indolyphosphate (BCIP). Finally, the developing step was stopped with PBS, and the samples were mounted in 80% glycerol and covered by coverslips. Pictures were taken using a Leica microscope (M125 C) and a Leica camera (DMC2900; Leica, Germany). For double-FISH experiments, worms were incubated with anti-FITC-POD (1:1,000) in FISH blocking solution (5% heat-inactivated horse serum and 0.5% Western Blocking Reagent in TNT) overnight at 4°C and washed in TNT. For tyramide signal amplification, worms were developed in TSA Plus working solution (TSA Plus Stock Solution 1:50 in 1X Amplification Diluent) (TSA Plus Cyanine 3) for 15-30 min at RT in the

dark; 300 µL of TSA Plus working solution was required per well. Following development, worms were washed in TNT. Quenched residual peroxidase activity was blocked with 100 mM sodium azide in TNT for 45 min at RT, washed in TNT. Following residual peroxidase inactivation, the worms were washed in TNT, incubated in anti-DIG-POD (1:1,000) in FISH blocking solution overnight at 4°C. This process was repeated with a different fluorescent-tyramide conjugate (TSA Plus Cyanine 5), the worms washed with TNT, and incubated with 0.1 µg/mL 2'-[4-ethoxyphenyl]-5-[4-methyl-1-piperazinyl]-2,5'-bi-1H-benzimidazole trihydrochloride trihydrate (Hoechst 33342) overnight at 4°C. Samples were mounted in Mount FlourCare for further analysis.

2.2.15. Synthesis of dsRNA

dsRNA was synthesized as described previously (Collins et al., 2010). Briefly, 500-800 bp of GOI was amplified by PCR from recombinant pJC 53.2 plasmids (**Chapter 2.2.11.4**).

dsRNA was synthesized by *in vitro* transcription with T7 RNA polymerases as follows:

15 µL reactions:	**Volume (µL)**	**Ingredients**
	5	PCR product
	10	Reaction buffer (10 ×)
	20	rNTPs (25 mM)
	5	T7 RNA polymerase (self-made)
	1	Pyrophosphatase, Inorganic (IPP)
	x	pJC53.2 based plasmid
	Up to 100	DEPC H_2O

The reaction was incubated for 4 h or overnight at 37°C. To remove any residual DNA, 5 µL of RNase-free DNase I (2 U/µL) was added, and the mix incubated for 30 min at 37°C. Precipitation was performed with 100 µL LiCl (7.5 M) at -20°C for 30 min. The samples were centrifuged at full speed for 30 min at 4°C, the pellet was washed with pre-cooled 70% EtOH and centrifuged again for 2-5 min at 4°C at full speed. Lastly, the pellet was air-dried and resuspended in DEPC H_2O. After *in vitro* transcription, the quantity of dsRNA was measured by spectrophotometer, and the quality was checked on 1.5% agarose gels. dsRNA was stored at -20°C until further use.

2.2.16. Statistical analysis

Statistically significant differences of the obtained data were performed using GraphPad Prism 7 or 9. A two-way ANOVA with Tukey's test for multiple comparisons (Midway et al., 2020) was used for monitoring egg production of the different groups. One-way ANOVA with Tukey's test for multiple comparisons was used for RT-qPCRs analyses. T-test was used for other experiments, unless otherwise states. Statistically significant indicated as: *P<0.05, **P<0.01, ***P < 0.001, and ****P < 0.0001. Error bars are representative of the mean ± SEM of at least three biological replicates.

3. Results

This work is divided in two parts. In the first part (3.1), I focus on the identification of *Sm*GPCR20-*Sm*NPPs interactions and characterization of *Smgpcr20-Smnpps* interactions including functional analyses. In the second part (3.2), I will describe the functional analyses of two decarboxylases, *Smtdc-1* and *Smddc-1*, and unravel their roles and the putative involvement of BAs and neuronal activities in the male-female interaction of *S. mansoni*.

3.1. Rhodopsin orphan GPCR (*Sm*GPCR20) interacts with the neuropeptides and mediates reproductive processes in *Schistosoma mansoni*

3.1.1. Sequence analyses of Smp_084270

To address on the role of GPCRs in *S. mansoni*, a first step of this work was the verification of the GPCR genes. Based on the available RNA-seq transcriptomic data of *S. mansoni* obtained in our group before (Lu et al., 2016; Lu et al., 2017; Hahnel et al., 2018), I investigated one putative Rhodopsin orphan GPCR gene (Smp_084270, *Sm*GPCR20) in more detail, which showed a sex- and pairing-influenced transcript pattern in *S. mansoni*. Gene and protein sequences of *Sm*GPCR20 were obtained from WormBase ParaSite and Uniprot (WormBase ParaSite: Smp_084270; Uniprot: A0A3Q0KIK8) (Howe et al., 2017). *In silico* analyses using DeepTMHMM and SACS HMMTOP showed the presence of 7-transmembrane (7-TM) domains in *Sm*GPCR20 (**Figure 3.1**), thus confirming *Sm*GPCR20 as a GPCR family member. Further analysis using the interpro website indicated that *Sm*GPCR20 belongs to the rhodopsin-like, 7TM (Accession: IPR017452) GPCR family. Proteins containing GPCR_Rhodpsn_7TM domains of multiple species were identified on the interpro website (**Supplementary Figure 1**). To identify orthologues and the closest "relatives" of *Sm*GPCR20, I performed a phylogenetic analysis using MEGA11. This analysis showed the existence of *Sm*GPCR20 orthologues in *S. japonicum*, *S. haematobium*, *Trichobilharzia regent*, *Clonorchis sinensis*, *Fasciola gigantica*, *Schmidtea mediterranea*, *Echinococcus granulosus*, *Taenia asiatica*, and *Protopolystoma xenopodis*. Two branches of this tree have unacceptably low support in terms of bootstrap replicates, thus including more sequences could improve this phylogenetic analysis. They form a GPCR20 helminth clade, which diverges from the nematode *Caenorhabditis elegans* and further invertebrates and vertebrates (**Figure 3.2**). The multiple sequence alignment using Clustal Omega showed highest identity of *Sm*GPCR20 (orange) to orthologues from *S. haematobium* (A0A095C4R8) (90.71% identity, pink) and *S. japonicum*

(A0A4Z2CQX1) (76.44% identity, blue). Furthermore, these sequences shared also highest homology of the predicted 7-TM domains (**Figure 3.3**).

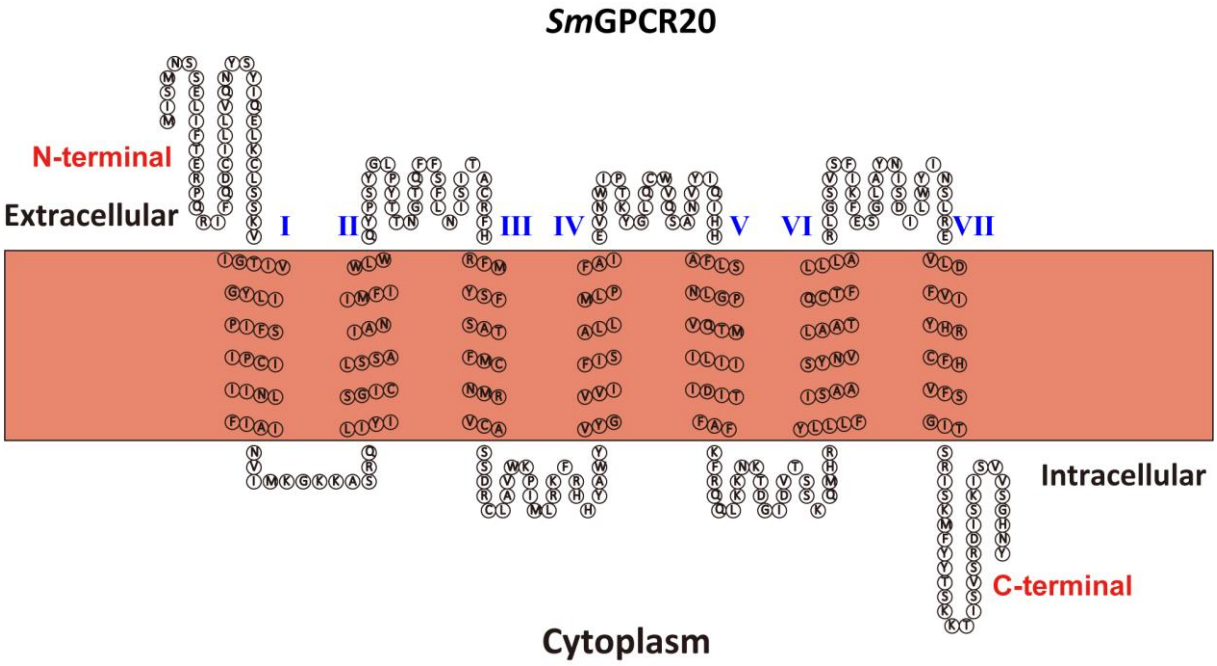

Figure 3.1: The transmembrane domain composition of *Sm*GPCR20 as predicted by DeepTMHMM and SACS HMMTOP.

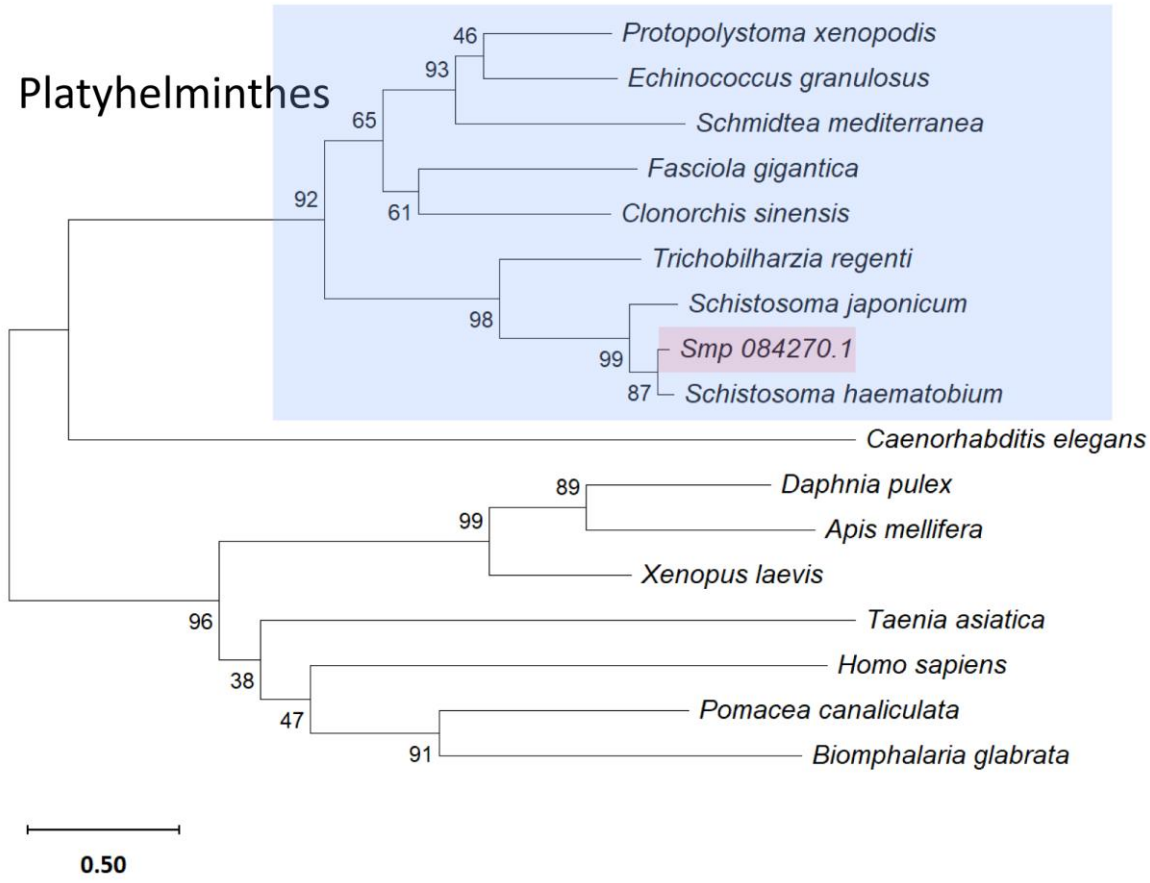

Figure 3.2: Phylogram of *Sm*GPCR20.

The following sequence IDs consist of the species and Uniprot entry names. Schistosomes (*Schistosoma japonicum* (A0A4Z2CQX1), *S. mansoni* (Smp_084270 (A0A3Q0KIK8)), *S. haematobium* (A0A095C4R8), and *Trichobilharzia regenti* (A0A183WMW7)); other trematodes (*Clonorchis sinensis* (H2KRY6) and *Fasciola gigantica* (A0A504Z2P0)); cestoda (*Echinococcus granulosus* (U6J3B5) and *Taenia asiatica* (A0A0R3W0W9)); monogenea (*Protopolystoma xenopodis* (A0A3S5CMM6)); turbellaria (*Schmidtea mediterranea* (A0A193KU74)); nematodes (*Caenorhabditis elegans* (G5EDR2)); molluscs (*Pomacea canaliculate* (A0A2T7PVN7) and *Biomphalaria glabrata* (A0A2C9LEA4)); arthropods (*Apis mellifera* (Q9NG02) and *Daphnia pulex* (E9G3B6)); amphibians (*Xenopus laevis* (B7ZRQ1)); mammals (*Homo sapiens* (Q14439)). Platyhelminthes are highlighted in light blue.

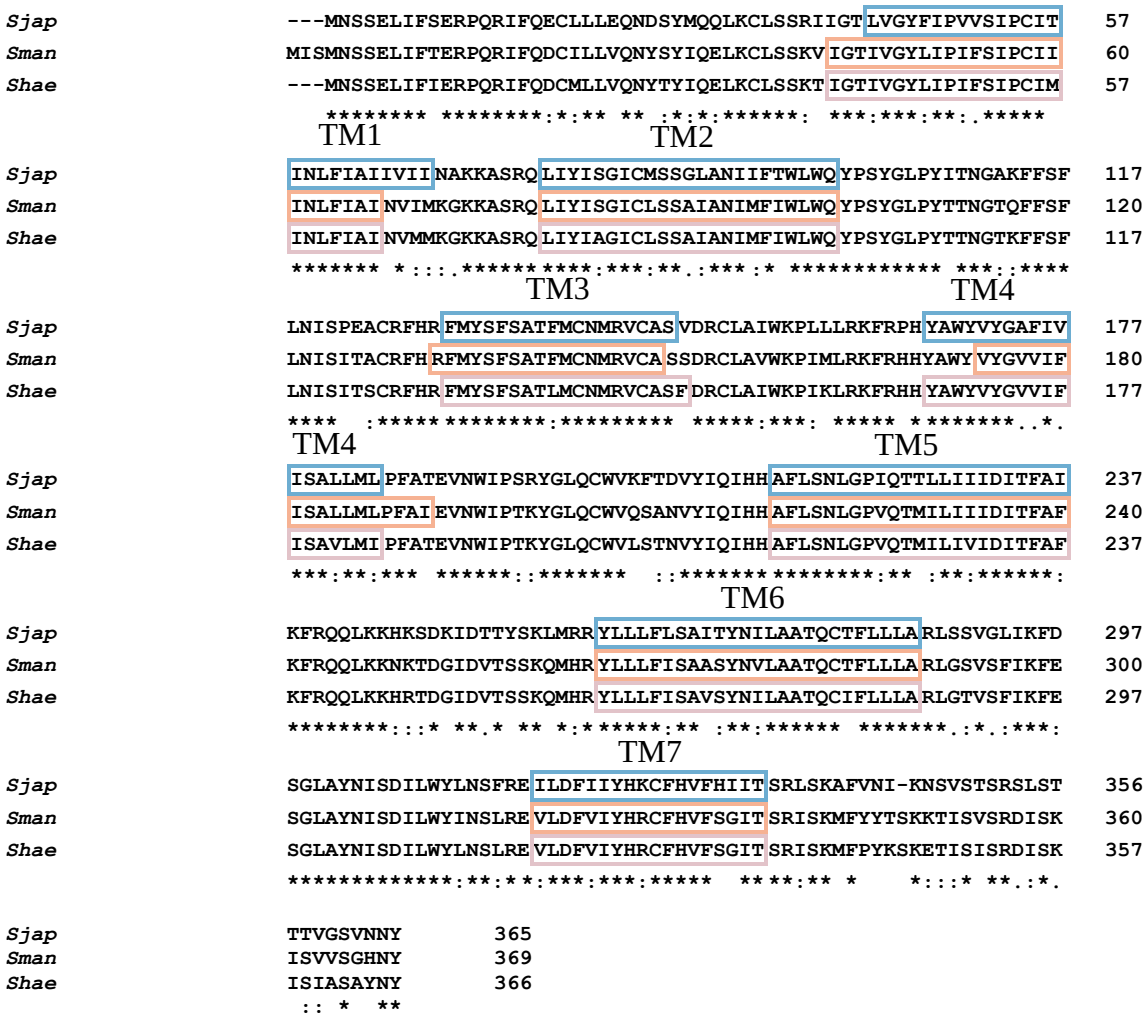

Figure 3.3: Multiple sequence alignment of *Sm*GPCR20 with the Rhodopsin-like orphan GPCR orthologues of other schistosome species.

Multiple protein alignment of *Sm*GPCR20 and its orthologues of *Schistosoma. haematobium* and *S. japonicum*. Highlighted are the 7-TM sequence motifs (TM1-TM7) (colored in blue, orange, and pink, respectively); * indicates sequence identity; : indicates strong sequence similarity; . indicates weak sequence similarity. *Sjap*, *S. japonicum* (A0A4Z2CQX1); *Shae*, *S. haematobium* (A0A095C4R8); *Sman*, *S. mansoni* (Smp_084270 (A0A3Q0KIK8)).

3.1.2. Identification of *Sm*GPCR20-*Sm*NPPs interactions in *S. mansoni*

In a first approach to deorphanize *Sm*GPCR20, the MALAR-Y2H system was employed that was previously shown to be suitable for ligand identification of GPCRs of *S. mansoni* (Weth et al., 2019). To this end, *Sm*GPCR20 was cloned as a fusion protein with the N-terminal part of ubiquitin, and the resulting construct was transformed into yeast strain Y187. As potential ligands, 47 NPP genes were each fused via a flexible linker to the WBP1 transmembrane domain of a yeast receptor for membrane integration (with the neuropeptide as

extracellular part). At the intracellular part of this fusion construct, the C-terminal part of the split ubiquitin system was cloned. These constructs were (individually) transformed into yeast strain AH109 and used SD-Leu/-Trp to select mated clones co-expressing bait and prey constructs. Using SD-Leu/-Trp/-His/-Ade plates, I further selected for interaction of the *Sm*GPCR20 receptor and presumptive ligands (Weth et al., 2019). Of 47 NPP candidates of *S. mansoni* (*Sm*_NPPs), only two allowed growths under selection conditions in diploid yeasts co-expressing *Sm*GPCR20. These two neuropeptides were *Sm*NPP26 (Smp_071050) and *Sm*NPP40 (Smp_004710) (**Figure 3.4**). Only weak or no growth was monitored for all other 45 NPPs (exemplified by *Sm*NPP16). As expected, the positive control (CXCR4/CXCL12) showed growth comparable to *Sm*GPCR20/*Sm*NPP26 or *Sm*GPCR20/*Sm*NPP40. In contrast, no growth was observed on the selective medium with the negative control (OST1/CXCL12). This suggested specific interactions between *Sm*GPCR20/*Sm*NPP26 and *Sm*GPCR20/*Sm*NPP40.

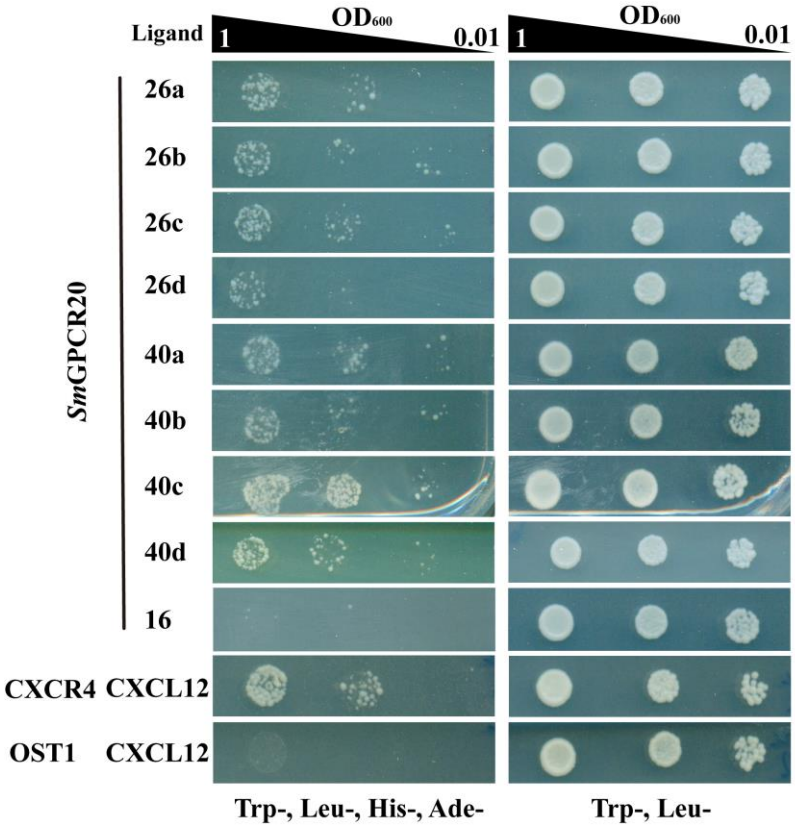

Figure 3.4: The MALAR-Y2H system identified interaction between *Sm*GPCR20 and two neuropeptides.

Shown are results of cell growth assays of yeast strain AH109 transfected with plasmids expressing the Sm_NPP fusion proteins. These cells were mated with yeast strain Y187, which had been transfected

with a plasmid expressing a SmGPCR20 fusion construct. The Trp-, Leu- control (right panel) indicated the successful transformation of yeast cells with all used plasmids. Trp-, Leu-, His-, and Ade- (left panel) showed growth under selection conditions for protein interaction, in this case with the candidate neuropeptides L26 and L40 (a, b, c, d indicate different fragments of SmNPP26 and SmNPP40). The classic chemokine CXCL12 and its known receptor CXCR4 were employed as positive control. OST1 is a transmembrane protein of S. cerevisiae and in combination with CXCL12 used as the negative control (Li et al., 2016).

3.1.3. Identification of *Sm*NPP26 and *Sm*NPP40 orthologues

Based on the available protein sequences of *Sm*NPP26 and *Sm*NPP40, I performed Blastp searches on NCBI with flatworm NPP sequences obtained from the literature (McVeigh et al., 2009; Koziol et al., 2016). Using the identified amino acid sequences of *Sm*NPP26 orthologues of flatworms, I employed multiple sequence alignment using Clustal Omega, and cleavage site prediction using the ProP1.0 server (http://www.cbs.dtu.dk/services/ProP/) (Duckert et al., 2004). As shown, N-terminal secretory signal peptides were identified (highlighted in yellow, italics, and underlined). Furthermore, potential peptides (amino acids colored in green and underlined) of *Sm*NPP26 (**Figure 3.5**) and *Sm*NPP40 (**Figure 3.6**) were predicted based on the presence of putative prohormone convertase (PPC) sites (K, R, KR, KK or RR, highlighted in red). The prediction indicated that both genes could code for multiple distinct peptides.

Smp_071050.1_*npp-26*

MKIYKFDNKMIIEQLFYCLLVFITFSSIVNAIPVHELNYVNHKTNDPIFG***RR***YEGRYPTDGNSRFIESEYSNFYP
MAF***KR***TLFNPILF***KR***NFDPILF***KR***SYFDPIIY***KR***SYFDPILF***KR***NEDRQFE***KR***EHFDPIIY

```
Smed                -MQFRF-----SKMTHV-TLLITVGLFH-----------------VISGYPQTYE-----          31
EgrG                ----------MRAM--LAVLLCALSFFGCVSM--AH--------------PLSDEES---          29
Csin                ---------MMQKNAARICTLCLVLLYLVEASQNMEEKSMDEQHEMFSAYPLSPHESPDI          51
Sjap                MKTYKL---NEKKMFIEQCFYLLLGLLIFSSTVNA--VTVREPN-------YENHGILGN          48
Sman                MKIYKFD----NKMIIEQLFYCLLVFITFSSIVNA--IPVHELN-------YVNHKTNDP          47
Shae                MKIYKFDHNNNNKMIIEQLFYCLLVLMAFSSIINA--IPVHELN-------YVNHKSNDH          51
                                      : :                      .

Smed                -LNQSDRGYYPILFDKRFDPIQFGKRFDPIQFGK--RFDPIQFGK--RFDPIQFGKR-FD          85
EgrG                ------------------LE-LFKRYFDPIRFAMG----PIR-------------------          48
Csin                LRQVSEDEHELMD-----SD-KRASHFDPIMFKRLSHFDPIMFKRRAHFDPIMFKRR---          102
Sjap                RLGKHFERQYFVESDY---P-DKRSYFDPIAFKRT-YFDPIAFKR--NFDRILFKRN---          98
Sman                IFGRRYEGRYPTDGNSRFIE-SEYSNFYPMAFKRT-LFNPILFKR--NFDPILFKRSYFD          103
Shae                MIGKQYDERYPTDGNTRFVE-SDYSNFYPMAFKRT-LFNPILMKR--NFDPIVFKRSYFD          107
                                        * *: *       **

Smed                PIQFG-KRFDPIQFGK--RFDPIQFGKRFDPIQFGKKFDPIQFGK--RFDPIMFGR--   136
EgrG                ------------------------TKED-------LDKREAVVASKRYFDPILFKHAY   75
Csin                ------AHFDPIMFKRRAHFDPIMFKRR-------AHFDPIMFKRRAYFDPIMF----   143
Sjap                --------FDPILFKR-SYFDPIAFKRN-------AD---HQFDKREYFDPIIY----   133
Sman                PI----------IYKR-SYFDPILFKRN-------ED---RQFEKREHFDPIIY----   136
Shae                PIIYKRSYFDPIIYKR-SYFDPILFKRN-------EN---RQLEKREYFDPIIY----   150
                                      .         .     .     ****::
```

Figure 3.5: Multiple sequence alignment of Smp_071050 (*Sm*NPP26) identified orthologues in other flatworms.

Shown are prohormone gene sequences with signal peptides highlighted in yellow, italics, and underlined. Identical aa residues are highlighted in black, and similar ones in light grey. The predicted propeptides of *Sm*NPP26 could be processed *in silico* into segments due to the occurrence of potential prohormone convertase (PPC) sites (K, R, KR, KK, or RR; highlighted in red). Putative mature neuropeptides are given in bold, underlined and green. *Smed*, *Schmidtea mediterranea* (*Smed-secreted peptide prohormone-15*); *Sjap*, *Schistosoma japonicum* (EWB00_010141); *Shae*, *S. haematobium* (SHAE1_39540); *Csin*, *Clonorchis sinensis* (Csin106202); *EgrG*, *Echinococcus granulosus* (EgrG_000239700.1). *indicate sequence identity, : indicates strong sequence similarity; . indicates weak sequence similarity.

Figure 3.6: Multiple sequence alignment of Smp_004710 (*Sm*NPP40) identified orthologues in other flatworms.

Shown are prohormone gene sequences with signal peptides highlighted in yellow, italics, and underlined. Identical aa residues are highlighted in black, and similar ones in light grey. The predicted propeptides of *Sm*NPP40 could be processed *in silico* into segments due to the occurrence of potential prohormone convertase (PPC) sites (K, R, KR, KK, or RR; highlighted in red); these sites were highlighted in red; Putative mature neuropeptides are in bold, underlined and in green. *Sjap*, *S. japonicum* (EWB00_006876); *Shae*, *S. haematobium* (Shae_MS3_00006162); *EgrG*, *E. granulosus* (EgrG_002016900); *Oviv*, *Opisthorchis viverrini* (T265_10151). *indicate sequence identity, : indicates strong sequence similarity; . indicates weak sequence similarity.

3.1.4. Expression patterns of *Smgpcr20*, *Smnpp26*, and *Smnpp40* in different sexes of *S. mansoni*

To unravel the gene transcript patterns of *Smgpcr20*, *Smnpp26*, and *Smnpp40* in different sexes of *S. mansoni*, total RNA was isolated from bF (paired (bisex) females), sF (unpaired (single-sex) females), bM (paired (bisex) males), and sM (unpaired (single-sex) males) worms, and cDNA synthesis was done as described above. To this end, the cDNA was diluted in 1:7-1:10 in RNase-free water for subsequent RT-qPCR analyses. The results showed *Smgpcr20* expression in a sex- and pairing-dependent pattern. Slightly higher transcript levels were found in sM compared with bM, and similarly low levels occurred in sF and bF (**Figure 3.7 left**). However, no statistically significant differences were observed. The results corresponded to previous RNA-seq results of gene expression profiles of paired and unpaired female and male *S. mansoni* (Lu et al., 2016) (**Figure 3.7 right**). With respect to males, *Smnpp26* and *Smnpp40* showed comparable expression to *Smgpcr20*, I obtained similar sM > bM transcript profiles (**Figure 3.7 left**). A comparable tendency (sF > bF) was also detected for females (**Figure 3.7 left**). This finding was similar to previous RNA-seq results (**Figure 3.7 right**), but the transcript profiles of *Smnpp26* and *Smnpp40* differed in male worms, especially, *Smnpp26* showed a statistically significant higher expression in sM compared to bM.

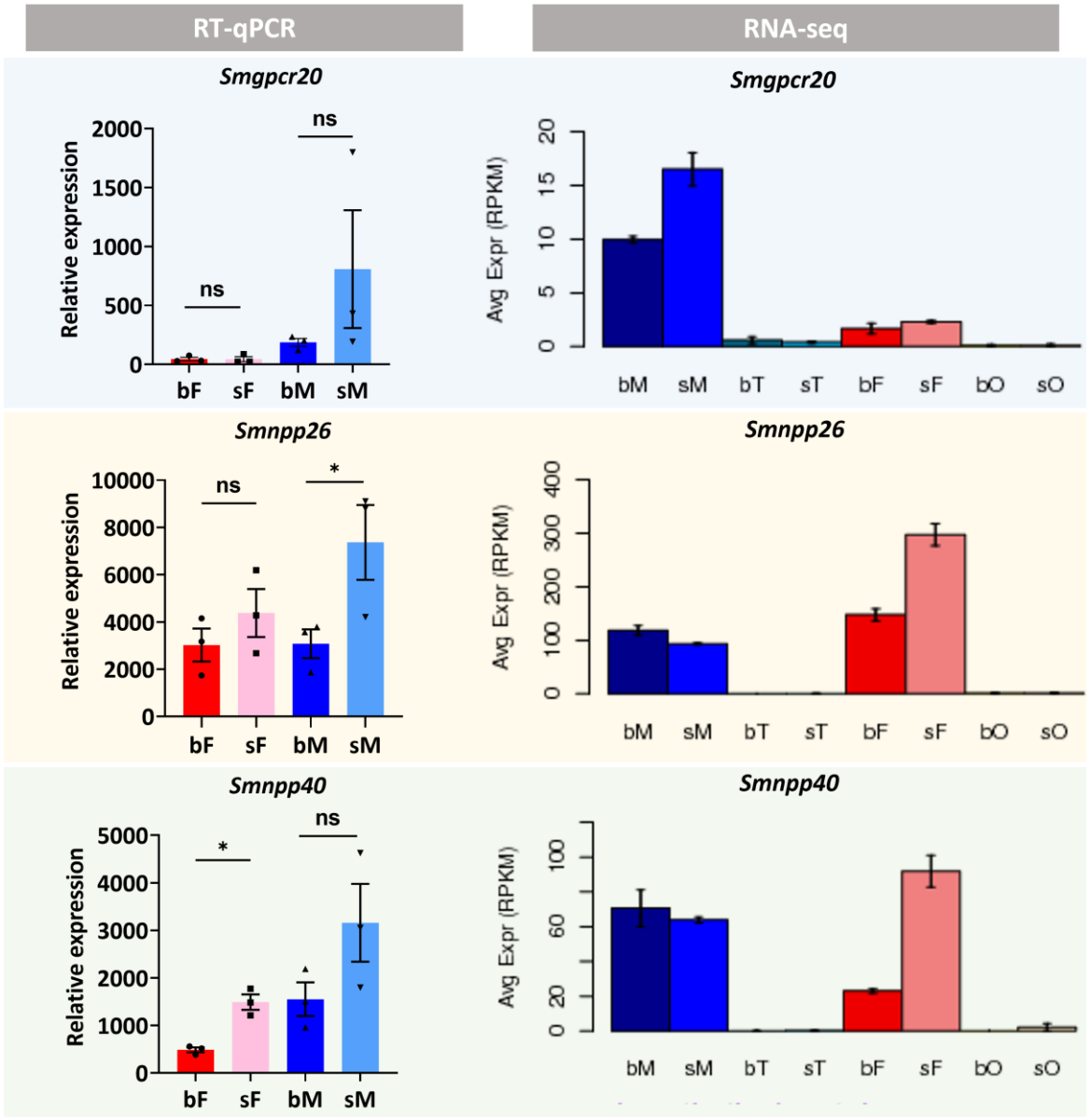

Figure 3.7: Expression patterns of *Smgpcr20*, *Smnpp26*, and *Smnpp40* in different sexes of *S. mansoni* using RT-qPCR (left) and RNA-seq data (right).

The relative expression levels of *Smgpcr20*, *Smnpp26*, and *Smnpp40* were quantified by normalization against reference gene *Smletm1* using RT-qPCR. Data represent the mean±SEM of three independent experiments. Significant differences were determined by One-way ANOVA with Tukey's test for multiple comparisons, as indicated: $^{****}P < 0.0001$, $^{***}P < 0.001$, $^{**}P < 0.01$, $^{*}P < 0.05$. bM = paired-males, sM = unpaired-males, bF = paired-females, sF = unpaired-females. RNA-seq data were collected from a previous study (Lu et al., 2016).

3.1.5. Localization of *Smgpcr20, Smnpp26,* and *Smnpp40* transcripts in different sexes of *S. mansoni*

To investigate the transcript localization of *Smgpcr20*, *Smnpp26*, and *Smnpp40* in adult worms, whole-mount *in situ* hybridization (WISH) experiments were performed. Especially for the neuropeptides, higher transcript levels in bM and sF were noted compared with bF, and for *Smnpp26*, signals were distributed along the whole body of bM and sF (**Figure 3.8B**). Moreover, distinct and similar, dot pattern-like signals were detected for all three transcripts (**Figure 3.8A-C**). Their occurrence resembled neuronal expression patterns as shown previously and supported by RNA-seq data (Lu et al., 2016). In bM and sF, these signals occurred along the body (**Figure 3.8A-C**). Remarkable differences were observed comparing sF and bF. In sF, signals were nearly evenly distributed along the whole body, whereas in bF, the signals dominated in the anterior part along the uterus and the ootype, which was especially evident for *Smgpcr20* and *Smnpp40* (**Figure 3.8A, C**). In the vitellarium of bF, no signals of these two genes occurred. In contrast, *Smnpp26* transcript signals were distributed along the whole body of bF, which was similar to sF (**Figure 3.8B**). In the posterior part of bF, it seemed that these signals occurred in the subtegumental region along the vitellarium but not within the vitellarium. As negative controls, sense probes of both genes were used and no signals detected (**Figure 3.8D**, **Supplementary Figure 2**). As positive control for males, a probe detecting transcripts of the tetraspanin gene (*Smtsp-2*) of *S. mansoni* was used (**Figure 3.8E**), which is transcribed in the tegument (Tran et al., 2010; Cogswell et al., 2011). Smp_165360, a presumptive vitellarium marker (*Smmyst4*) (Lu et al., 2016; Möscheid et al., in preparation), was used as a positive control for bF. As expected, Smp_165360 transcripts were detected in the vitellarium (**Figure 3.8F**).

To provide further evidence for potential interactions of *Smgpcr20* with *Smnpp26* and *Smnpp40*, co-localization experiments of *Smgpcr20* with *Smnpp26* and *Smnpp40* were performed by double-FISH in sF. To this end, an antisense RNA probe labelled by FITC was used for *Smgpcr20* FISH, whereas *Smnpp26* and *Smnpp40* antisense RNA probes were labelled by DIG. In the head region and along the body of sF, transcripts of *Smgpcr20/Smnpp26* (**Figure 3.9A**) and *Smgpcr20/Smnpp40* (**Figure 3.9B**) co-localized. As negative controls, sense probes of each gene were used, and no signals detected (**Figure 3.9C**). In addition, co-localization experiments by double-FISH showed *Smgpcr20* and *Smnpp40* transcripts in cells surrounding the ootype (**Figure 3.10C-D**), where no *Smnpp26* signals occurred (**Figure 3.10A-B**).

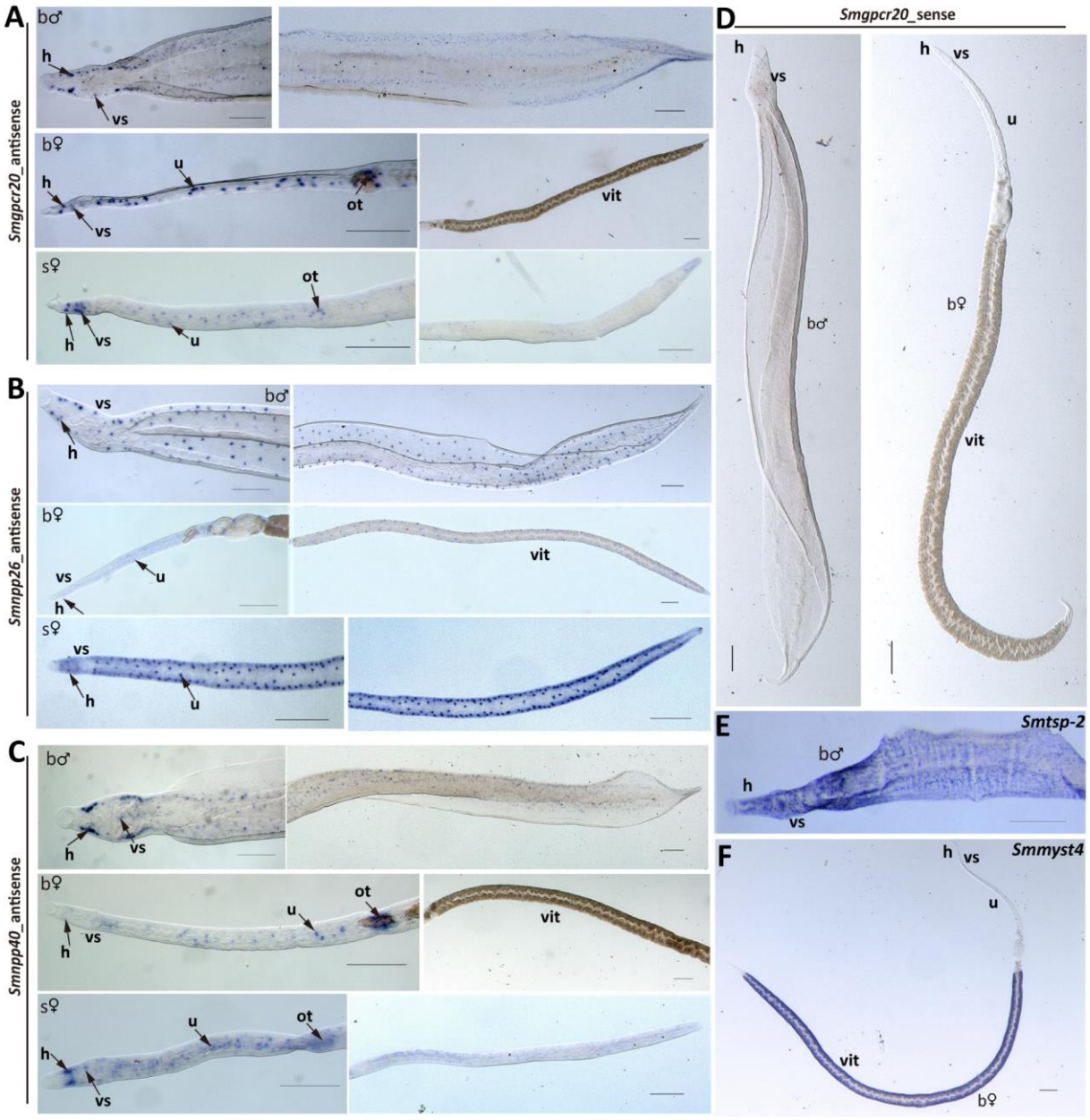

Figure 3.8: WISH of *Smgpcr20*, *Smnpp26*, and *Smnpp40* in different sexes of *S. mansoni* indicated mainly neuronal expression.

Representative results of WISH experiments showing the expression of *Smgpcr20* (**A**), *Smnpp26* (**B**), and *Smnpp40* (**C**) in the body of bM, bF, and sF. The sense probe of *Smgpcr20* served as negative control showed no signals detected (**D**). As positive control, I used a probe detecting *Smtsp-2* (**E**), a tetraspanin gene with known expression pattern along tegumental surface area of *S. mansoni* (Tran et al., 2010; Cogswell et al., 2011). *Smmyst4* (Möscheid et al., in preparation) was used as a positive control for female worms, its transcripts were detected in the vitellarium (**F**). bM = paired-males; bF = paired-females; sF = unpaired-females; vit = vitellarium; ov = ovary; u = uterus; ot = ootype; h = head; vs = ventral sucker. Scale bars: 200 µm.

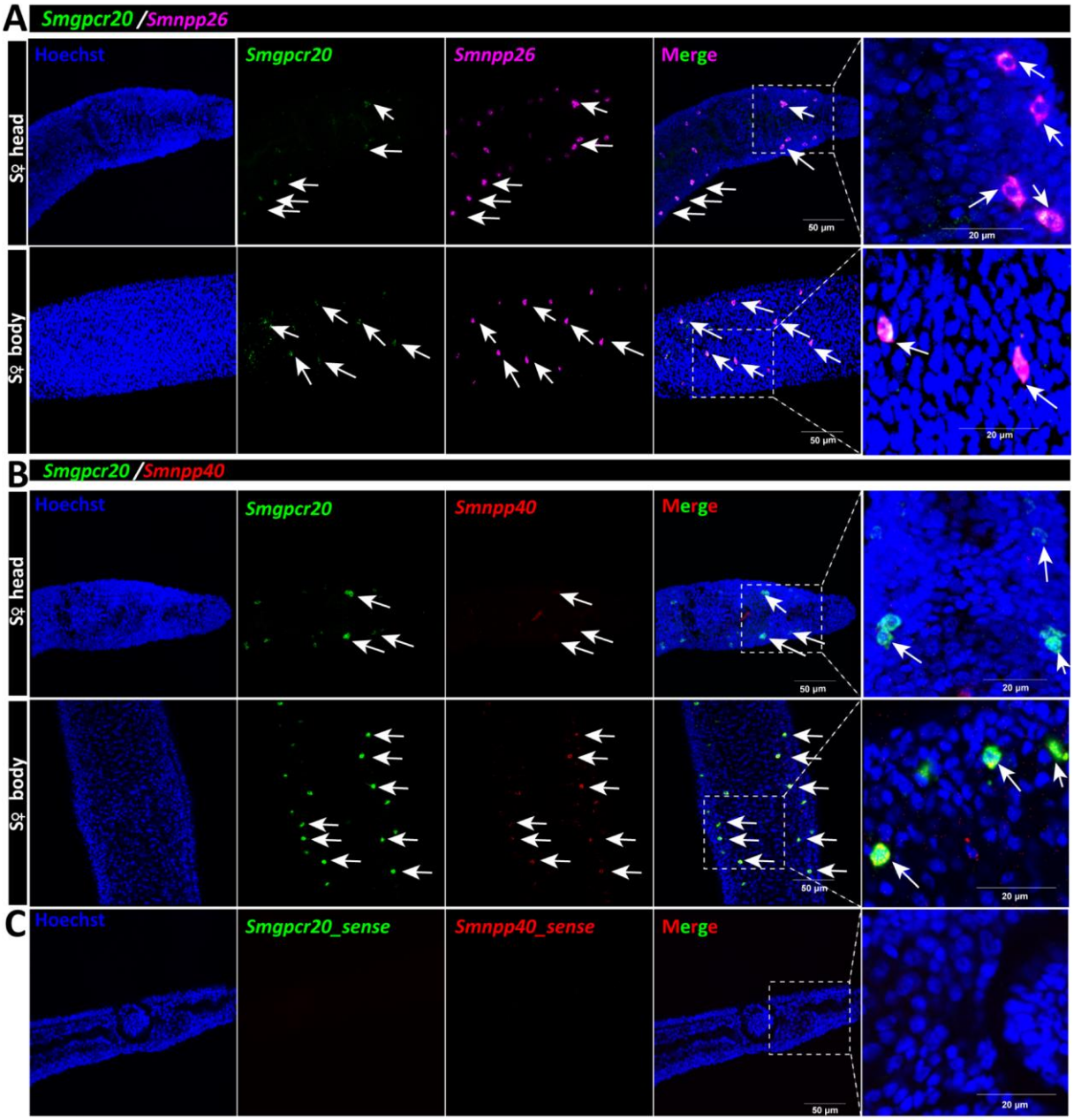

Figure 3.9: Double-FISH showed co-localization of *Smgpcr20*, *Smnpp26*, and *Smnpp40* in *S. mansoni* sF.

(**A**) Results of double-FISH experiments showing *Smgpcr20* and *Smnpp26* transcript co-localization in neuronal cells within the head region and along and body of sF. FITC-labelled *Smgpcr20* transcripts are shown in green, and DIG-labelled *Smnpp26* transcripts are shown in magenta. (**B**) Results of double-FISH experiments showing *Smgpcr20* and *Smnpp40* transcript co-localization in the head and body regions of sF. FITC-labelled *Smgpcr20* transcripts are shown in green, and DIG-labelled *Smnpp40* transcripts are shown in red. The sense probe of each gene served as negative control and showed no signals (**C**). For counter staining, cells were labelled by Hoechst 33342 (blue). Scale bars: 50 µm; right panel: 20 µm.

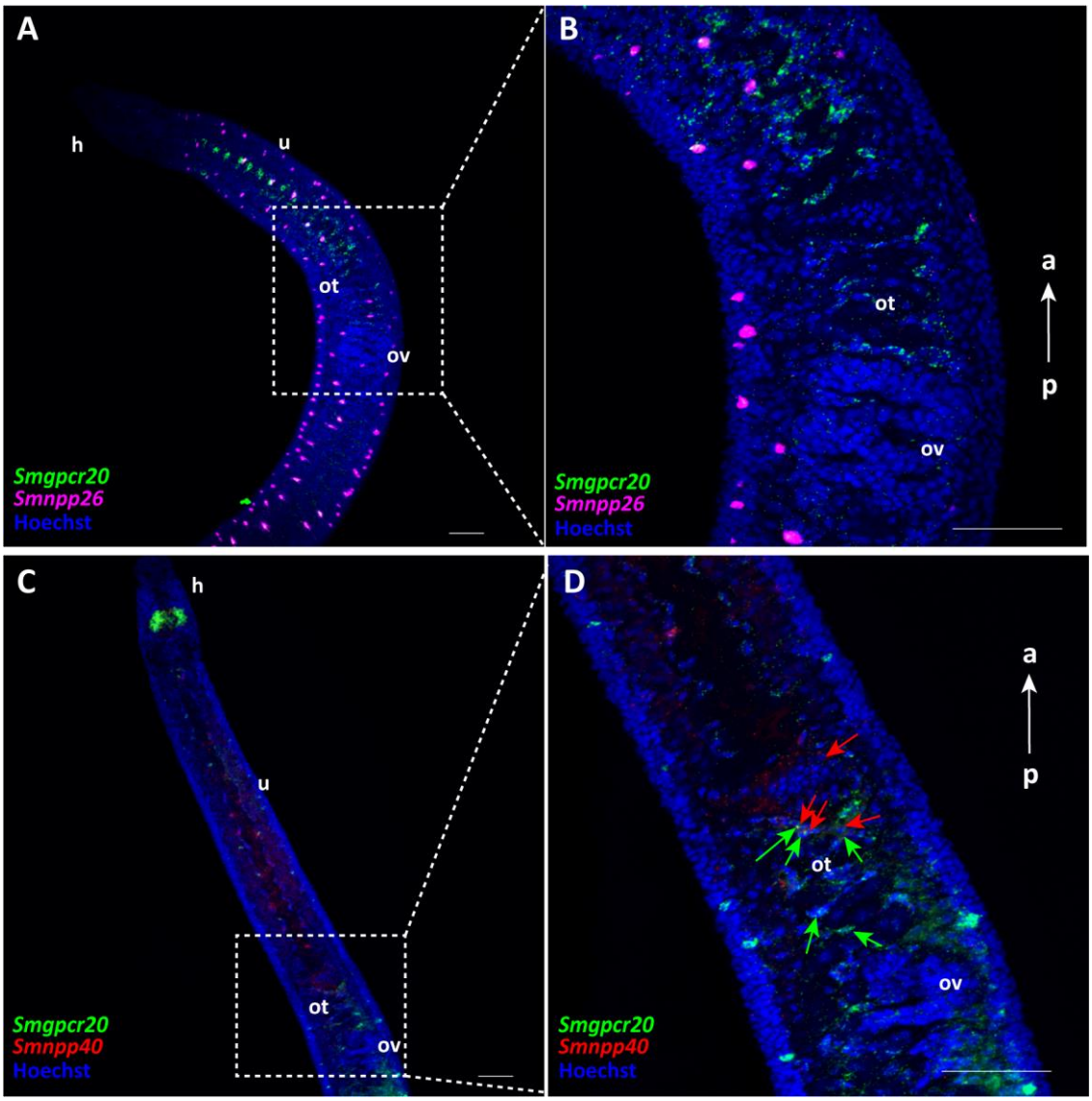

Figure 3.10: Double-FISH analyses revealed co-localization of *Smgpcr20*, *Smnpp26*, and *Smnpp40*. (**A**) Representative images of double-FISH experiments showing *Smgpcr20* and *Smnpp26* transcripts in the anterior part of sF. (**B**) Representative images of double-FISH experiments showing *Smgpcr20* and *Smnpp26* transcripts not co-localizing in cells around the ootype of sF. For counter staining, cells were labelled by Hoechst 33342 (blue). FITC-labelled *Smgpcr20* transcripts are shown in green, and DIG-labelled *Smnpp26* transcripts are shown in magenta. White arrows indicate the direction of sF from posterior (p) to anterior (a). (**C**) Results of double-FISH experiments showing *Smgpcr20* and *Smnpp40* transcripts in the anterior part of sF. (**D**) Results of double-FISH experiments showing *Smgpcr20* and *Smnpp40* transcripts co-localization in the ootype of sF. Cells were labelled by Hoechst 33342 (blue), FITC-labelled *Smgpcr20* transcripts are shown in green, and DIG-labelled *Smnpp40* transcripts are shown in red. White arrows indicate the direction of sF from posterior (p) to anterior (a). ov = ovary; u = uterus; ot = ootype; h = head. Scale bars: 50 µm.

3.1.6. RNAi-mediated KD of *Smgpcr20*, *Smnpp26*, and *Smnpp40* in *S. mansoni*

As a next step, RNAi-mediated knock-down (KD) was performed to functionally characterize *Smgpcr20*, *Smnpp26*, and *Smnpp40*. *S. mansoni* couples were exposed to 30-60 µg/mL specific double stranded-(ds-) RNA (over a period of 15 days with changing of culture medium and dsRNA every 48 h) by the soaking method (Krautz-Peterson et al., 2007) *in vitro* to silence the target genes. Couples without treatment were used as control. In preliminary single-gene RNAi experiments with dsRNA against *Smgpcr20*, or *Smnpp26*, or *Smnpp40*, the KD efficiencies were determined by RT-qPCR following RNAi, which varied in the range of 67-99% depending on the gene (**Figure 3.11A**), single-gene RNAi against either *Smgpcr20*, or *Smnpp26*, or *Smnpp40* showed in no case clear effects on physiological parameters like motility, viability, pairing-stability (**Figure 3.11B**), but a decline of egg production was observed (**Figure 3.11C**).

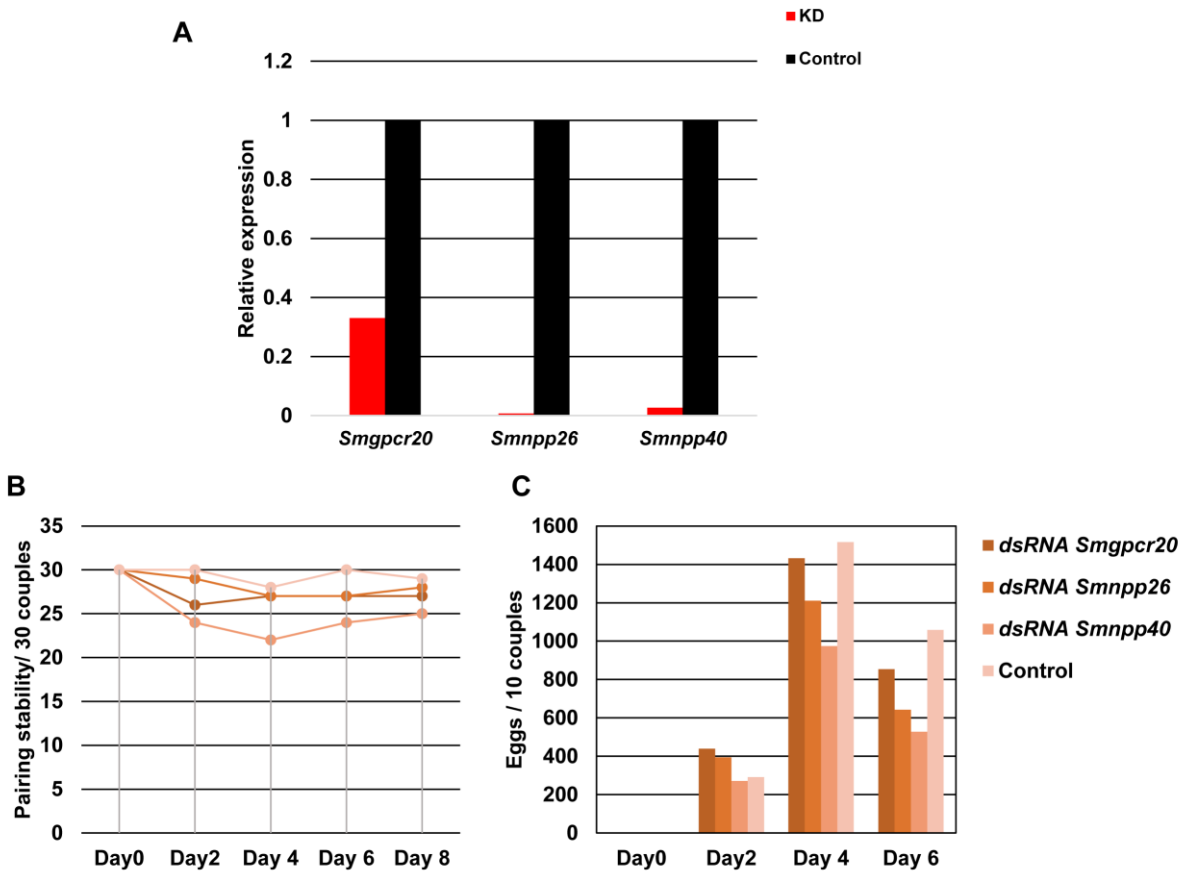

Figure 3.11: RNAi with specific dsRNA against *Smgpcr20*, or *Smnpp26*, or *Smnpp40* caused effects on egg production.

The transcripts levels of *Smgpcr20*, or *Smnpp26*, or *Smnpp40* were quantified after 8 d of *in vitro* culture by RT-qPCR (**A**). The results were normalized compared to the transcript level of the control (untreated

worms). Relative expression levels were calculated with the $2^{-\Delta\Delta Ct}$ method. *Smletm1* was used for normalization and compared to the transcript level of the control. Following KD, the number of couples (**B**) and the total number of eggs of 10 couples laid *in vitro* (**C**) were determined. Untreated worms (no dsRNA addition) were used as controls (n = 1; each n with 30 worms). All worms maintained *in vitro* were kept under the same conditions for 8 d.

To gain more insights into the effect, combinations of dsRNA against *Smgpcr20*/*Smnpp26*, *Smgpcr20*/*Smnpp40*, or a combination of all three gene-specific dsRNAs were tested. The RT-qPCRs showed that the transcript level of *Smgpcr20* in worms treated with dsRNA combinations *Smgpcr20* and *Smnpp26*, *Smgpcr20* and *Smnpp40*, or a combination of all three specific dsRNAs decreased by 72-73%, respectively (**Figure 3.12A**), compared with the untreated control. Similarly, transcript abundance of *Smnpp26* in worms treated with dsRNA combinations of *Smgpcr20* and *Smnpp26* or a combination of all three specific dsRNAs decreased by 94-96%, respectively (**Figure 3.12B**). For *Smnpp40*, dsRNA combination of two or three dsRNAs led to a significant decrease in transcript levels for each gene by 79-87% compared to the control (**Figure 3.12C**). At the physiological level, no clear effects on pairing-stability and motility were observed upon dsRNA treatment (**Figure 3.13**).

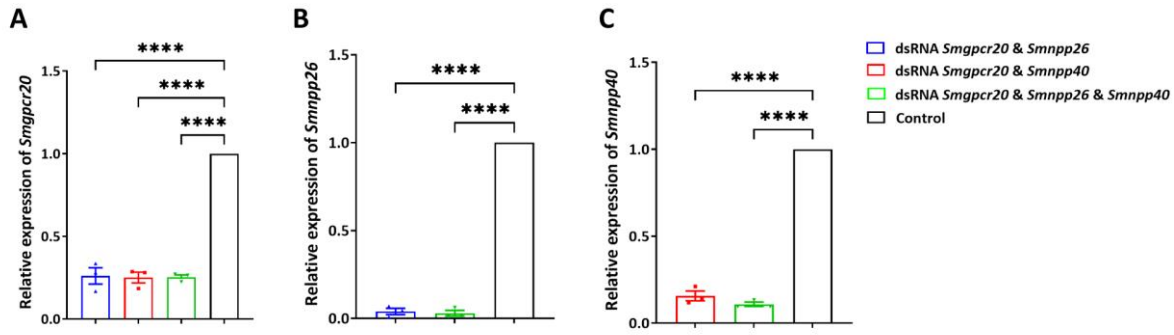

Figure 3.12: RNAi resulted in significantly reduced transcript levels of *Smgpcr20*, *Smnpp26*, and *Smnpp40* in adult *S. mansoni*.

RT-qPCRs showed significant reduction of the transcript levels of *Smgpcr20* (**A**), *Smnpp26* (**B**), and *Smnpp40* (**C**) upon dsRNA treatment. Relative expression levels were calculated with the $2^{-\Delta\Delta Ct}$ method. *Smletm1* was used for normalization. Results of biological triplicates with SEM are shown. Significant differences were determined by One-way ANOVA with Tukey's test for multiple comparisons, as indicated: $^{****}P < 0.0001$.

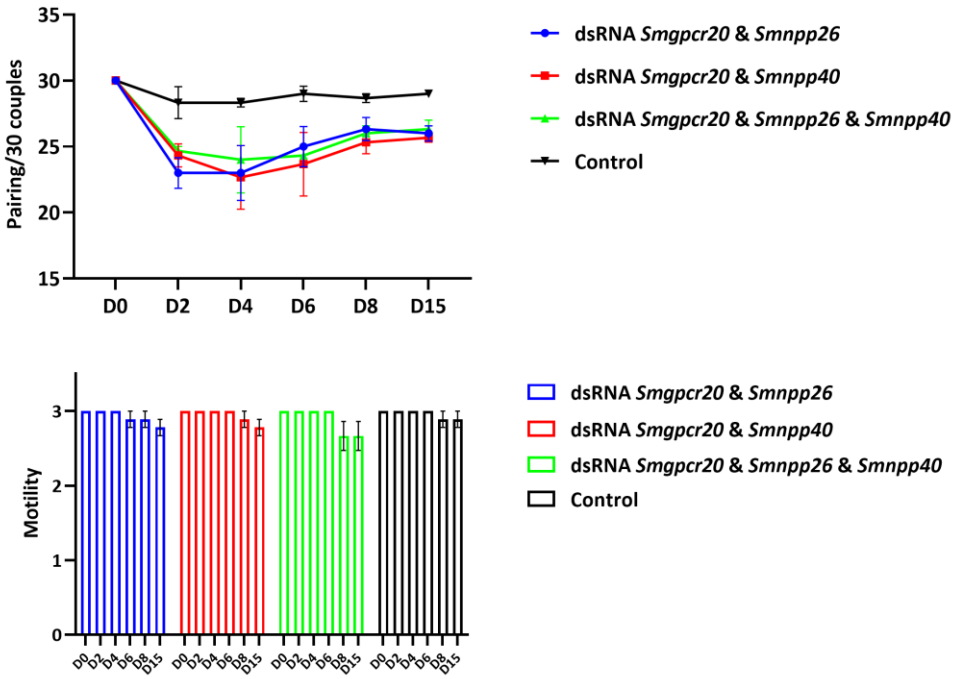

Figure 3.13: RNAi against *Smgpcr20*, *Smnpp26*, and *Smnpp40* had no influence on pairing stability and motility of *S. mansoni* couples.

Shown are the results of pairing stability and motility analyses of *S. mansoni* couples *in vitro* following RNAi with dsRNA combinations of *Smgpcr20* and *Smnpp26*, *Smgpcr20* and *Smnpp40* dsRNA, or a combination of three specific dsRNAs. Untreated worms (no dsRNA addition) were used as controls (n = 3; each n with 30 worms). No statistically significant differences were observed. All worms were kept under the same *in vitro* conditions for 15 d.

Next, egg production was monitored in dsRNA-treated and control *S. mansoni* couples, which was conducted every two days. The obtained results exhibited a decline of egg production after four days upon treatment with dsRNA combinations of *Smgpcr20* and *Smnpp26*, *Smgpcr20* and *Smnpp40*, or a combination of all three dsRNAs. There was no decline in the control group (**Figure 3.14A**). After six days, the levels of egg production decreased about 50-60% in all treatment groups. Correspondingly, the total number of eggs laid during the whole treatment period decreased about 40% compared to the control (**Figure 3.14B**).

Morphological analysis of the eggs showed an increase of abnormally shaped eggs in the RNAi groups but not in the control (**Figure 3.14C-F**). Since pairing stability and motility were not affected in the RNAi groups, the observed decline in egg production and the increase of morphological aberrations of eggs cannot be explained by the loss of the physical contact to the male. This explanation was supported by CLSM analyses, which exhibited abnormal eggs

(smaller, spine missing) inside the ootypes of dsRNA-treated, paired females (**Figure 3.15A-C**), while eggs of the paired control females appeared normal in shape and size (**Figure 3.15D**).

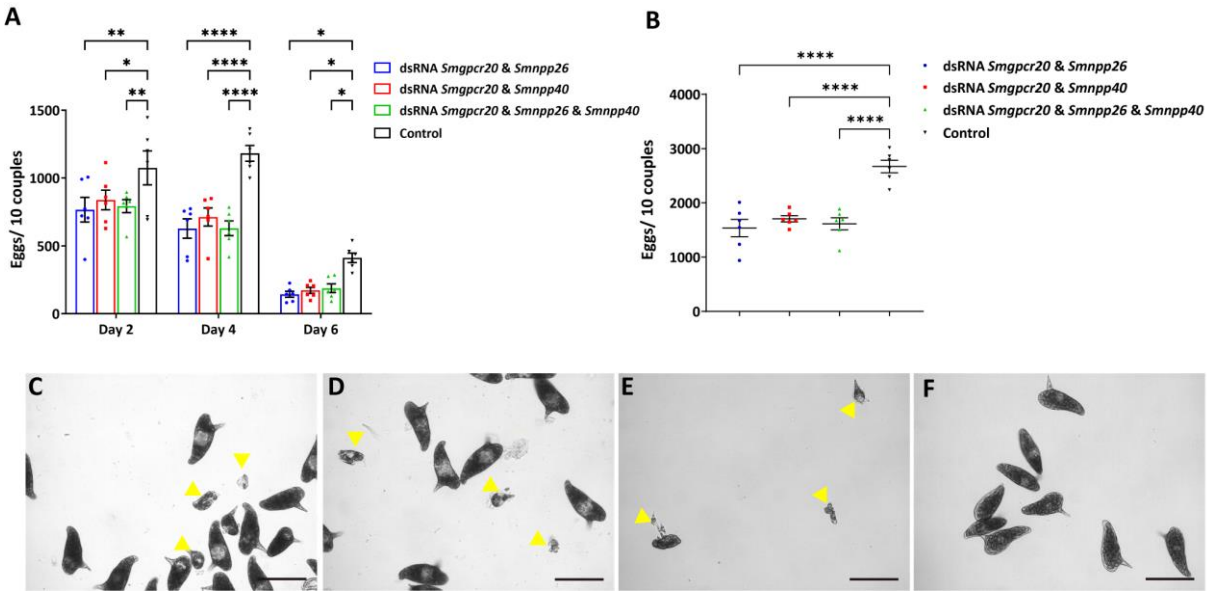

Figure 3.14: RNAi against *Smgpcr20, Smnpp26* and *Smnpp40* influenced egg production and quality in *S. mansoni* couples.

Number of eggs laid at days 2, 4, and 6 (**A**), and the total number of eggs (**B**) laid by females *in vitro* treated with dsRNA combinations of *Smgpcr20* and *Smnpp26* dsRNA, *Smgpcr20* and *Smnpp40* dsRNA, or all three dsRNAs. (**C-F**) After the dsRNA treatments with *Smgpcr20*/*Smnpp26* (**C**), *Smgpcr20*/*Smnpp40* (**D**), or a combination of the three gene-specific dsRNAs (**E**), a higher number of malformed eggs were found in all RNAi groups compared to the control group (**F**). Data are representative of the mean ± SEM of three biological experiments. Significant differences were determined by Two-way ANOVA (**B**) or One-way ANOVA (**A**) with Tukey's test for multiple comparisons, indicated as: $^{****}P < 0.0001$, $^{***}P < 0.001$, $^{**}P < 0.01$, $^{*}P < 0.05$. Scale bars: (**C-F**) 100 µm.

In addition to the physiological parameters, CLSM revealed a reduction in the length and width of the ovary of females from the RNAi groups, compared with the control (**Figure 3.15E-H)**. The number of mature oocytes in the posterior part of the ovary was decreased upon treatment with the dsRNA combinations *Smgpcr20* and *Smnpp26*, *Smgpcr20*, and *Smnpp40* (**Figure 3.15E, F**), compared with the control (**Figure 3.15H**). Whereas the combination of three specific dsRNAs led to a decrease of the number of immature oocytes in the anterior parts part of the ovary (**Figure 3.15G**). In control females, the ovary shows a typical oval structure with small, stem cell-like oogonia in the anterior part and immature oocytes as well as large mature oocytes in the posterior part (**Figure 3.15H**). No obvious morphological changes were

detected in the vitellarium of dsRNA-treated females (**Figure 3.15I-K**), compared to the control (**Figure 3.15L**).

Finally, morphological changes were also investigated in males and their gonads. Here, no obvious morphologic changes were detected, neither along the male worm body nor in the testes (number and size of the testicular lobes) nor in the seminal vesicle, which in all cases was filled with differentiated sperm (**Figure 3.15M-O**). Testes and seminal vesicles of males of the RNAi groups showed no differences to control males, which contained seminal vesicles filled with sperm and testicular lobes filled with numerous spermatogonia and spermatocytes at different stages of maturation (**Figure 3.15P**).

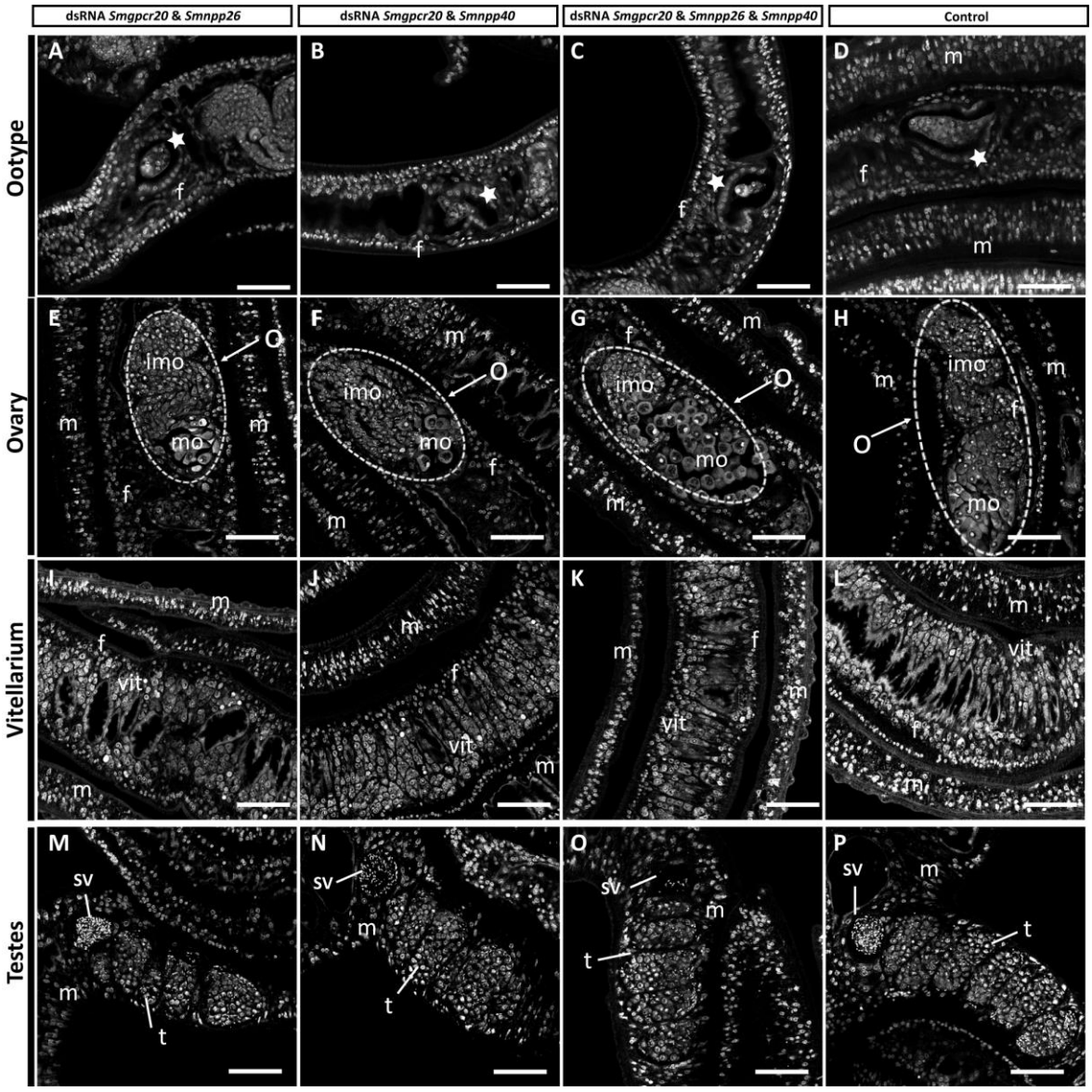

Figure 3.15: Clear morphologic changes occurred in the ovary of *S. mansoni* females following treatment with *Smgpcr20*, *Smnpp26*, and *Smnpp40* dsRNA.

CLSM analysis of *S. mansoni* males and females treated for 15 days with different combinations of dsRNA (as indicated) (**A**, **E**, **I**, **and M**) *Smgpcr20* and *Smnpp26* dsRNA; (**B**, **F**, **J**, **and N**) *Smgpcr20* and *Smnpp40* dsRNA; (**C**, **G**, **K**, **and O**) a combination of the three gene-specific dsRNAs; (**D**, **H**, **L**, **and P**) control worms maintained under the same culture conditions but without dsRNA (n = 5 per experiment). f = female; m = male; o = ovary; imo = immature oocytes; mo = mature oocytes; sv = sperm vesicle; t = teste; vit = vitellarium; white asterisk indicates ootype of females. Scale bar: 50 μm.

3.1.7. Culture conditions improvement assured optimal re-pairing rates of *S. mansoni in vitro*

To strengthen functional characterization, *in vitro* culture conditions were optimized to achieve high efficiency re-pairing rates over time. According to literature, an improved medium ABC169 was identified to support female development following pairing, which finally leads to enhanced egg production over time (Wang et al., 2019). Here, due to restricted availability, I replaced the porcine cholesterol originally used as additive for ABC169 (Wang et al., 2019) by human LDL. To test pairing efficiencies under these conditions, I started with different concentrations of LDL (0 - 2%) and equal numbers of male and female worms (5 per sex, respectively). Concentrations between 0.125% - 0.5% LDL were most suitable to achieve high re-pairing efficiency (**Table 3.1**), while worm vitality was assured (**Table 3.2**). A concentration of 2% LDL showed lethal effects within three days of culture. Furthermore, I compared ABC169/LDL (0.25%) medium to the standard M199 medium for schistosome culture and observed a higher re-pairing rate with ABC169/LDL (0.25%), when male: female ratios were 6:2 or 15:10 in 5 mL medium. Under these conditions, 100% re-pairing was achieved within 48 -72 h (**Table 3.3**). The improved *in vitro*-culture conditions with the male: female ratio 15:10 (in 5 mL medium) was subsequently used for re-pairing experiment. In addition, to investigate oocyte differentiation as a biological marker for female sexual maturation, I investigated couples at days 4, 8, 12, 16, and 21 after re-pairing by fixing couples of each time point for subsequent morphological analyses. CLSM analyses indicated that oocyte differentiation and vitellarium development started at day 8 of re-pairing under these conditions (**Figure 3.16**). After 16 d, first-time paired sF were morphologically similar to paired females recovered from hamsters immediately after perfusion (**Figure 3.16**).

Table 3.1: Different LDL concentrations affect re-pairing efficiency

Re-paired worms	2% LDL	1% LDL	0.5% LDL	0.25% LDL	0.125% LDL	0% LDL
Day 2	2.7%	67.0%	88.0%	88.0%	82.0%	69.0%
Day 4	0	42.0%	85.0%	90.0%	82.0%	76.0%

Table 3.2: Different LDL concentrations influence worm vitality

Dead worms	2% LDL	1% LDL	0.5% LDL	0.25% LDL	0.125% LDL	0% LDL
Day 2	14.5%	0	0	0	0	0
Day 4	50.9%	5%	0	0	0	0

Table 3.3: Media compositions (ABC169/LDL (0.25%) vs M199) and varying ratios of males and females affect re-pairing efficiency

	4:4	3:9	6:2	15:10	4:4	3:9	6:2	15:10
Day 1	63.90%	81.48%	66.67%	77.50%	25.00%	62.96%	50.00%	50.00%
Day 2	83.33%	96.29%	100.00%	92.50%	61.11%	81.48%	61.11%	70.00%
Day 3	94.44%	96.29%	100.00%	100.00%	52.78%	77.77%	50.00%	83.33%

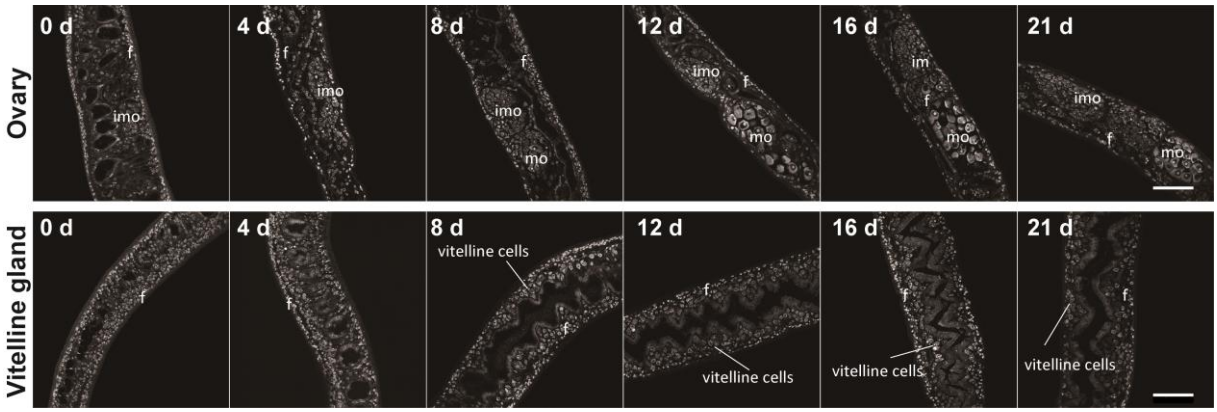

Figure 3.16: Reproductive changes of paired single-sex female parasites during *in vitro* culture. CLSM analyses showing the maturation of oocytes and vitellocytes *in vitro* with the optimized culture medium ABC169/LDL (0.25%) during d0 - d21. Representative images from three biological replicates are shown. With n ≥ 10 parasites. f = female; imo = immature oocytes; mo = mature oocytes. Scale bars: 50 µm.

3.1.8. *Smgpcr20*, *Smnpp26*, and *Smnpp40* are required for male-stimulated growth and sexual maturation of the female

With the optimized culture condition described above, I investigated if *Smgpcr20*, *Smnpp26*, and *Smnpp40* may be involved in male-stimulated female growth and developmental processes associated with sexual maturation. For this purpose, I performed re-pairing experiments combined with RNAi. I employed RNAi on sF and bM (males with previous pairing experience recovered from hamsters immediately after perfusion) for 7 d, and then paired these dsRNA-treated worms with opposite sex parasites for 21 d (**Figure 3.17A**). Since cooperative RNAi effects were assumed upon KD of *Smgpcr20* and one or both of its potential *Sm_npp*

binding partners, I used different combinations of dsRNAs. Thus, before pairing, sF and bM were (pre-) treated with *Smgpcr20* and *Smnpp26* dsRNA, *Smgpcr20* and *Smnpp40* dsRNA, or a combination of the three dsRNAs. For control, sF and bM were maintained under the same *in vitro* culture conditions but without dsRNA treatment. At day 21, RT-qPCR was performed with one part of the newly formed couples. KD efficiencies of ~50% were obtained for *Smgpcr20,* and about 80% for *Smnpp26* and *Smnpp40* (**Figure 3.17B-D**). This was comparable to the KD efficiency of pairing-experienced females (**Figure 3.12**). At day 21, females were manually separated fom their male partners and used for length determination by ImageJ. Compared with the control, the length of first-time paired females was significantly reduced upon treatment with the dsRNA combination *Smgpcr20*/*Smnpp26* (**Figure 3.17E**), and the combination of all three dsRNAs (**Figure 3.17G**). The lengths of these females was shortened 21.1% ($P<0.0001$) and 18.6% ($P<0.001$), respectively (**Figure 3.17I**). In contrast, body-size shortening was not observed in re-paired females treated under the same conditions with *Smgpcr20* and *Smnpp40* dsRNAs (**Figure 3.17F, I)**.

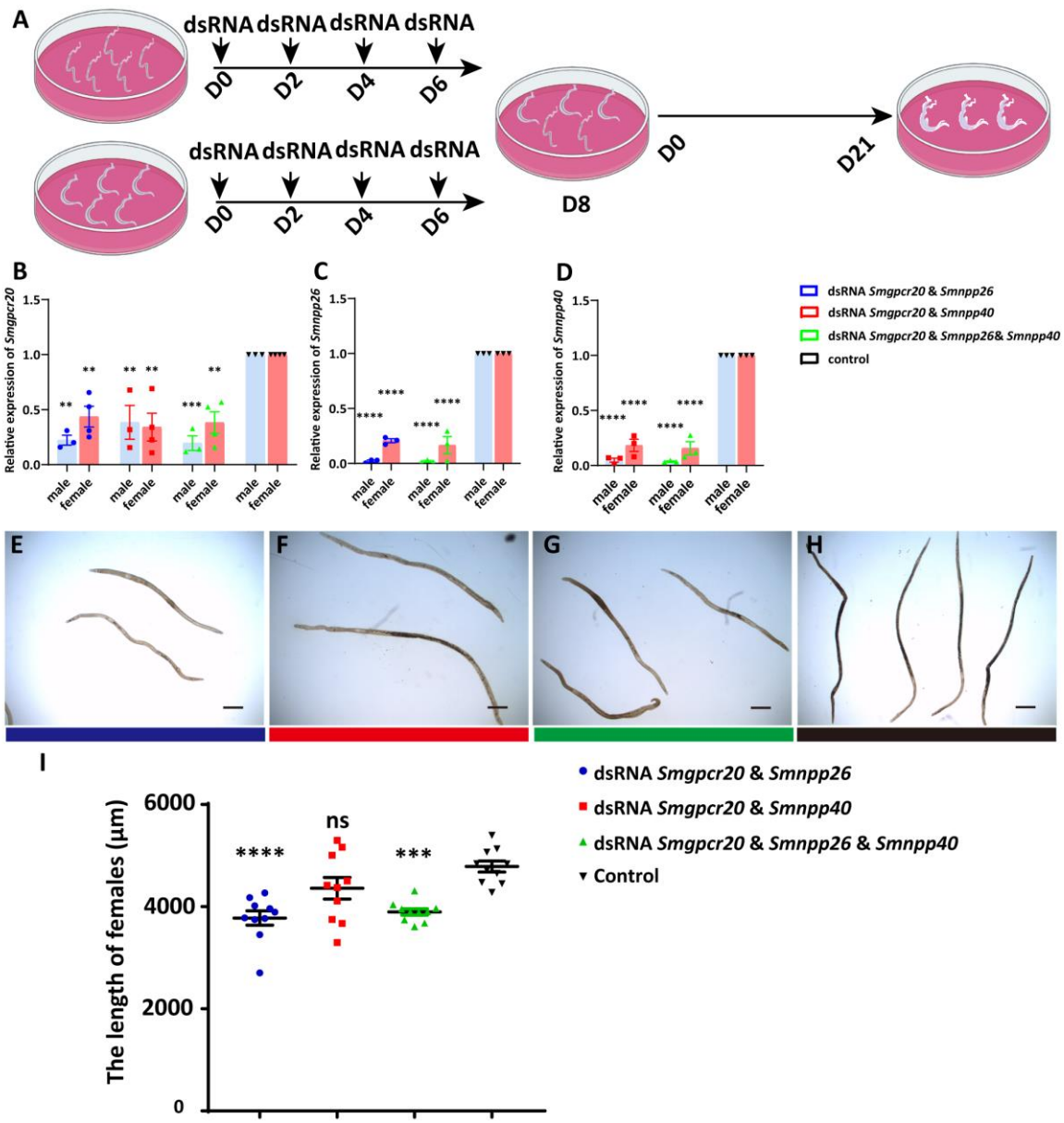

Figure 3.17: *Smgpcr20, Smnpp26,* and *Smnpp40* are required for growth of first-time paired *S. mansoni* females *in vitro*.

(**A**) Schematic overview of the experiment to evaluate effects of *Smgpcr20*, *Smnpp26* and *Smnpp40* KD on the growth of first-time paired females. Single-sex females and mature males (with previous pairing experience) were maintained *in vitro* (still separated by gender), and dsRNA was added at days 0, 2, 4, and 6. Subsequently, males and females were allowed to pair, and as couples they were maintained *in vitro* for another 21 d (n = 3). (**B-D**) RT-qPCRs showed a significant reduction of the transcript levels of *Smgpcr20*, *Smnpp26*, and *Smnpp40* upon RNAi. Relative expression levels were calculated with the $2^{-\Delta\Delta Ct}$ method, and *Smletm1* was used for normalization. Light microscopy showing first-time paired females of the RNAi groups, *Smgpcr20* and *Smnpp26* (**E**), *Smgpcr20* and *Smnpp40* (**F**), or a combination of all three dsRNAs (**G**), and the control (**H**), at d21 after pairing. Scale bars: 500 µm. (**I**) Comparison

of worm length of the RNAi groups, *Smgpcr20* and *Smnpp26*, *Smgpcr20* and *Smnpp40* dsRNA, or a combination of all three dsRNAs. As control, worms (sF and bM) were kept under the same *in vitro* culture conditions but without dsRNA treatment. The results of biological triplicates with SEM are shown. Significant differences were determined by One-way ANOVA with Tukey's test for multiple comparisons, indicated as: $^{****}P < 0.0001$, $^{***}P < 0.001$, $^{**}P < 0.01$, $^{*}P < 0.05$.

Furthermore, CLSM analyses showed that the dsRNA combination *Smgpcr20*/*Smnpp26*, and the combination of all three dsRNAs resulted in poorly developed ovaries (**Figure 3.18A-D**). Compared to ovaries of first-time paired (control) females, which were kept under the same conditions *in vitro* but without adding any dsRNA (**Figure 3.18D**), ovaries of treated females were reduced in size and exhibited lower amounts of mature oocytes in the posterior part and immature oocytes in the anterior part (**Figure 3.18A, C**). In contrast, no significant morphological change of ovaries was observed in paired females treated with the dsRNA combination *Smgpcr20*/*Smnpp40* (**Figure 3.18B**). In addition, EdU incorporation assays demonstrated that *Smgpcr20*/*Smnpp26* double KD (**Figure 3.18E**) and triple KD (**Figure 3.18G**) impaired gonadal stem-cell proliferation compared to the control (**Figure 3.18H**). Hoechst was used as background staining (**Figure 3.18E-H**). *Smgpcr20*/*Smnpp26* double KD and the triple KD also reduced the number of proliferating cells in the vitellarium compared to control worms. In contrast, no changes were observed in gonad of male worms (**Supplementary Figure 3**).

Since the dsRNA-induced phenotypes in paired and first-time paired females indicated negative effects on egg production and poorly developed ovaries of paired females, I analyzed potential effects of RNAi on the transcript level of selected genes (**Table 3.4**) known to be involved in egg production, stem cell proliferation, meiosis, epigenetic processes in the vitellarium, and stress-responses in *S. mansoni*. Among these genes were the egg-shell precursor protein genes *Sm*p14 (Smp_131110) (Bobek et al., 1986), *fs*800-like (Smp_000270) (Reis et al., 1989), *tyrosinase 1* (*Sm*TYR1; Smp_050270) (Fitzpatrick and Hoffmann, 2006; Fitzpatrick et al., 2007; deWalick et al., 2012), *tyrosinase 2* (*Sm*TYR2; Smp_013540) (Fitzpatrick and Hoffmann, 2006; Fitzpatrick et al., 2007; deWalick et al., 2012), the germline stem-cell (GSC) marker *nanos-1* (Smp_055740) (Wang et al., 2007; Wang et al., 2018), the neoblasts (somatic stem cells in flatworms) marker *nanos-2* (Smp_051920) (Collins et al., 2013), the GSC progeny marker *Smmeiob* (meiosis-related protein, Smp_333540) (Möscheid et al., in preparation), extracellular superoxide dismutase *sod* [Cu-Zn] (*Sm*SOD; Smp_095980) (Fridovich, 1975; Cogswell et al., 2011), and histone acetyltransferase *myst4* (*Smmyst4*; Smp_165360) (Möscheid et al., in preparation). To this end, RNA was extracted from first-time

paired and dsRNA-treated females, and control females, after manual separation from their male partners. Then, RT-qPCR analyses were done using the reference gene *Smletm1* (Haeberlein et al., 2019), which was shown before to be a suitable control for this kind of *in vitro* culture experiments. The transcript levels of the egg-shell precursor protein genes *Smp14*, *fs800*, and the egg-shell-forming genes *Smtyr1* and *Smtyr2* were significantly decreased upon treatment with the dsRNA combination *Smgpcr20*/*Smnpp26*, and the combination of all three dsRNAs (**Figure 3.18I**). Only upon combining all three dsRNAs, the transcript level of *nanos-1* was significantly decreased (**Figure 3.18I**). In contrast, the transcript levels of *nanos-2* and the GSC progeny marker *Smmeiob* were not downregulated following RNAi (**Figure 3.18I**). A significant decrease of the transcript levels of *Smmyst4* (a putative vitellarium marker) (Lu et al., 2016) and *Smsod* in dsRNA combinations *Smgpcr20*/*Smnpp26* and all three dsRNAs was also found. In contrast, there was no significant difference in the transcript levels of all selected genes between the control and dsRNA combination *Smgpcr20*/*Smnpp40*.

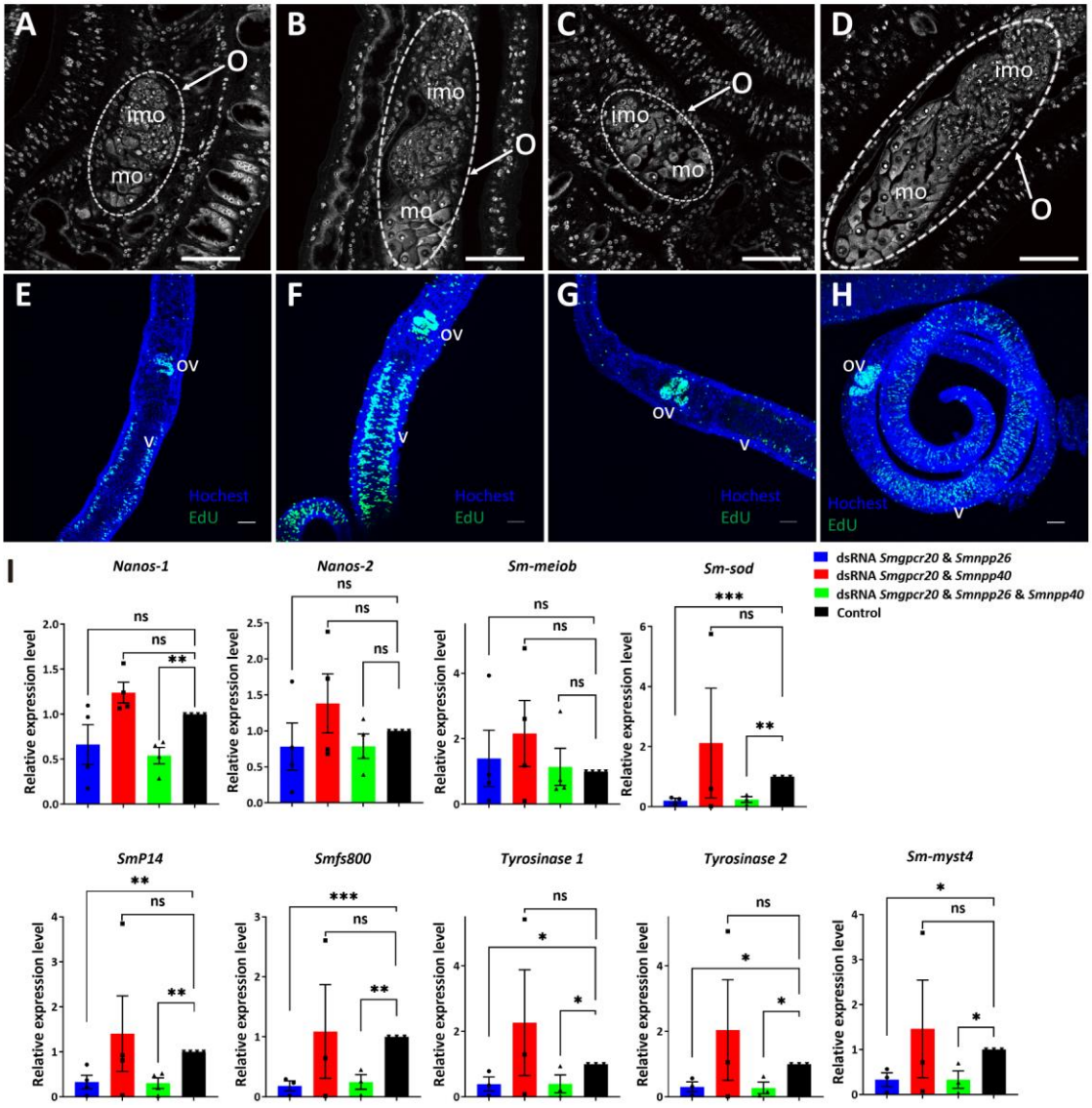

Figure 3.18: RNAi against *Smgpcr20*, *Smnpp26*, and *Smnpp40* affected gonad development, oocyte differentiation, and gene expression in first-time paired *S. mansoni* females.

CLSM analysis showing representative pictures of *S. mansoni* females post pairing for 21 d (see **Figure 3.17A**) in the presence of *Smgpcr20*/*Smnpp26* dsRNA (**A**), *Smgpcr20*/*Smnpp40* dsRNA (**B**), or a combination of *Smgpcr20*/*Smnpp26*/*Smnpp40* dsRNAs (**C**). First-time paired females maintained under the same conditions but without dsRNA served as control (**D**) (n=5). O = ovary; imo = immature oocytes; mo = mature oocytes; scale bars: 50 µm. (**E-H**) Results of EdU staining of paired females following dsRNA treatment; Hoechst 33342 was used as counter staining (blue), ov = ovary; v = vitellarium. The order of (**E-H**) is as in (**A-D**). Compared to the control (**H**), a reduction of the number of EdU-stained cells was mainly observed in the *Smgpcr20*/*Smnpp26* (**E**) and the triple dsRNA treatment groups (**G**). (**I**) Results of RT-qPCR experiments to determine transcript levels of selected genes. Fold change of gene expression levels were calculated using the $2^{-\Delta\Delta Ct}$ method. The transcript levels of genes encoding *nanos-1*, *nanos-2*, *Smp14*, *fs800*, *Smtyr*1, *Smtyr*2, *Smmyst*4, and *Smsod* were significantly lower than in the

control group; *nanos-2*, and *Smmeiob* transcript levels showed no significant differences among the RNAi and the control groups ($n \geq 3$). Data are representatives of the mean ± SEM of three separate experiments. Significant differences determined by T-test were indicated as: $^{****}P < 0.0001$, $^{**}P < 0.01$, $^{*}P < 0.05$.

Table 3.4: Genes selected for RT-qPCR experiments.

Selected genes	Gene ID	Expression (References)
Smnanos-1	Smp_055740	germline stem cells (Wang et al., 2007; Wang et al., 2018)
Smnanos-2	Smp_051920	somatic stem cells (Collins et al., 2013)
Smfs800	Smp_000270	vitellocytes (Reis et al., 1989)
Smmeiob	Smp_333540	germline stem cells progeny (Möscheid et al., in preparation)
Tyrosinase-1	Smp_050270	vitellocytes (Fitzpatrick and Hoffmann, 2006; Fitzpatrick et al., 2007; deWalick et al., 2012)
Tyrosinase-2	Smp_013540	vitellocytes, oocytes (Fitzpatrick and Hoffmann, 2006; Fitzpatrick et al., 2007; deWalick et al., 2012)
Smmyst4	Smp_165360	vitellocytes (Lu et al., 2016; Moescheid et al., in preparation)
Smp14	Smp_131110	vitellocytes (Bobek et al., 1986)
Smsod	Smp_095980	vitellocytes (Fridovich, 1975; Cogswell et al., 2011)

3.2. Functional analyses of *Smtdc-1* and *Smddc-1* unraveled their roles, and the putative involvement of BAs and neuronal activities in the male-female interaction of *S. mansoni*

BAs like dopamine, serotonin, histamine, and tryptamine are major modulators of neuromuscular function controlling movement, attachment, and behavior, including copulation (Pax et al., 1984; Ribeiro et al., 2012; Will et al. 2014). BAs are molecules with one or several amine groups. They are basic, nitrogenous compounds synthesized by the decarboxylation of amino acids or by the amination and transamination of aldehydes and ketones. BA synthesis is controlled by decarboxylases, enzymes that add or remove a carboxyl groups from organic molecules.

According to previous *in silico* analyses, Smp_135230 represents an L-tyrosine decarboxylase (*Smtdc-1*), whereas Smp_171580 is a DOPA decarboxylase (*Smddc-1*), which was substantiated in this work by phylogenetic analyses (**Supplementary Figure 4**). Due to the interesting biological roles of BAs and based on evidence from our RNA-seq studies for pairing-dependent expression of Smp_135230 and Smp_171580 especially in males, the aim of this part of my project was the functional characterization of *Smtdc-1* and *Smddc-1*.

3.2.1. Expression patterns of *Smtdc-1* and *Smddc-1* in different sexes of *S. mansoni*

Bioinformatics analyses of previous transcriptomic studies (microarray, SuperSAGE, and RNA-seq analyses) of male and female *S. mansoni* and their gonads indicated that *Smtdc-1* and *Smddc-1* are expressed in male-specific and pairing-dependent patterns (Leutner et al., 2013; Lu et al., 2016) (**Figure 3.19**). To confirm the preliminary transcript profiles, I performed RT-qPCR analyses comparing the transcript levels in sM, bM, sF, and bF. The RT-qPCR results of *Smtdc-1* showed male-specific expression with higher transcript abundance in bM than in sM. Nearly no transcripts were found in bF and sF (**Figure 3.19**). For *Smddc-1*, RT-qPCR indicated also a bM > sM bias in transcript abundance. In contrast, females showed a sF > bF bias in transcript abundance, but the overall transcript level in females was lower than in males (**Figure 3.19**). All RT-qPCR data showed transcript patterns that were comparable to the RNA-seq data.

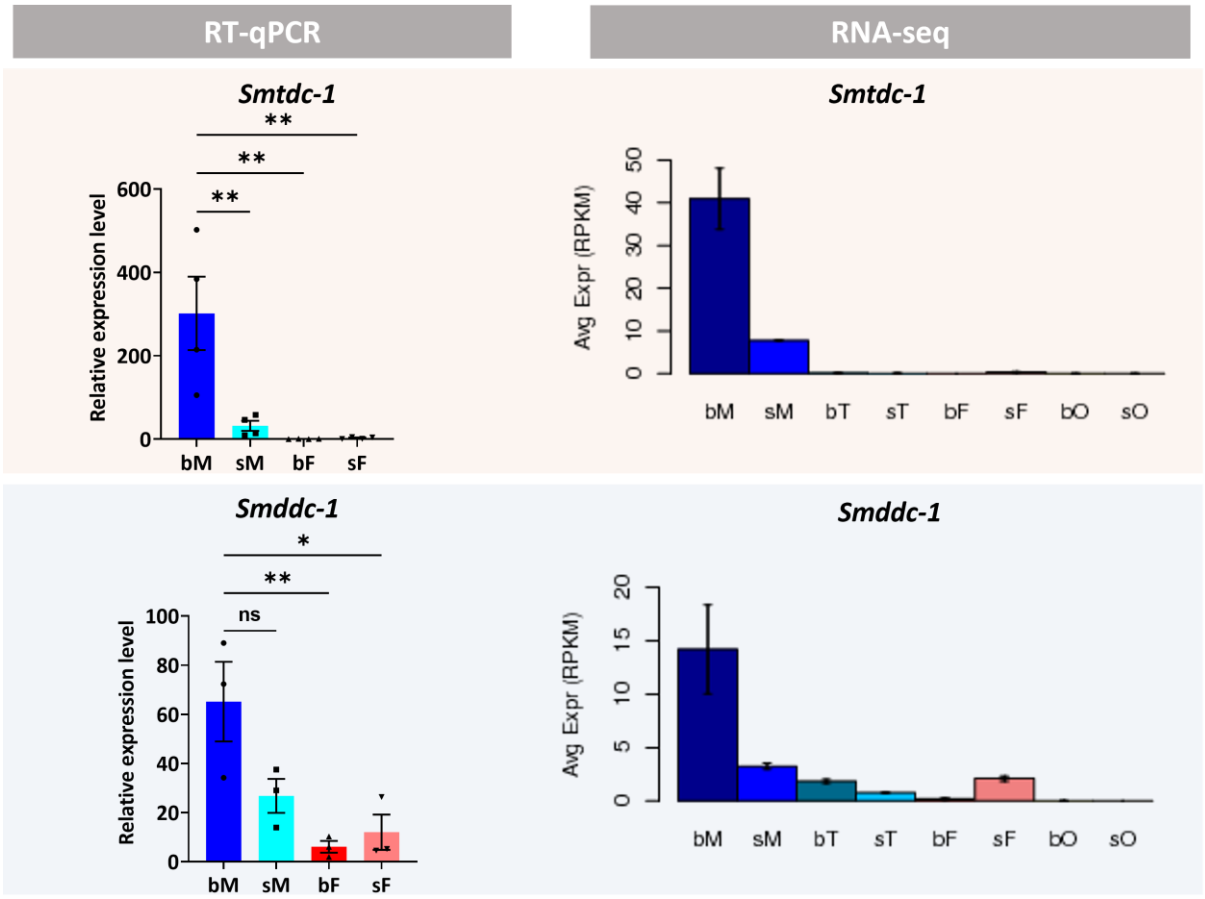

Figure 3.19: RT-qPCR analyses confirmed RNA-seq data showing sex- and pairing-dependent transcript profiles of *Smtdc-1* and *Smddc-1* in *S. mansoni*.

Relative expression of *Smtdc-1* and *Smddc-1* as determined by RT-qPCR (left) was quantified by normalization against reference gene *Smletm1*. For comparison, previous RNA-seq data (Lu et al., 2016) are presented (right). Both data sets show corresponding transcript profiles. Data represent the mean±SEM of three independent experiments (n = 3). Significant differences were determined by One-way ANOVA with Tukey's test for multiple comparisons, as indicated: $^{**}P < 0.01$, $^{*}P < 0.05$. bM = paired-males, sM = unpaired-males, bF = paired-females, sF = unpaired-females.

3.2.2. WISH analyses showed neuronal patterns of *Smtdc-1* and *Smddc-1* transcripts

To localize transcripts of *Smtdc-1* and *Smddc-1*, WISH was performed using a specific anti-sense probe coupled with digoxygenin. Transcripts of both genes showed strong signals in males but not in females (**Figure 3.20**). Transcripts of both genes were detected in an area near the gynaecophoric canal of the male worms (**Figure 3.20**), which represents the contact zone to the female during pairing. Transcripts were also detected in the anterior part of the male, the "head region" (**Figure 3.20**). This localization was comparable to the occurrence of *Smnrps*

transcripts (**Figure 3.20**). *Smnrps* were identified in neuron-2 cluster (Wendt et al., 2020; Chen et al., 2022), and their transcript abundance is higher in bM, bF versus sM, sF (Lu et al., 2016). *Sm*NRPs generate a BATT dipeptide that is released by ciliated sensory neurons into the gynaecophoric canal (Chen et al., 2022). The signals along the male gynaecophoric canal region and the head suggested similar expression patterns of *Smtdc-1*, *Smddc-1*, and *Smnrps* (**Figure 3.20**). In females, *Smtdc-1* and *Smddc-1* transcripts were only found along the uterus (**Figure 3.20**). No signal was detected using sense probes of both genes (**Figure 3.20**). *Smtsp-2*, a tegument marker (Tran et al., 2010), was used as a positive control. As expected, signals were detected along the tegument area (**Figure 3.20**).

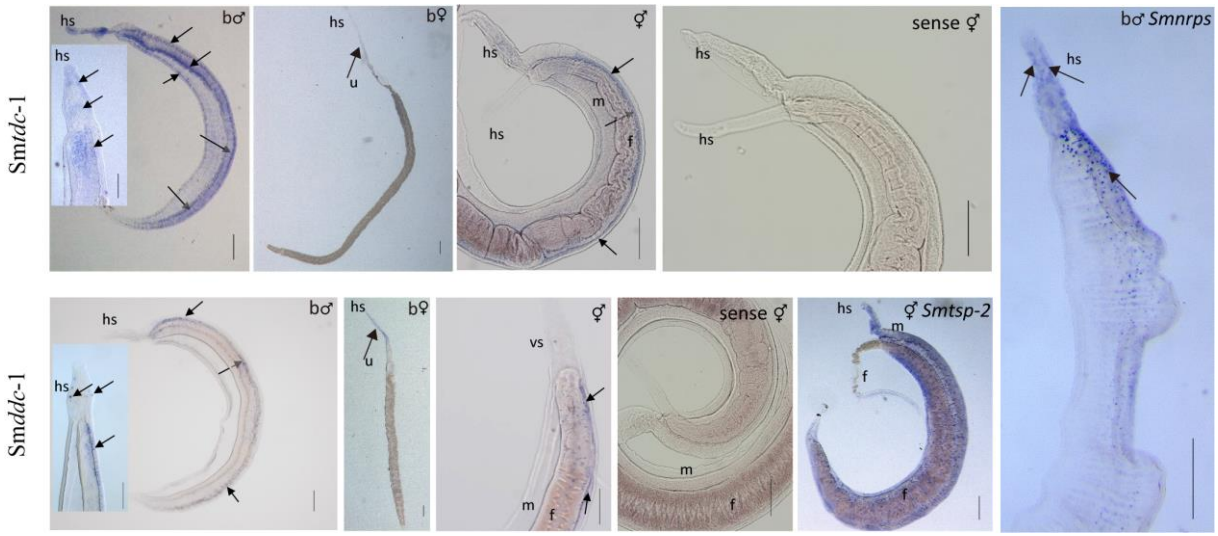

Figure 3.20: WISH analyses localized *Smtdc-1* and *Smddc-1* transcripts in different regions of both sexes of *S. mansoni*.

Localization of *Smtdc-1* and *Smddc-1* transcripts in male worms was performed by WISH using anti-sense probes. A sense probe served as negative control and showed no signals. An antisense probe against *Smtsp-2* served as positive control and showed signals along the tegument area. An antisense probe against *Smnrps* showed signals along the gynaecophoric canal and in the head of males. Signals of *Smtdc-1* and *Smddc-1* were mostly detected along the gynaecophoric canal and in the head of males, and along the uterus of females. bo♂ = paired males, b♀ = paired females, ♂♀ = couples, f = female; m = male; hs = head sucker; u = uterus. Scale bars: 200 µm.

To examine the localization in more detail, I performed FISH using FITC-labelled *Smtdc-1* anti-sense and DIG-labelled *Smddc-1* anti-sense probes. Again, *Smtdc-1* and *Smddc-1* transcripts were detected in the head region but also along the body of male worms (**Figure 3.21A**). This corresponded to the WISH data (**Figure 3.20**). Since the single cell-atlas data (Wendt et al., 2020) showed similar distributions of *Smtdc-1* and *Smddc-1*, mainly in neuronal

cluster-2 cells (**Figure 3.21B**), I also performed co-localization studies of *Smtdc-1* and *Smddc-1* by double-FISH, using FITC-labelled *Smtdc-1* anti-sense and DIG-labelled *Smddc-1* anti-sense probes. The obtained results demonstrated the co-localization of *Smtdc-1* and *Smddc-1* transcripts along the body of males worms (**Figure 3.21C**).

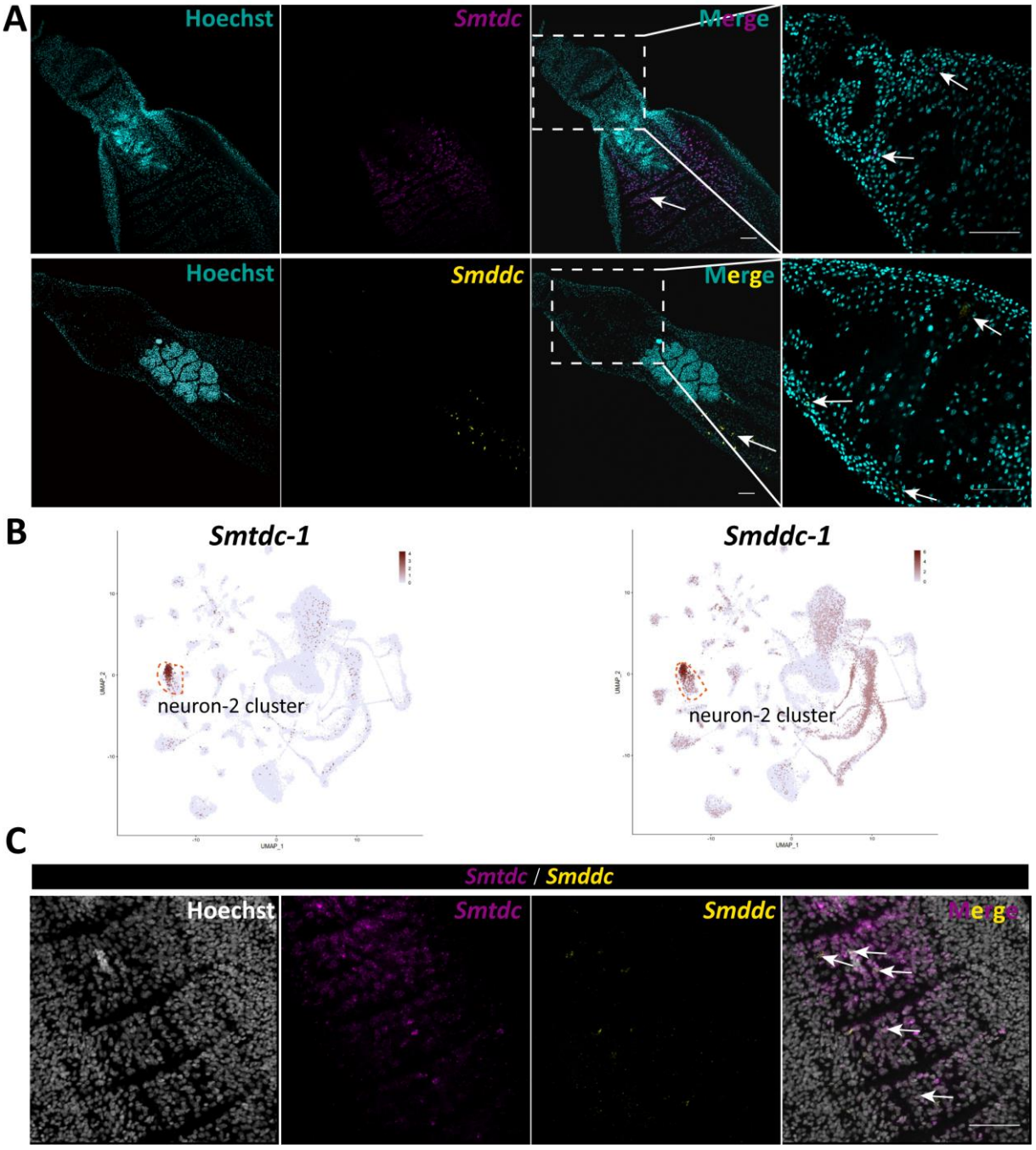

Figure 3.21: *Smtdc-1* and *Smddc-1* transcripts mainly localize in neuronal cells of male *S. mansoni*. (**A**) Localization of *Smtdc-1* and *Smddc-1* transcripts in male worms was done with anti-sense probes labelled by FITC and DIG using FISH. The sense probe served as negative control and showed no signal (data not shown). (**B**) Single cell-atlas data showing *Smtdc-1* and *Smddc-1* transcripts widely distributed in different cell clusters, including neuron cells, neoblast cells, tegument cells, and muscle cells (Wendt

et al., 2020) with a clear dominance in cells of the neuron-2 cluster. (**C**) Double-FISH with *Smtdc-1* and *Smddc-1* in male worms of *S. mansoni* showing co-localization. Nuclei were stained cyan (**A**) or grey (**C**) (Hoechst 33342), FITC-labelled *Smtdc-1* was stained magenta, DIG-labelled *Smddc-1* was stained yellow. Identified areas of co-localization are indicated by arrows. Scale bars: 50 µm.

3.2.3. RNAi against *Smtdc-1* and *Smddc-1* indicated roles for female sexual maturation

To characterize the potential functions of *Smtdc-1* and *Smddc-1*, I performed KD approaches in bM and bF by RNAi. In these days, our lab had a shortage of single-sex worms. To overcome this problem, I generated females with a sF-like status by separating bF directly after perfusion from their male partners. These females were kept as female-only population for 7-14 days *in vitro* to induce a sexual de-differentiation status of these females (Popiel and Basch, 1984; Kunz, 2001; Grevelding, 2004). In the following sections, these de-differentiated females are named as group 1. After the working group got access to sF again for experiments at a later time point of my work, I used these females for (first-time-) pairing experiments and named these females group 2. Re-pairing (group 1) and first-time pairing experiments (group 2) were conducted using the improved culture condition described before (**Chapter 3.1.7**). For RNAi experiments, 4 µg/mL dsRNA of *Smtdc-1* or *Smddc-1* were used, individually, or in combination. Based on the results obtained for pairing experiments with the optimized culture conditions and the time needed for the sexual maturation of sF after first-time pairing *in vitro*, the experimental period was extended to 21 d, with the renewal of culture medium and dsRNA every 2 d. Worms maintained under the same conditions but without dsRNA served as control.

For studying RNAi effects on pairing stability, males and group 1 females were treated with dsRNA, and re-pairing frequency, egg production, motility, and vitality were monitored every 2 d. After this period, the experiment was finished by separating reformed couples to extract RNA. By RT-qPCR, the KD efficiencies were determined, which varied between 50-90% depending on the gene (**Figure 3.22**). RNAi against either *Smtdc-1* or *Smddc-1* had no influence on motility and vitality (not shown). Re-pairing of group 1 females occurred within 2-3 days, and no statistically significant differences were observed for re-pairing frequencies of males and group 1 females following RNAi with dsRNA targeting *Smtdc-1* and *Smddc-1*, either individually or in combination (**Figure 3.23**).

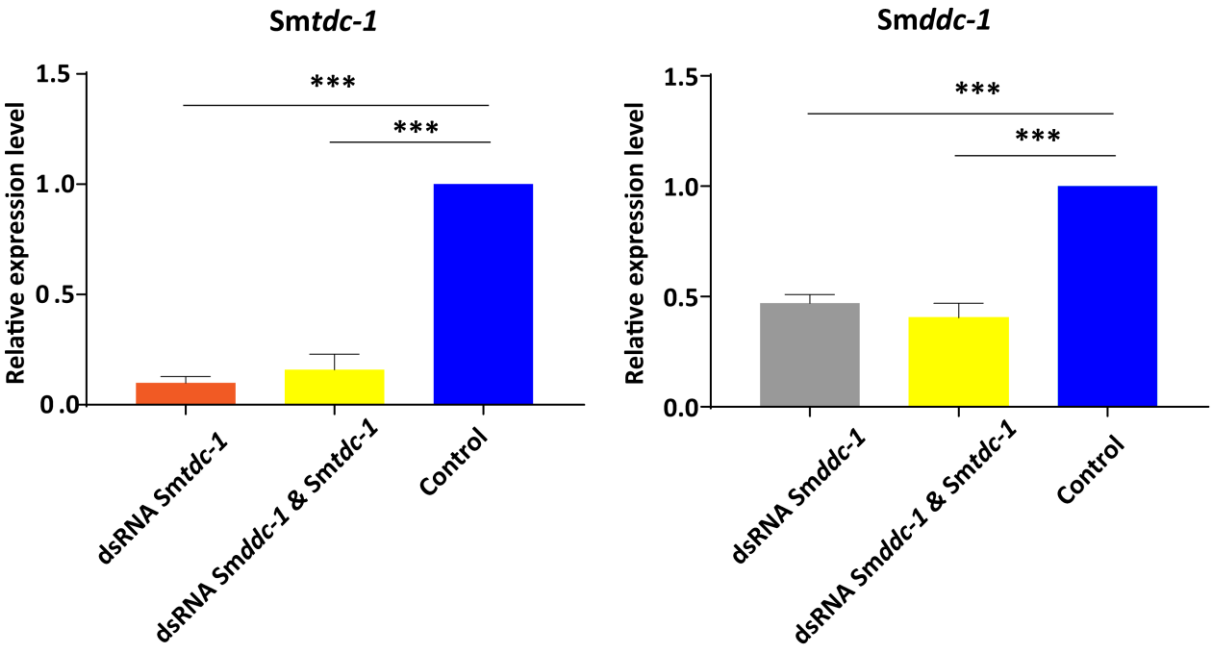

Figure 3.22: RNAi caused significant KD of *Smtdc-1* and *Smddc-1* transcripts in bM and group 1 females.

The transcripts level of *Smtdc-1* and *Smddc-1* were quantified after 21 d of culture. RT-qPCR data were normalized compared to the transcript level of the control (untreated worms). Relative expression levels were calculated with the $2^{-\Delta\Delta Ct}$ method. *Smletm1* was used for normalization, compared to the transcript level of the control (untreated worms). Biological triplicates with SEM are shown. Significant differences were determined by One-way ANOVA with Tukey's test for multiple comparisons were indicated as: $^{***}P < 0.001$.

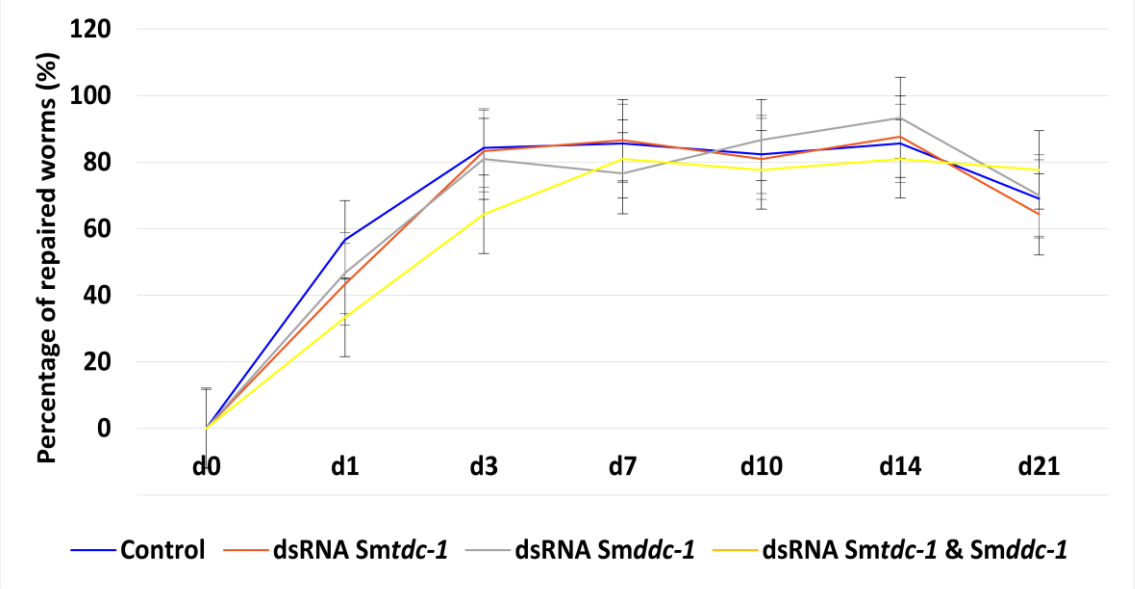

Figure 3.23: RNAi against *Smtdc-1* and *Smddc-1* had no influence on re-pairing frequencies of bM and group 1 females.

The diagram shows the summary of re-pairing frequencies of *S. mansoni* males with group 1 females *in vitro* following RNAi with dsRNA targeting *Smtdc-1* and *Smddc-1*, either individually (grey and orange lines) or in combination (yellow line; n = 3; each n with 10-15 worms of both genders). Control, untreated worms maintained *in vitro* for re-pairing under the same conditions (blue line; n = 3; each n with 10-15 worms of both genders). No statistically significant differences were observed.

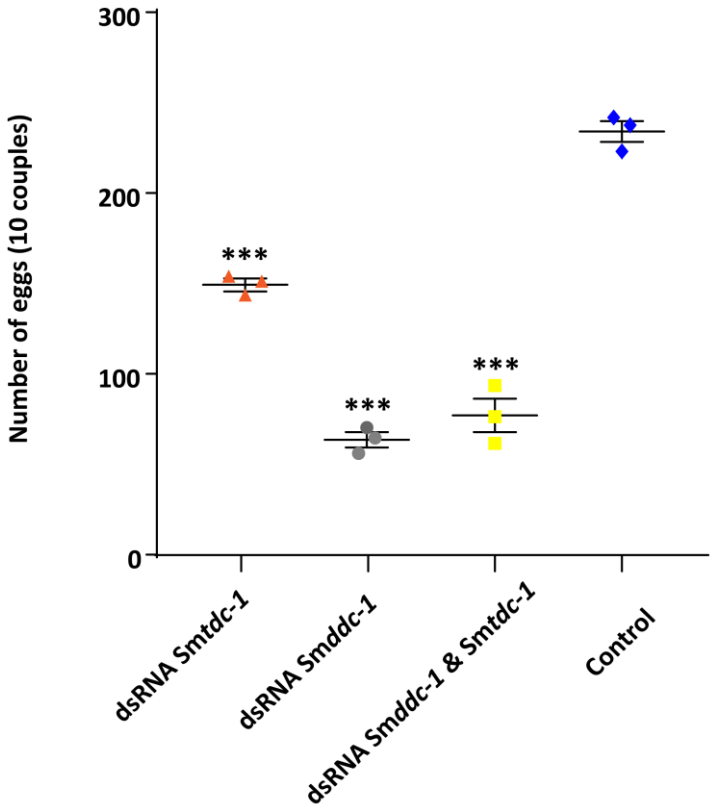

Figure 3.24: RNAi against *Smtdc-1* and *Smddc-1* in bM and group 1 females affected egg production *in vitro*.

Summary of egg counts over the observation period of 21 d. In all treatment groups, egg production significantly decreased compared to the control. Results of biological triplicates with SEM are shown. Significant differences were determined by One-way ANOVA with Tukey's test for multiple comparisons were indicated as: $^{***}P < 0.001$.

Analyzing egg production over the complete observation period of 21 d, significantly lower numbers of eggs were detected in the treatment groups compared to untreated control couples (**Figure 3.24**). In addition to these physiological effects, CLSM analyses showed that treatment with either *Smtdc-1* or *Smddc-1* led to a decrease in the number of mature oocytes in all treatment groups (**Figure 3.25**).

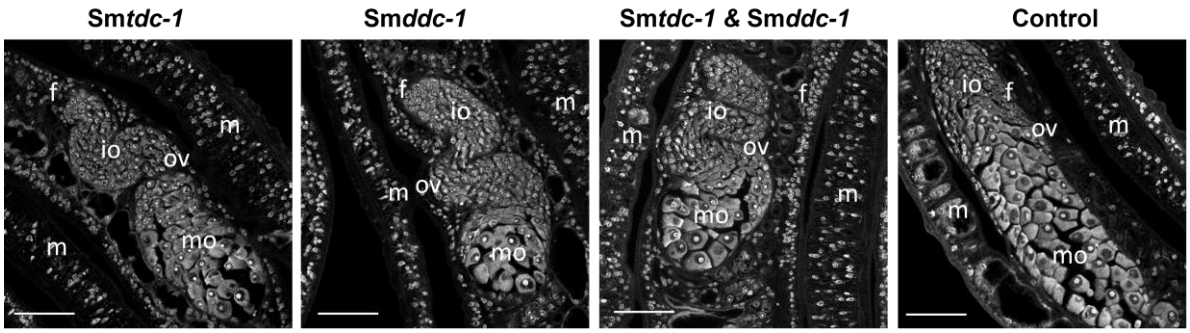

Figure 3.25: RNAi against *Smtdc-1* and *Smddc-1* decreased the number of mature oocytes produced by group 1 females.

CLSM analyses showed lower numbers of differentiated oocytes in all treatment groups (*Smtdc-1*, or *Smddc-1*, or a combination of both) compared to the control at d 21 after re-pairing. f = female, m = male, mo = mature oocytes, io = immature oocytes; ov = ovary. Scale bars: 50 µm.

For group 2 females, the transcript level was also examined following *Smtdc-1* and *Smddc-1* RNAi by RT-qPCR. KD efficiencies were in similar to those obtained from group 1 with a range of 60-90% following RNAi with dsRNA targeting *Smtdc-1* and *Smddc-1*, either individually or in combination (**Figure 3.26**). No statistically significant differences were observed for motility and vitality of *S. mansoni* males with group 2 females *in vitro* following RNAi with the mentioned dsRNA combinations. Also, re-pairing efficiencies were comparable to those of the controls (**Figure 3.27A**). However, the total number of eggs laid over the complete culture period of 21 d showed significant reduced egg numbers following RNAi with dsRNA targeting *Smtdc-1* and *Smddc-1*, compared to untreated control (**Figure 3.27B**). In addition, the morphology of eggs laid by KD females at d 14 showed significant differences as compared to eggs of the control group, and many abnormally formed eggs were found (**Figure 3.27C**).

Finally, CLSM analysis showed a decrease in the number of mature oocytes for re-paired females from group 2 treated with either *Smtdc-1* or *Smddc-1* or a combination of both dsRNAs, compared to the control (**Figure 3.28**). However, the observed differences appeared not to be substantial. There is no morphological change of the gonads in male worms after all dsRNA treatments (data not shown).

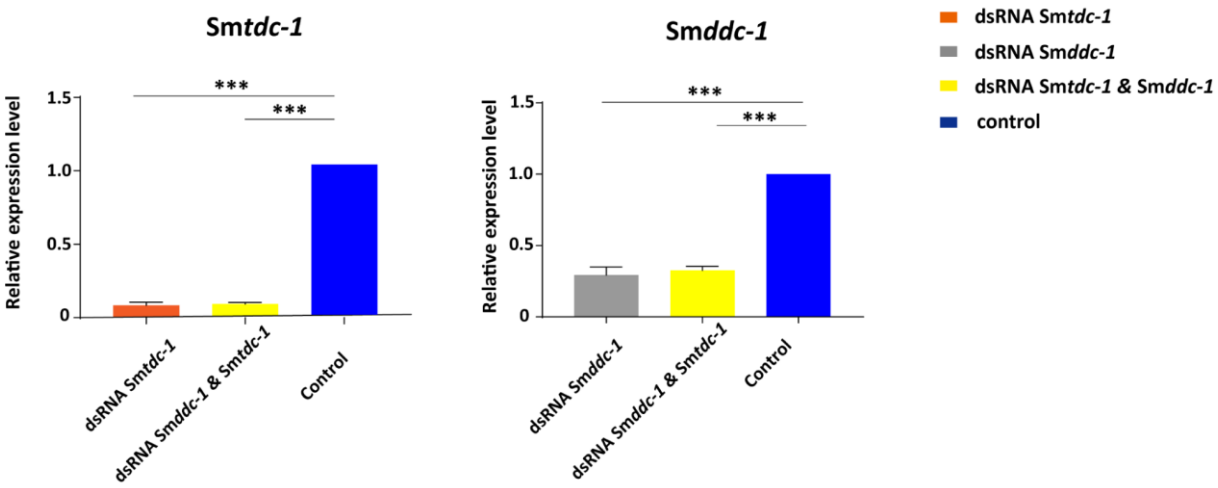

Figure 3.26: RNAi significantly reduced transcript levels of *Smtdc-1* and *Smddc-1* in bM and females from group 2.

The transcripts levels of *Smtdc-1* and *Smddc-1* were quantified after 21 d of culture by RT-qPCR. The results were normalized compared to the transcript level of the control (untreated worms). Relative expression levels were calculated with the $2^{-\Delta\Delta Ct}$ method. *Smletm1* was used for normalization and compared to the transcript level of the control (untreated worms). Biological triplicates with SEM are shown. Significant differences were determined by One-way ANOVA with Tukey's test for multiple comparisons were indicated as: $^{***}P < 0.001$.

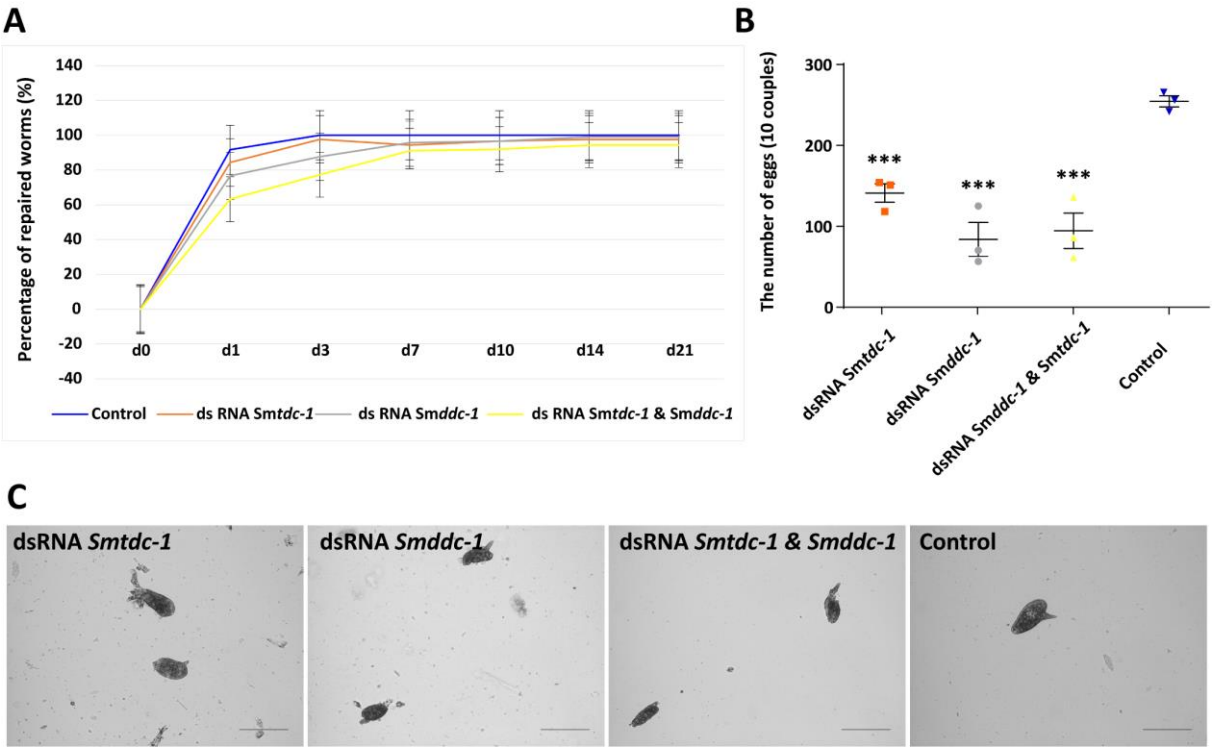

Figure 3.27: RNAi against *Smtdc-1* and *Smddc-1* caused effects on egg production in group 2 females.

Following KD, the number of re-paired couples (**A**) and the total number of eggs of 10 couples laid *in vitro* (**B**) were determined. (**C**) Images showing abnormal eggs upon dsRNA treatment at d 14, mostly normal eggs were observed in the control group. Results of biological triplicates with SEM (**A, B**) are shown, and representative pictures in (**C**). Significant differences were determined by One-way ANOVA with Tukey's test for multiple comparisons were indicated as: $^{***}P < 0.001$.

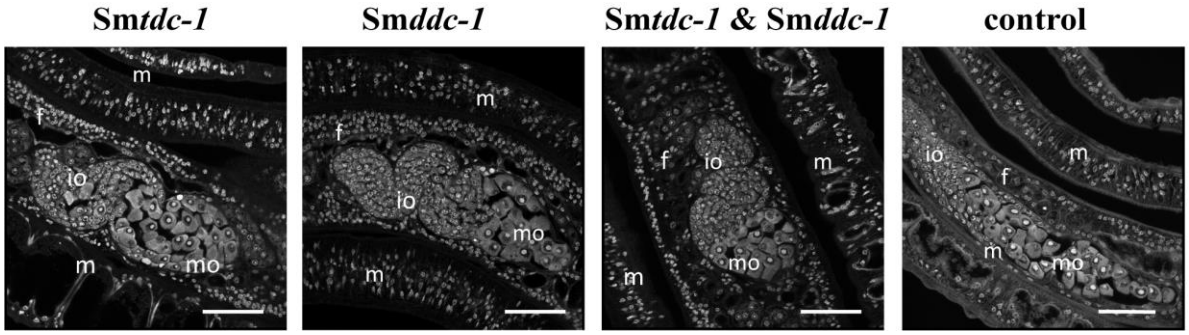

Figure 3.28: Morphologic changes occurred in the ovaries of group 2 females following *Smtdc-1* and *Smddc-1* RNAi.

CLSM images of female worms treated with either *Smtdc-1* or *Smddc-1* or a combination of dsRNAs targeting both genes. Untreated worms served as control, m = male; f = female; imo = immature oocytes; mo = mature oocytes. Scale bars: 50 µm.

3.2.4. The addition of dopamine might compensate the loss of *Smtdc-1* and/or *Smddc-1* function

Since *Smddc-1* is supposed to be a DOPA decarboxylase, I intended in a kind of pilot experiment to investigate whether the addition of dopamine to couples *in vitro* may rescue the effects caused by *Smtdc-1* and *Smddc-1* KD. To this end, I performed RNAi against *Smtdc-1* and *Smddc-1* and added 30 µM dopamine to one of the experimental groups. The groups consisted of males and group 2 females. Untreated worms (no dsRNA, no dopamine) maintained *in vitro* for re-pairing under the same conditions were served as control. As found before, RT-qPCR analyses showed similar KD efficiencies in the range of 60-90% following RNAi. The treatment period for all groups was 21 d. Egg count determination at the end of the observation period revealed significant differences between the *Smtdc-1* and *Smddc-1* double

KD-only group and the control. However, the egg production of the KD group treated with dopamine was comparable to those of the double KD-only group (**Figure 3.29**).

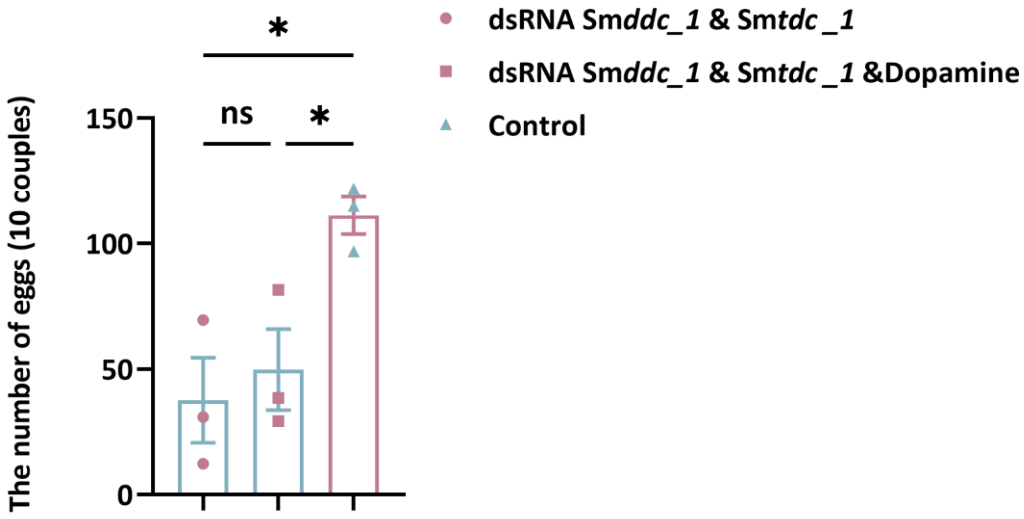

Figure 3.29: Dopamine slightly increased egg numbers of females treated with *Smtdc-1* and *Smddc-1* dsRNA.

Summary of egg counts over the observation period of 21 d. Following treatment, the total number of eggs of 10 couples laid *in vitro* was compared to the control. Untreated worms (no dsRNA, no dopamine) maintained *in vitro* for re-pairing under the same conditions were served as control. Biological triplicates with SEM are shown. A significant difference determined by One-way ANOVA with Tukey's test for multiple comparisons were indicated as: $^{*}P < 0.05$.

In addition, females treated with dsRNA against *Smtdc-1* and *Smddc-1* showed relatively small ovaries and reduced numbers of mature oocytes compared to the control, a finding that is similar to the one found before. It appeared that females of the double KD groups that were treated with dopamine showed a higher number of mature oocytes, which was comparable to the completely untreated control group, than females of the double-KD only group (**Figure 3.30**). As a further negative control, sF were kept under the same *in vitro* culture conditions, and no mature oocytes appeared in the ovaries (**Figure 3.30**). In conclusion, the addition of dopamine seemed to compensate the loss of *Smtdc-1* and/or *Smddc-1* function at least partially.

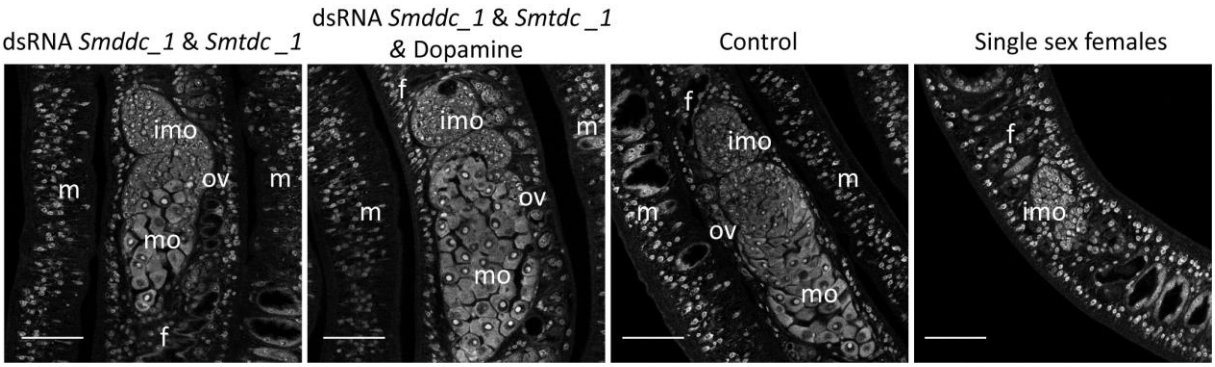

Figure 3.30: The addition of dopamine caused an increase of the number of mature ooyctes in females treated with dsRNAs against *Smtdc-1* and *Smddc-1*.

CLSM analyses of *S. mansoni* females treated with *Smtdc-1* and *Smddc-1* dsRNA, *Smtdc-1* and *Smddc-1* dsRNA and 30 µM dopamine. As further control, sF were used, without treatment. m = male; f = female; ov = ovary; imo = immature oocytes; mo = mature oocytes. Scale bars: 50 µm.

4. Discussion

4.1. Rhodopsin orphan GPCR *Sm*GPCR20 interacts with the neuropeptides and mediates reproductive processes in *S. mansoni*

4.1.1. The occurrence of GPCRs in schistosomes

Schistosomes have a unique male-female interaction, because the female has to pair with a male partner in order to fully develop and mature sexually. Schistosomes were historically noted to be difficult to culture and hard to work with experimentally (Geary and Maule, 2010). Those limitations have been overcome by the long history of schistosome research, which has provided a number of useful bioassays for biological insights. In the recent decade, especially the genome sequence data have placed schistosome research in a very good position providing novel experimental opportunities to study this important parasite. In this context, GPCR signaling studies have come into focus, on the one hand because not much is known about the biological meaning of the probably 126 GPCRs in *S. mansoni* (Hahnel et al. 2018, Kamara et al., 2023). For instance, some studies in schistosomes have reported about GPCRs involved in neuromuscular function (Ribeiro et al., 2012), reproduction (Hahnel et al., 2014; 2018), and chemosensation (Wheeler et al., 2022). On the other hand, GPCRs have been proven as suitable drug targets in different organisms including helminths (Larhammar et al., 1993; Holden-Dye and Walker, 2007; Hauser et al., 2017; Odoemelam et al., 2020; Liu et al., 2021; Orr-Burks et al., 2021; Montazeri et al., 2022).

With respect to the transcriptomic data from various studies in *S. mansoni* (Lu et al., 2016; Wendt et al., 2020; Buddenborg et al., 2021), *in silico* analyses uncovered GPCRs as the largest superfamily of transmembrane receptors, and all major subfamilies were represented, including a platyhelminth-specific rhodopsin subfamily (PROF) (Zamanian et al., 2011; Campos et al., 2014). In *S. haematobium*, a GPCR*ome* similar to that of *S. mansoni* was described (Campos et al., 2014). Although some GPCRs of *S. mansoni* have been characterized as receptors responding to different BAs, most GPCRs were shown to be involved in neuromuscular function (Hamdan et al., 2002; El-Shehabi et al., 2009; 2012; Taman and Ribeiro, 2009; 2011; Protasio et al., 2012; MacDonald et al., 2015). Despite this, not much is known so far about potential ligands binding to orphan schistosome GPCRs.

4.1.2. *In silico* analyses defined *Sm*GPCR20 as a PROF subfamily member of GPCRs

One part of my work was to characterize the Rhodopsin-family orphan receptor *Sm*GPCR20 of *S. mansoni*. As the first step towards structural analysis, *in silico* studies indicated that *Sm*GPCR20 has a typical composition with 7-TM domains. Furthermore, highly conserved orthologues exist in *S. japonicum* and *S. haematobium*. Based on phylogenetic analyses, I detected a close relationship of *Sm*GPCR20 to orthologues in other Platyhelminthes, whereas *Sm*GPCR20 is rather distantly related to orthologues of the nematode *Caenorhabditis elegans*, the intermediate host snail *B. glabrata*, *Homo sapiens* and other species. This finding grouped *Sm*GPCR20 into the PROF subfamily (Campos et al., 2014). The high conservation in different schistosome species identified by the multiple sequence alignment suggested a specific role(s) of *Sm*GPCR20 for members of the family Schistosomatidae.

4.1.3. The MALAR-Y2H analysis identified neuropeptides *Sm*NPP26 and *Sm*NPP40 as potential interaction partners of *Sm*GPCR20

Towards deorphanization of *Sm*GPCR20, potential neuropeptide ligands of *Sm*GPCR20 were tested by the MALAR-Y2H system (Weth et al. 2019). As before with other *S. mansoni* GPCR-NPP ligand interaction, also in my study evidence for specific *Sm*_NPPs as interaction partners were obtained. *Sm*NPP26 and *Sm*NPP40 were shown to specifically bind to *Sm*GPCR20 in this yeast system by growth on media selective for the presence of bait and prey plasmids as well as for interaction. In contrast to all other *Sm*_NPPs tested, only *Sm*NPP26 and *Sm*NPP40 in combination *Sm*GPCR20 led to results that were similar to the positive control (CXCR4/CXCL12). Therefore, *Sm*NPP26 and *Sm*NPP40 are potential ligands of *Sm*GPCR20.

4.1.4. Analyzing the expression profiles of *Smgpcr20*, *Smnpp26*, and *Smnpp40* showed mainly neuronal expression, and higher transcript levels in sM, sF compared with bM, bF of *S. mansoni*

To investigate the transcript profiles of *Smgpcr20*, *Smnpp26*, and *Smnpp40*, RT-qPCR analyses were performed showing that the transcript levels of *Smgpcr20* dominated in sM, bM, and sF. This indicates that the transcript patterns of these genes in sF seem to be more closely related to the appropriate ones in males than to bF. For *Smnpp26* and *Smnpp40*, a male-preferential transcript profile (with a sM >bM tendency) were observed, and for both *npp* genes higher mRNA levels in unpaired vs paired worms. The *Smgpcr20* and both *npp* genes with the higher transcript levels in unpaired worms may contribute to processes in male and female attraction, or in the involvement or/and establishing the pairing contact, and then may trigger

female maturation. Since transcript levels may not be representative for protein levels, and because also a low amount of protein can be of high cell biological and/or physiological importance, further studies are needed to substantiate the pairing influence on the protein expression of these three genes. Therefore, with regard to the male-female interaction of *S. mansoni*, these results also suggest that *Smgpcr20*, *Smnpp26*, and *Smnpp40* circuits may have a higher importance in sM and sF until pairing. Studies in *S. japonicum* also showed a clear reduction of the expression of *npps* after pairing (Wang et al., 2017), which indicated that the observed reduction of the transcript levels of these genes may be a schistosome-wide biological pattern. Recently, transcriptomic analysis in *F. hepatica* showed that the GPCRs and *npp*-encoding genes are being produced at a decreased rate *in vivo* compared with *in vitro* maintained juveniles. This may coincide with a more rapid growth and development along with the downregulation of peptidergic neuronal signaling components *in vivo* compared with the *in vitro* maintained juveniles and supports a role for the GPCRs and *npp*-encoding genes in regulating liver fluke growth and development (Robb et al., 2022).

In addition, my RT-qPCR data were supported by the detection of transcripts of all three genes by WISH. Signals of transcripts of all genes were detected in both genders, and a regular, widely, punctate signal pattern was observed. The latter suggests transcript occurrence in neuronal cells. This result is consistent with the similar patterns obtained by WISH in previous studies of neuronal genes in *S. mansoni* (Taman and Ribeiro, 2011; Patocka et al., 2014; Diaz Soria et al., 2020; Wendt et al., 2020). In addition, NPPs were found to be involved in regeneration processes of the central nervous system in the free-living flatworm *S. mediterranea* (Fraguas et al., 2012). WISH results of my study showed *Smgpcr20* to be mostly transcribed in the neuronal and tegument area (parenchyma, neoblast cells) (**Supplementary Figure 6**). A similar result was obtained in the previous single-cell atlas study of *S. mansoni*, according to which *Smgpcr20* appeared to be transcribed in the parenchyma, the neuronal clusters 1, 2, and 4, as well as in neoblasts (Wendt et al., 2020, **Supplementary Figure 5B**). Furthermore, the overall transcript levels of *Smgpcr20*, *Smnpp26*, and *Smnpp40* across the majority of tissues were lower in bF than sF, which corresponds to the RNA-seq data (Lu et al., 2016) and our RT-qPCR data. The occurrence of *Smnpp26* transcript in females depended on the pairing status. Higher transcript levels were obtained from sF than bF, which corresponds to the *Smgpcr20* transcript pattern. According to the single-cell atlas, transcripts of *Smnpp26* are widely distributed in all males tissues, but the highest transcript abundance was found in neuron cluster 14 (Wendt et al., 2020, **Supplementary Figure 5C**). Moreover, *Smnpp26* was

also found to be preferentially transcribed in neuron cluster 14, also in sF and bF. Differently, the transcript level of *Smnpp26* in neuron cluster 4 was influenced by pairing status, which was higher in bF than sF, while WISH showed quantitative differences of the *Smnpp26* signal patterns with more intensive signals in sF compared to bF in the head region of females. In this case, we hypothesize that these additional signals in the head region of sF may belong to neuron cluster 14, while neuron cluster 4 cells occur along the body of females, and in bF from the uterus down to the posterior part containing the vitellarium tissue (*Smmyst4* localized area, **Figure 3.8F**). This finding suggests that *Smnpp26* transcripts localize in similar regions as *Smgpcr20* transcripts. Indeed, co-localization experiments by double-FISH in sF showed *Smgpcr20* and *Smnpp26* transcripts in cells positioned in the same subtegumental area of the head region and along the body.

In addition, *Smnpp40* transcripts also occurred differently in females, with a more abundant overall transcript level throughout the majority of tissues in sF than bF. According to the single-cell atlas, *Smnpp40* transcript dominantly occur in neuronal cells, preferentially in the clusters 1, 8, 13, 15, and 21-23 in sF and bF, whereas the transcript level of *Smnpp40* in neuron cluster 1 was found to be higher in sF compared to bF (Wendt et al., 2020, **Supplementary Figure 5D**). My WISH experiments showed quantitative differences between females and males, transcript levels appeared to be higher in bM than in females in neuron clusters 2, 4, 6, 10, 16, and 30. In contrast, lower transcript levels in bM than females occurred in cluster 1. Furthermore, co-localization experiments by double-FISH showed *Smgpcr20* and *Smnpp40* transcripts in cells positioned in the subtegumental area of the head region and along the body, as observed by WISH with these individual genes/transcripts. The positions of the WISH signals for *Smnpp40* in the head region overlapped to some extent with the signals of *Smgpcr20* and *Smnpp26*. In addition, we observed *Smnpp40* signals also around the ootype, where no *Smnpp26* signals occurred by WISH. This ootype localization of *Smnpp40* transcripts coincided with the WISH signals obtained for *Smgpcr20.* Indeed, co-localization experiments by double-FISH showed *Smgpcr20* and *Smnpp40* transcripts in cells surrounding the ootype where no *Smnpp26* signals occurred.

Several studies have shown the localization of neuropeptides in somatic gonad tissue, such as ootype in other organisms. For instance, a neuropeptide of the NPY family was found in the shell glands that are supposed to be involved in egg encapsulation and deposition in *S. mediterranea* (Stunkard, 1951; Shinn, 1993); In *F. hepatica*, FMRFamide-immunoreactive cell bodies have been observed amongst the cells of Mehlis' gland around the ootype (Magee et al.,

1989). In *S. mansoni*, expression of an NPY-like family member has been demonstrated in the region of Mehlis' gland around the ootype (Skuce et al., 1990). Here, according to the multiple sequence alignment, *Sm*NPP26 and *Sm*NPP40 are not homologues of NPY and FMRFamide neuropeptides (**Figure 3.5, 3.6**). Thus, the area surrounding the ootype may be equipped with neuronal cells harboring NPY-like and FMRFamide as well as novel NPP families such as *Sm*NPP40 in parasitic flatworms, which have not yet been classified, even though there are similar peptides in free-living flatworms. Accordingly, from the localization results, we hypothesize that *Sm*GPCR20 in combination with *Sm*NPP40 may have a function in regulating egg-forming processes in the ootype such as contractions, which influence the shape of the schistosome egg. In addition, signals were also found along the uterus (**Figure 3.10**), indicating that *Sm*GPCR20 in combination with *Sm*NPP40 might be also involved in the egg release from the ootype to the environment (Spence and Silk, 1971a; deWalick et al., 2012). This result corresponded to the RNAi phenotype, since *Smgpcr20/Smnpp40* double KD led not only to a decreased number of eggs compared to the control, but also to more abnormally formed eggs, a phenotype also observed upon *Smgpcr20/Smnpp26/Smnpp40* triple KD. This is consistent with previous studies showing that malformed eggs were observed in the ootypes of RNAi-treatment groups by CLSM analyses, also including the *Smgpcr20/Smnpp26* double KD. This suggests an additional role of this neuropeptide for egg formation, although *Smnpp26* transcripts were not localized within the ootype.

Morphologically, the region around the ootype of schistosomes is filled by the Mehlis´ glands, and egg-shell formation is supported by the Mehlis´ glands products that are released in granules into the ootype (Spence and Silk, 1971b; Moczon et al., 1992). However, the list of genes found to be expressed in the Mehlis´ glands according to the single-cell atlas does not contain one of the three genes in focus. In future studies, indirect immunofluorescence experiments using antisera of pancreatic polypeptides including NPY could clarify this (Spence and Silk, 1971b; Skuce et al., 1990). With respect to the transcript presence of the three studied genes in the single-cell atlas, it is tempting to speculate that cells of the clusters 1 and/or 3, in which both *Smgpcr20* and *Smnpp40* are transcribed, may represent the WISH-positive cells circularly surrounding the uterus. Antibody-based mapping of neuropeptides and other marker cells for neuronal clusters may solve this and similar questions in the future.

4.1.5. KD of *Smgpcr20, Smnpp26,* and *Smnpp40* by RNAi

Recently, RNAi has been widely used in adult *S. mansoni* at small-scale (Guidi et al., 2015) and large-scale (Wang et al., 2020b) to KD GOIs. In this study, to characterize *Smgpcr20* and its interaction partners *Smnpp26* and *Smnpp40*, I knocked down the transcripts of *Smgpcr20, Smnpp26,* and *Smnpp40* in paired worms via RNAi and monitored phenotypic effects every two days. In preliminary single-gene RNAi experiments with dsRNA against *Smgpcr20*, or *Smnpp26*, or *Smnpp40*, I detected tendencies towards reduced egg production of bF but without significance (**Figure 3.11**). Provided that *Sm*GPCR20 interacts with both NPPs, I assumed that combinations of dsRNAs against *Smgpcr20/Smnpp26*, *Smgpcr20*/*Smnpp40*, and the combination of all three gene-specific dsRNAs may enhance the phenotype. The obtained results showed a significant decrease of egg production in all RNAi groups. Furthermore, RNAi against *Smgpcr20, Smnpp26,* and *Smnpp40* decreased the length and width of the ovary in females, while a remarkable decline of mature oocytes was found in both double KDs (*Smgpcr20/Smnpp26, Smgpcr20/Smnpp40*), along with a reduction of immature oocytes in the triple KD. However, transcripts of all three genes were not detected in the ovary or other reproductive organs of female worms by WISH. This could be explained by indirect RNAi effects, which may have downregulated neuronal and/or neuromuscular activities, which may influence reproduction-associated processes such as the pairing-controlled maintenance of the developmental status of the ovary including oocyte differentiation.

Of note, in *Drosophila melanogaster* it was shown that molecular communication between the gut and the ovary contributes to the mating-induced activation of gametogenesis in *D. melanogaster* (Ameku et al., 2018). The higher expression levels of *Smgpcr20* and *Smnpp40* in bM than bF (similar levels for *Smnpp26*), suggest that *Smgpcr20* interactions with both *npps* may fulfill a similar male-dependent role in schistosomes. At the physiological (vitality, motility, pairing stability *in vitro*) and morphological levels, there was no visible phenotype in males that provide an explanation for a male-only or male-preferential role of these three genes. However, it may be possible that these three genes contribute to the male´s molecular communication repertoire used for the induction and/or maintenance of female sexual maturation, here mainly the ovary differentiation status.

It is also important to point out that, further to the egg-production and gonad phenotypes observed, my results also showed a negative growth effect in first-time paired females upon KD. *Smgpcr20*/*Smnpp26* double KD and triple KD caused a remarkable decrease of the length

of first-time paired females compared to control females, which were maintained under the same conditions with no dsRNA added. However, this effect was not significant with *Smgpcr20*/*Smnpp40* double KD. Furthermore, I also detected a reduced size of ovaries of females from all RNAi groups compared to the control, this change was more intense in the *Smgpcr20*/*Smnpp26* and triple KD groups than in *Smgpcr20*/*Smnpp40* KD group. Moreover, less mature and immature oocytes were observed in the *Smgpcr20*/*Smnpp26* double KD and triple KD groups, while the number of immature oocytes in the *Smgpcr20*/*Smnpp40* double KD group was comparable to the control but the number of mature oocytes was also lower. Overall, these findings in the ovary were similar to the results of the RNAi approach with pairing-experienced females.

Since egg production and ovary function were both affected, I investigated the RNAi influence on the expression levels of marker genes that were known to be involved in egg synthesis, oocyte differentiation, or stem-cell activities. The egg-shell precursor genes *Sm*p14 (Bobek et al., 1986), *fs800* (Reis et al., 1989), and the egg-synthesis genes *Smtyr1* (Fitzpatrick et al., 2007; deWalick et al., 2012), and *Smtyr2* (Fitzpatrick et al., 2007; deWalick et al., 2012) were significantly down-regulated in the *Smgpcr20*/*Smnpp26* double KD and the triple KD groups. In these two groups, the transcript levels of the germline stem-cell marker *nanos-1* (Wang et al., 2018) and bF expression-biased genes *Smmyst4* (vitellarium marker) (Möscheid et al., in preparation) and *Smsod* (redox marker expressed in the vitellarium) (Cogswell et al., 2011) were also decreased upon RNAi. This corresponded to results obtained after *Smgpcr20*/*Smnpp26* double KD and triple KD which caused negative effects on gonadal stem-cell proliferation. However, the expression levels of the somatic stem-cell marker *nanos-2* (Wang et al., 2018) and GSC progeny marker *Smmeiob* (Wendt et al., 2020) were not affected in first-time paired females upon any dsRNA treatment. Moreover, the expression levels of these genes showed no significant changes in the *Smgpcr20*/*Smnpp40* KD group.

The results of the growth analysis of first-time paired females and RNAi effects on ovaries and oocytes, and the molecular data including WISH indicate that the potential ligands *Sm*NPP26 and *Sm*NPP40 may only in part have similar roles downstream of activating *Sm*GPCR20. Although in all RNAi combinations, egg production was affected in quantity and quality in mature females, differences were found concerning the ovary phenotypes of bF and first-time paired females. Overall, the majority of clear RNAi phenotypes was seen in the *Smgpcr20*/*Smnpp26* double KD group, which suggests that the neuropeptide *Smnpp26* plays a major role in this context. Indeed, roles of neuropeptides for reproduction have also been

investigated in planarians. For instance, the neuropeptide receptor NPYR1 of neuroendocrine cells receives signals from NPY8, which is taking place in the CNS to regulate germline development including GSC differentiation in *S. mediterranea* (Collins et al., 2010; Saberi et al., 2016). *Sm*SOD is a redox protein that belongs to the Cu-Zn superoxide dismutase family and involved in defending cells against reactive oxygen species by converting the superoxide radical to molecular oxygen and hydrogen peroxide (Fridovich, 1975; Cogswell et al., 2011), *Smsod*-mRNA was localized in the vitellarium of the female (Cogswell et al., 2011). The down-regulated expression of *Smsod* indicates that the *Sm*GPCR20-*Sm*NPPs interactions could also be involved in redox processes in the female reproductive system. *Sm*MEIOB has been shown to regulate meiosis progression of GSC progeny (Li et al., 2021). Since no evidence for differential regulation upon RNAi was obtained, it can be concluded that *Sm*GPCR20-*Sm*NPPs interactions may not be engaged in meiosis. In contrast, transcript levels of egg production-associated genes were significantly reduced upon *Smgpcr20*/*Smnpp26* RNAi, which associates with the observed negative effects on egg production in this KD group. In addition, at the morphological level, the ovary showed a reduced size, and oocyte differentiation seemed affected, while no phenotype was found in the vitellarium. Since vitellocytes contain two types of large cytoplasmic inclusions: lipid droplets and vitelline droplets, Oil Red O (labels neutral triglycerides and lipids) or Fast Blue BB (labels vitelline droplets) could be used for future experiments determining the amount of neutral lipids in vitelline cells to clarify an additional effect on the vitellarium (Ramírez-Zacarías et al., 1992; Wang et al., 2019).

4.2. Functional analyses of *Smtdc-1* and *Smddc-1* revealed their roles as male-competence factors for the sexual maturation of the *S. mansoni* female

4.2.1. The hypothesis of male-competence factors in *S. mansoni*

During the last decade, several studies have demonstrated a variety of communication principles among different organisms. This includes parasites and their interactions with the environment (Roditi, 2016). Among these parasites are schistosomes, the only flatworms of mammals that have evolved separate sexes. Although this phenomenon is long known (Severinghaus, 1928; Clough, 1981), unknown are what stimuli may be passed from male to female, and how does the female sense and “interpret” these signals during a pairing contact? And do female factors exist that may induce a kind of male competence, which enables the partner to subsequently induce female sexual maturation? Several transcriptomics studies have delivered comprehensive resources to investigate the impact of pairing on the expressed gene

repertoire of schistosome females and their reproductive biology (Fitzpatrick and Hoffmann, 2006; Cai et al., 2016; Lu et al., 2016; Wang et al., 2017). Results of these studies indicate that the contribution of the male is not restricted to nutritional care and muscular power to transport the female partner lodging inside the male´s gynaecophoric canal, to the final tissue destination, e.g. the mesenteric veins of the gut (*S. mansoni, S. japonicum* and other species) or the bladder plexus (*S. haematobium*). However, our detail knowledge about the bidirectional molecular communication during male-female interaction is still fragmentary (Lu et al., 2019). This interaction seems more complex than previously expected (Gupta and Basch, 1987; Basch and Nicolas, 1989) and involves a flow of information between the partners to direct transcriptional processes in females but also in males, as shown for S. *mansoni* (Fitzpatrick and Hoffmann, 2006; Lu et al., 2016) and *S. japonicum* (Cai et al., 2016). Results of previous studies indicated that pairing-experienced *S. mansoni* bM are able to stimulate mitogenic activity in bF faster than sM without pairing-experience can do (Den Hollander and Erasmus, 1985). In addition, studies also showed that pairing with amputated male worm segments induce development of the female reproductive organs only in regions in contact with the male (Wang et al., 2019). Recently, a first factor involved in this process has been identified, the dipeptide BATT (β-alanyl-tryptamine) which is produced by *Sm*NRPs and secreted into the environment. Treatment of sF worms with this dipeptide partially induced their sexual development of the female in the absence of the male (Chen et al., 2022). These data support the hypothesize of a kind of male molecular competence a male has to reach before it gains the capacity to deliver signals of low size and a hormone-like activity to govern female sexual maturation (Lu et al., 2019).

4.2.2. *Smtdc-1* and *Smddc-1* represent two decarboxylases, respectively, with pairing-dependent expression profiles

To unravel male competence, it is interesting to study genes that show a bM > sM expression pattern, which indicates the relevance of appropriate genes following pairing. Among such genes could be competence factors synthesized by the male to fulfill its bidirectional partner role. Among these GOIs with a bM > sM transcript profile were *Smtdc-1* or *Smddc-1*. This tendency of expression was correspondingly found in SuperSAGE and microarray experiments (Leutner et al., 2013), RNA-seq (Lu et al., 2016), and RT-qPCR analyses of a former (Haeberlein et al., 2019) and this study. According to sequence analyses, Smp_135230 was classified as a L-tyrosine decarboxylase (*Smtdc-1*) and Smp_171580 as a

DOPA decarboxylase (*Smddc-1*), which was supported by our pervious phylogenetic analyses (kindly provided by PD Dr. Simone Haeberlein) (**Supplementary Figure 4**).

To investigate the expression profiles of *Smtdc-1* and *Smddc-1*, RT-qPCR and WISH analyses were performed. The WISH results corresponded to the RT-qPCR data with respect to male-specific/-preferential transcript occurrence, with no or less transcripts in bF or sF. In addition, WISH showed that both genes are localized at the ventral surface area of the male, the gynaecophoric canal. This is consistent with *in situ* hybridization results of a Smp_171580 orthologue of *S. japonicum*, *Sj*AADC (CCD58963.1; EWB00_004068.2) (Wang et al., 2017). Also, *Sj*AADC transcripts localized at the male gynaecophoric canal. For *Smtdc-1* and *Smddc-1*, WISH uncovered a spotty signal pattern in the head region, which together with FISH analysis indicated the transcript occurrence of both genes in neuronal cells. Indeed, in the single-cell atlas for *S. mansoni*, highest transcript levels of both genes were found in cells of the neuron-2 cluster (Wendt et al., 2020, **Supplementary Figure 5E, F**). Taken together with the WISH data obtained, transcripts of *Smtdc-1* and *Smddc-1* probably occur in neuronal cells at the ventral side of the male along the gynaecophoric canal. A similar pattern of ventral cells was recently observed in WISH analyses of *Smnrps+* cells, which were also identified as part of the neuron-2 cluster (**Figure 3.20**). These cells may secrete BATT (**Chapter 4.2.1**), which is at least partly able to induce sF development in the absence of a male worms (Chen et al., 2022). Furthermore, the *Sjaadc* transcript profile exhibited a similar pattern with higher abundance in males between days 14-18 of pairing in *S. japonicum*, while its transcript level remained low and pairing-independent in females. *Sjaadc* was hypothesized as being important for movement, and motility to maintain copulatory activity of male *S. japonicum* (Wang et al., 2017). Similar to this pattern, a meta-analysis of gene expression profiles during *S. mansoni* development showed that the transcript level of *Smtdc-1* is upregulated in the juvenile stage between days 21 and 28, while the transcript level of *Smddc-1* increased already in 24 h old schistosomula (Lu et al., 2018). Moreover, the transcript levels of both genes decreased in females after pairing, while the transcript levels remained high in their male partners.

4.2.3. KD of *Smtdc-1* and *Smddc-1* by RNAi revealed their essential roles during male-female interaction

To gain more insight into their functions, RNAi was performed against *Smtdc-1* and *Smddc-1*. The results exhibited complementing, reproduction-associated phenotypes in the female upon RNAi. Egg production was significantly reduced in both groups of females,

pairing-experienced females that were separated and later re-paired as well as single-sex females paired for the first time. However, there was no significant effect on pairing-stability during the treatment period in both groups. Therefore, the decline in egg-production must have reasons independent of the separation of couples. Further morphological analyses by CLSM showed a substantial decrease of mature oocytes in both female groups following RNAi. This phenotype was also observed in single-gene KD experiments, but it was more pronounced upon simultaneous KD of both transcripts. This finding suggests that both genes fulfill complementary or additive roles in oocyte maturation.

It is also important to point out that these experiments were done using optimized *in vitro*-culture conditions using a medium containing human LDL and a male: female ratio of 1.5:1. These conditions resulted in 100% re-pairing frequency within 2-3 days (Li et al., 2023). Moreover, separation and re-pairing experiments were accompanied by CLSM analyses and showed that a separation period from males for 6-14 days is sufficient for dedifferentiation and the loss of mature oocytes of (previously paired) females. Similarly, previous studies showed a rapid loss in the ability of cultured parasites to generate vitellocytes in the absence of male worms in BM169, a medium that was able to support the *in vitro* growth of larval parasites to adulthood (Basch, 1981; Wang et al., 2019). However, this could vary from worm batch to worm batch, from the culture conditions (including serum source and batch), and from the schistosome strain used. Therefore, female gonad dedifferentiation following the separation of couples should generally be monitored by CLSM (**Supplementary Figure 7**).

Previous BrdU (5-bromo-2'-deoxyuridine) incorporation experiments demonstrated a tremendous decline of mitogenic activity in bF in the absence of male worms within 2-5 days. After re-paring of separated females, a resumption of mitogenic activity was observed after 7 days (Knobloch et al., 2002; Galanti et al., 2012), which corresponds to my results. In addition, my results also meet the hypothesis that the induction of mitogenic activity in females is the first process induced by pairing and a prerequisite for subsequent differentiation processes in the female, especially the gonads (Den Hollander and Erasmus, 1985). In my experiments, oocyte maturation and egg production resumed within 11 days following re-pairing (**Figure 3.16**). Beyond that, the presented *in vitro* pairing approach with (previously) pairing-experienced and for six days separated females, which were reset to a virgin-like female status, this way opens an alternative strategy for experiments with a focus on female-gonad differentiation in case of limited access to virgin females from single-sex infections.

All in all, the results of the RNAi experiments suggest essential roles of *Smtdc-1* and *Smddc-1* for male-female interaction and the pairing-dependent gonad development and differentiation of mature oocytes in female. As male-specifically (*Smtdc-1*) or male-preferentially (*Smddc-1*) and strictly pairing-dependently expressed genes, *Smtdc-1* and *Smddc-1* fulfill the definition of male-competence factors, whose existence has previously been hypothesized (Lu et al., 2019). L-tyrosine decarboxylases and the aromatic-L-amino-acid decarboxylase are potentially involved in the synthesis of BAs like dopamine, serotonin, histamine, and tryptamine, which can act as neurotransmitters. To get first evidence, which BAs may be involved, a rescue experiment with 30 µM dopamine was performed with worms that had been treated with *Smtdc-1* and *Smddc-1* dsRNA. Indeed, RNAi of first-time paired females followed by dopamine addition induced a slight increase in the number of eggs compared with the RNAi-only group, although the observed differences were not statistically significant. Nonetheless, there is first weak evidence that dopamine could be one of the BAs that are synthesized by the enzyme activities of *Smtdc-1* and *Smddc-1*.

Elder studies in *S. mansoni* indicated the presence of biosynthetic pathways for the major BA classes, for BA receptors, and for role of BAs as major modulators of neuromuscular function regulating movement, attachment, and behavior (Pax et al., 1984; Ribeiro et al., 2012). In the 1980s, the presence of serotonin was shown in sensory nerve endings located near the surface of the parasite (Gustafsson, 1987). Finally, bioinformatics analyses suggested the existence of probably 24 BA receptors in *S. mansoni* (Zamanian et al., 2011). Altogether, these results suggest major biological functions of BAs for this parasite. From our data, it appears tempting to speculate that BAs might contribute to the male-dependent control of female sexual maturation. In the absence of a tryptophan decarboxylase- annotated orthologue in *S. mansoni* (according to WormBase ParaSite), one of the putative roles of the aromatic L-amino acid/DOPA decarboxylase *Sm*DDC-1 could be to provide the tryptamine substrate for the nonribosomal peptide synthetase, an enzyme that is expressed in males upon pairing to generate BATT. This is a pheromone-like dipeptide, and it was recently shown that BATT can induce part of the sexual maturation and egg production in sF without pairing (Chen et al., 2022). Even though, compared to untreated bF as control, egg number and quality as well as ovary differentiation were inferior in BATT-only treated but otherwise un-paired sF. This suggests that further factors may be important in conjunction with BATT to organize the sexual maturation of the paired female, and *Smtdc-1* and *Smddc-1* may contribute to this process. In the future, visualizing the spatial distribution of neurotransmitters (dopamine, serotonin,

histamine, and tryptamine), also in *Smtdc-1* and *Smddc-1* KD worms by using high-resolution AP-SMALDI mass spectrometry imaging (Shariatgorji et al., 2014) will be helpful in understanding the hypothesized roles of these neurotransmitters. In addition, a more complete overview of the downstream effects of RNAi against *Smtdc-1* and *Smddc-1* could be achieved by a transcriptomics approach to get an overview about all genes up- or down-regulated upon treatment.

5. Summary

Schistosomes are parasitic flatworms that cause schistosomiasis, a NTD of worldwide importance for human and animal health. Standard treatment of schistosomiasis relies on a single drug, praziquantel (PZQ). However, several reports discussed the possibility of resistance development in *Schistosoma mansoni* against PZQ, and a vaccine is not yet available. Therefore, alternative treatment options are urgently needed, which requires substantial efforts in basic and applied research.

Schistosomes are the only mammalian flatworms that have evolved separate sexes. Furthermore, female development in schistosomes is tightly controlled by the male partner and characterized by a high turn-over of gonadal cells in the female. This finally leads to egg production, which represents the major cause for clinical symptoms and the pathologic consequences of schistosomiasis. In this context, goal of my study was to characterize genes that are involve in the male-female interaction of schistosomes, and which may contribute to female sexual maturation. Previous *omic* studies have detected several genes as being significantly differentially transcribed between pairing experienced males (bM), pairing-unexperienced males (sM), pairing experienced females (bF), and pairing-unexperienced females (sF).

Among these were genes involved in neuronal processes, including some G protein-coupled receptor (GPCR) genes, for which a pairing-influenced transcript occurrence was discovered with high transcript levels in bM, sM, and sF, whereas comparably low or no transcripts of these GPCRs occurred in bF. Besides their interesting roles in controlling diverse biological processes, GPCRs also represent promising targets for new anthelmintics. Although GPCRs represent a prominent receptor class in schistosomes, functional studies are limited as well as our knowledge about their ligands. Candidate ligands are neuropeptides acting as neurotransmitters, neuromodulators, or hormones in the nervous system. Transcriptomics studies in *S. mansoni* indicated that nearly all neuropeptide genes (*Sm_npps*) and a subgroup of GPCRs exhibited sex- and pairing-dependent expression profiles. Among these was the rhodopsin orphan GPCR20 (*Sm*GPCR20), which was characterized in my study. Here, first evidence is provided for specific interactions between *Sm*GPCR20 and two unclassified *Sm_npps*, *Smnpp26*, and *Smnpp40*, using bioinformatics, molecular, physiological, and biochemical approaches. According to functional analyses by RT-qPCR, *Smgpcr20*, *Smnpp26*, and *Smnpp40* showed sex- and/or pairing-influenced transcript profiles. Whole-mount *in situ*

hybridization (WISH) exhibited transcripts of these three genes in neuronal cells, sub-tegumental cells, and the parenchyma of both sexes. Transcripts of these genes co-localized in the anterior "head" region of sF and in particular patterns along the worm body indicating neuronal expression. RNA interference (RNAi) experiments with dsRNAs against these three genes resulted in reduced egg production, while pairing stability was unaffected. Furthermore, confocal microscopy (CLSM) revealed morphologic changes in the female gonads. RNAi in first-time paired females caused a reduced length of females after double RNAi against *Sm*GPCR20 and *Sm*NPP26, and morphological changes in the ovary. In addition, reduced transcript levels of egg formation-associated and gonad-specifically transcribed genes and the stem-cell marker *nanos-1* were found. The obtained results suggest that *Sm*NPP26 and *Sm*NPP40 are potential ligands of *Sm*GPCR20, and they point to a multifaceted role of *Sm*GPCR20 in concert with *Sm*NPP26 and *Sm*NPP40 for the growth of first-time paired females, oogenesis, and egg-production. Therefore, the results obtained in my study contribute to the understanding of Rhodopsin-family GPCRs, their potential ligands, and their potential roles for the biology of *S. mansoni*. Further studies are needed to substantiate the specificity of *Sm*NPP-GPCR20 interaction, e.g., by FRET analysis or related techniques, which will finally lead to its complete deorphanization. With respect to their druggability and the urgent need to find alternative treatment options to fight schistosomiasis, unravelling the biological function(s) of GPCRs will lead us to potential targets for the design of novel drugs - especially when receptors are in focus that exhibit a low homology to their host counterparts.

Further differentially transcribed genes analyzed in my work with an expression bias towards paired males were annotated as decarboxylases (DDC or TDC), Smp_135230 and Smp_171580, enzymes involved in neurotransmitters and neuromodulator synthesis. For both genes, previous RNA-seq analyses showed significantly higher transcript levels in bM compared to sM, and no transcripts occurred in bF or sF. Results of RT-qPCR analyses with RNA from males following pairing, separation, and re-pairing *in vitro* supported the RNA-seq data and demonstrated an influence of pairing on the upregulation of *Smddc-1* in bM. With respect to their male-specific/preferential transcript occurrence, both genes were hypothesized as male-competence factors, which were defined as gender-specifically and/or preferentially as well as pairing-dependently regulated genes transcribed in males to contribute to the induction and/or maintenance of female sexual maturation. According to sequence analyses, Smp_135230 is an L-tyrosine decarboxylase (*Smtdc-1*), while Smp_171580 is a DOPA decarboxylase (*Smddc-1*). Both genes are male-specifically/preferentially transcribed and in a

pairing-dependent manner which was confirmed by RT-qPCR analyses. WISH experiments located transcripts in neuronal cells of the male´s ventral surface, the gynaecophoric canal, which faces the female during pairing. Based on improved *in vitro*-culture conditions for re-pairing experiments of *S. mansoni in vitro*, RNAi experiments against these genes resulted in reduced egg production, which was partly rescued by dopamine treatment. In addition, conclusive evidence was provided that these genes are part of the molecular communication processes between males and female during pairing, and they control ovary differentiation as part of the pairing-induced female sexual maturation.

6. Zusammenfassung

Schistosomen sind parasitäre Plattwürmer, die Schistosomiasis verursachen, eine NTD von weltweiter Bedeutung für die Gesundheit von Mensch und Tier. Die Standardbehandlung der Schistosomiasis beruht auf einem einzigen Medikament, Praziquantel (PZQ). In mehreren Berichten wurde jedoch die Möglichkeit einer Resistenzentwicklung bei *Schistosoma mansoni* gegen PZQ erörtert, und ein Impfstoff ist derzeit nicht verfügbar. Daher werden dringend alternative Behandlungsmöglichkeiten benötigt, was substantielle Anstrengungen in der Grundlagen- und angewandten Forschung erfordert.

Schistosomen sind die einzigen Plattwürmer der Säugetiere, die getrennte Geschlechter entwickelt haben. Darüber hinaus wird die weibliche Entwicklung bei Schistosomen durch den männlichen Partner streng kontrolliert und ist durch einen hohen Umsatz von Gonadenzellen im Weibchen gekennzeichnet. Dies führt schließlich zur Eiproduktion, die die Hauptursache für die klinischen Symptome und die pathologischen Folgen der Schistosomiasis darstellt. In diesem Zusammenhang war das Ziel meiner Studie, Gene zu charakterisieren, die an der Interaktion zwischen Männchen und Weibchen bei Schistosomen beteiligt sind und die möglicherweise zur sexuellen Reifung der Weibchen beitragen. Frühere *omics*-Studien haben gezeigt, dass mehrere Gene zwischen paarungserfahrenen Männchen (bM), paarungsunerfahrenen Männchen (sM), paarungserfahrenen Weibchen (bF) und paarungsunerfahrenen Weibchen (sF) signifikant unterschiedlich transkribiert werden.

Darunter befanden sich Gene, die an neuronalen Prozessen beteiligt sind, einschließlich einiger G-Protein-gekoppelter Rezeptorgene (GPCR), für die ein paarungsabhängiges Transkriptaufkommen mit hohen Transkriptmengen in bM, sM und sF entdeckt wurde, während in bF vergleichsweise geringe oder keine Transkripte dieser GPCRs auftraten. Neben ihrer interessanten Rolle bei der Steuerung verschiedener biologischer Prozesse stellen GPCRs

auch vielversprechende Ziele für neue Anthelminthika dar. Obwohl GPCRs eine wichtige Rezeptorklasse in Schistosomen darstellen, sind funktionelle Studien ebenso begrenzt wie unser Wissen über ihre Liganden. Mögliche Liganden sind Neuropeptide, die als Neurotransmitter, Neuromodulatoren oder Hormone im Nervensystem wirken. *Transcriptomics*-Studien in *S. mansoni* zeigten, dass fast alle Neuropeptidgene (*Sm_npps*) und eine Untergruppe von GPCRs geschlechts- und paarungsabhängige Expressionsprofile aufweisen. Dazu gehörte auch der Rhodopsin-GPCR20 (*Sm*GPCR20), welcher in meiner Studie charakterisiert wurde. Mit Hilfe von bioinformatischen, molekularen, physiologischen und biochemischen Ansätzen wurden erstmals Hinweise auf spezifische Interaktionen zwischen *Sm*GPCR20 und zwei nicht klassifizierten *Sm_npps*, *Smnpp26* und *Smnpp40*, geliefert. Nach funktionellen Analysen mittels RT-qPCR-Analysen zeigten *Smgpcr20*, *Smnpp26* und *Smnpp40* geschlechts- und/oder paarungsabhängige Transkript-profile. Mittels Whole-Mount-In-situ-Hybridisierung (WISH) wurden Transkripte dieser drei Gene in neuronalen Zellen, subtegumentalen Zellen und im Parenchym beider Geschlechter nachgewiesen. Transkripte dieser Gene kolokalisierten in der vorderen "Kopf"-Region von sF und in bestimmten Mustern entlang des Wurmkörpers, die auf eine neuronale Expression hindeuten. RNA-Interferenz (RNAi)-Experimente mit dsRNAs gegen diese drei Gene führten zu einer verringerten Eiproduktion, während die Paarungsstabilität nicht beeinträchtigt wurde. Darüber hinaus zeigte die konfokale Mikroskopie (CLSM) morphologische Veränderungen in den weiblichen Gonaden, vor allem dem Ovar. RNAi in erstmalig gepaarten Weibchen führte zu einer reduzierten Länge der Weibchen nach Doppel-RNAi von *Sm*GPCR20 und *Sm*NPP26 und zu morphologischen Veränderungen im Ovar. Darüber hinaus wurden verringerte Transkriptmengen von mit der Eibildung assoziierten und gonadenspezifisch transkribierten Genen sowie des Stammzellmarkers *nanos-1* festgestellt. Die erzielten Ergebnisse deuten darauf hin, dass *Sm*NPP26 und *Sm*NPP40 potenzielle Liganden von *Sm*GPCR20 sind, und sie deuten auf eine vielschichtige Rolle von *Sm*GPCR20 im Zusammenspiel mit *Sm*NPP26 und *Sm*NPP40 für das Wachstum von erstmals gepaarten Weibchen, die Oogenese und die Eiproduktion hin. Daher tragen die in meiner Studie erzielten Ergebnisse zum Verständnis der GPCRs der Rhodopsin-Familie, ihrer potenziellen Liganden und ihrer möglichen Rolle in der Biologie von *S. mansoni* bei. Weitere Studien sind erforderlich, um die Spezifität der Interaktion zwischen *Sm*NPP und GPCR20 zu belegen, z. B. durch FRET-Analyse oder verwandte Techniken, was schließlich zu seiner vollständigen Deorphanisierung führen wird. Im Hinblick auf die Medikamentenverfügbarkeit und die dringende Notwendigkeit, alternative Behandlungsmöglichkeiten zur Bekämpfung der Bilharziose zu finden, wird uns die

Entschlüsselung der biologischen Funktion(en) der GPCRs zu potenziellen Zielen für die Entwicklung neuer Medikamente führen - insbesondere dann, wenn Rezeptoren im Fokus stehen, die eine geringe Homologie zu ihren Wirts-Pendants aufweisen.

Weitere differenziell transkribierte Gene, die in meiner Arbeit analysiert wurden und deren Expression eher bei gepaarten Männchen auftrat, wurden als Decarboxylasen (DDC oder TDC), Smp_135230 und Smp_171580 annotiert, Enzyme, die an der Synthese von Neurotransmittern und Neuromodulatoren beteiligt sind. Eine frühere RNA-seq-Analyse zeigte für beide Gene signifikant höhere Transkriptmengen in bM im Vergleich zu sM, während in bF oder sF keine Transkripte auftraten. Die Ergebnisse von RT-qPCR-Analysen mit RNA von Männchen nach Paarung, Trennung, und erneuter Paarung *in vitro* bestätigten die RNA-seq-Daten und zeigten einen Einfluss der Paarung auf die Hochregulierung von *Smddc-1* in bM. Im Hinblick auf ihr männchenspezifisches/-präferentielles Transkriptvorkommen wurden beide Gene als Kompetenzfaktoren des Mänchens definiert, d. h. als geschlechtsspezifisch und/oder präferentiell sowie paarungsabhängig regulierte Gene, die in Männchen transkribiert werden und zur Induktion und/oder Aufrechterhaltung der weiblichen Geschlechtsreifung beitragen. Sequenzanalysen zufolge handelt es sich bei Smp_135230 um eine L-Tyrosindecarboxylase (*Smtdc-1*) und bei Smp_171580 um eine DOPA-Decarboxylase (*Smddc-1*). Beide Gene werden männerspezifisch/präferentiell und paarungsabhängig transkribiert, was durch RT-qPCR-Analysen bestätigt wurde. In WISH-Experimenten wurden die Transkripte in neuronalen Zellen der ventralen Oberfläche des Männchens, dem gynäkophoren Kanal, der dem Weibchen während der Paarung zugewandt ist, nachgewiesen. Auf der Grundlage verbesserter *in-vitro*-Kulturbedingungen für Re-Paarungsexperimente von *S. mansoni in vitro* führten RNAi-Experimente gegen diese Gene zu einer verringerten Eiproduktion, die durch eine Dopaminbehandlung teilweise wiederhergestellt werden konnte. Darüber hinaus wurde schlüssig nachgewiesen, dass diese Gene Teil der molekularen Kommunikationsprozesse zwischen Männchen und Weibchen während der Paarung sind und die Differenzierung des Ovars als Teil der paarungsinduzierten weiblichen Geschlechtsreifung steuern.

7. References

Adekiya, T.A., Aruleba, R.T., Oyinloye, B.E., Okosun, K.O., and Kappo, A.P. (2019). The effect of climate change and the snail-schistosome cycle in transmission and bio-control of schistosomiasis in sub-Saharan Africa. *Int J Environ Res Public Health* 17(1), 181. doi: 10.3390/ijerph17010181.

Amare, A., Hummon, A.B., Southey, B.R., Zimmerman, T.A., Rodriguez-Zas, S.L., and Sweedler, J.V. (2006). Bridging neuropeptidomics and genomics with bioinformatics: Prediction of mammalian neuropeptide prohormone processing. *J Proteome Res* 5(5), 1162-1167. doi: 10.1021/pr0504541.

Ameku, T., Yoshinari, Y., Texada, M.J., Kondo, S., Amezawa, K., Yoshizaki, G., et al. (2018). Midgut-derived neuropeptide F controls germline stem cell proliferation in a mating-dependent manner. *PLoS Biol* 16(9), e2005004. doi: 10.1371/journal.pbio.2005004.

Attwood, T. K., and Findlay, J. B. (1994). Fingerprinting G-protein-coupled receptors. *Protein engineering*, 7(2), 195–203. doi: 10.1093/protein/7.2.195.

Attwood, T.K., Bradley, P., Flower, D.R., Gaulton, A., Maudling, N., Mitchell, A.L., et al. (2003). PRINTS and its automatic supplement, prePRINTS. *Nucleic Acids Res.* 31(1), 400-402. doi: 10.1093/nar/gkg030.

Barakat, R., and El Morshedy, H. (2011). Efficacy of two praziquantel treatments among primary school children in an area of high *Schistosoma mansoni* endemicity, Nile Delta, Egypt. *Parasitology* 138(4), 440-446. doi: 10.1017/s003118201000154x.

Basch, P.F. (1981). Cultivation of *Schistosoma mansoni in vitro*. I. Establishment of cultures from cercariae and development until pairing. *J Parasitol* 67(2), 179-185. doi: 10.2307/3280632.

Basch P.F., and Nicolas C. (1989). *Schistosoma mansoni*: pairing of male worms with artificial surrogate females. *Exp Parasitol* 68(2):202-7. doi: 10.1016/0014-4894(89)90098-2

Beckmann, S., and Grevelding, C.G. (2010). Imatinib has a fatal impact on morphology, pairing stability and survival of adult *Schistosoma mansoni in vitro*. *Int J Parasitol* 40(5), 521-526. doi: 10.1016/j.ijpara.2010.01.007.

Bergquist, R., and McManus, D.P. (2017). "Schistosomiasis vaccine development: the missing link," in *Schistosoma*. CRC Press, 470-486. doi: https://www.taylorfrancis.com/chapters/edit/10.1201/9781315368900-29.

Bergquist, R., Utzinger, J., and Keiser, J. (2017). Controlling schistosomiasis with praziquantel: How much longer without a viable alternative? *Infect Dis Poverty* 6(1), 74. doi: 10.1186/s40249-017-0286-2.

Berlin, S., Keren-Raifman, T., Castel, R., Rubinstein, M., Dessauer, C. W., Ivanina, T., and Dascal, N. (2010). G alpha(i) and G betagamma jointly regulate the conformations of a G betagamma effector, the neuronal G protein-activated K^+ channel (GIRK). *J Biol Chem* 285(9), 6179-6185. doi: 10.1074/jbc.M109.085944.

Berriman, M., Haas, B.J., LoVerde, P.T., Wilson, R.A., Dillon, G.P., Cerqueira, G.C., et al. (2009). The genome of the blood fluke *Schistosoma mansoni*. *Nature* 460(7253), 352-358. doi: 10.1038/nature08160.

Bertoldi, M. (2014). Mammalian Dopa decarboxylase: structure, catalytic activity and inhibition. *Arch Biochem Biophys* 546, 1-7. doi: 10.1016/j.abb.2013.12.020.

Bobek, L., Rekosh, D.M., Van Keulen, H., and LoVerde, P.T. (1986). Characterization of a female-specific cDNA derived from a developmentally regulated mRNA in the human blood fluke *Schistosoma mansoni. Proc Natl Acad Sci U S A* 83(15), 5544-5548. doi: 10.1073/pnas.83.15.5544.

Boissier, J., Grech-Angelini, S., Webster, B.L., Allienne, J. F., Huyse, T., Mas-Coma, S., et al. (2016). Outbreak of urogenital schistosomiasis in *Corsica* (France): an epidemiological case study. *Lancet Infect. Dis* 16(8), 971-979. doi: 10.1016/S1473-3099(16)00175-4.

Booden, M.A., Siderovski, D.P., and Der, C.J. (2002). Leukemia-associated Rho guanine nucleotide exchange factor promotes G alpha q-coupled activation of RhoA. *Mol Cell Biol* 22(12), 4053-4061. doi: 10.1128/mcb.22.12.4053-4061.2002.

Boyer, J.L., Waldo, G.L., and Harden, T.K. (1992). Beta gamma-subunit activation of G-protein-regulated phospholipase C. *J Biol Chem* 267(35), 25451-25456. doi: https://doi.org/10.1016/S0021-9258(19)74062-9.

Boyle, J.P., Zaide, J.V., and Yoshino, T.P. (2000). *Schistosoma mansoni*: effects of serotonin and serotonin receptor antagonists on motility and length of primary sporocysts *in vitro*. *Exp Parasitol* 94(4), 217-226. doi: 10.1006/expr.2000.4500.

Bradbury, A.F., and Smyth, D.G. (1991). Peptide amidation. *Trends Biochem Sci* 16(3), 112-115. doi: 10.1016/0968-0004(91)90044-v.

Bruce, J.I.E., Straub, S.V., and Yule, D.I. (2003). Crosstalk between cAMP and Ca^{2+} signaling in non-excitable cells. *Cell Calcium* 34(6), 431-444. doi: 10.1016/s0143-4160(03)00150-7.

Buddenborg, S.K., Tracey, A., Berger, D.J., Lu, Z., Doyle, S.R., Fu, B., et al. (2021). Assembled chromosomes of the blood fluke *Schistosoma mansoni* provide insight into the evolution of its ZW sex-determination system. *bioRxiv*, 2021.2008.2013.456314. doi: 10.1101/2021.08.13.456314.

Budke, C.M., White, A.C., Jr., and Garcia, H.H. (2009). Zoonotic larval cestode infections: neglected, neglected tropical diseases? *PLoS Negl Trop Dis* 3(2), e319. doi: 10.1371/journal.pntd.0000319.

Cai, P., Liu, S., Piao, X., Hou, N., Gobert, G.N., McManus, D.P., et al. (2016). Comprehensive transcriptome analysis of sex-biased expressed genes reveals discrete biological and physiological features of male and female *Schistosoma japonicum*. *PLoS Negl Trop Dis* 10(4), e0004684. doi: 10.1371/journal.pntd.0004684.

Campos, R., Moreira, A.A., Sette, H., Jr., Chamone, D.A., and Da Silva, L.C. (1976). Hycanthone resistance in a human strain of *Schistosoma mansoni*. *Trans R Soc Trop Med Hyg* 70(3), 261-262. doi: 10.1016/0035-9203(76)90061-4.

Campos, T.D., Young, N.D., Korhonen, P.K., Hall, R.S., Mangiola, S., Lonie, A., et al. (2014). Identification of G protein-coupled receptors in *Schistosoma haematobium* and *S. mansoni* by comparative genomics. *Parasit Vectors* 7, 242. doi: 10.1186/1756-3305-7-242.

Camps, M., Carozzi, A., Schnabel, P., Scheer, A., Parker, P.J., and Gierschik, P. (1992). Isozyme-selective stimulation of phospholipase C-β2 by G protein βγ-subunits. *Nature* 360(6405), 684-686. doi: 10.1038/360684a0.

Catalano, S., Sène, M., Diouf, N.D., Fall, C.B., Borlase, A., Léger, E., et al. (2018). Rodents as natural hosts of zoonotic *Schistosoma* species and hybrids: An epidemiological and evolutionary perspective from west Africa. *J Infect Dis* 218(3), 429-433. doi: 10.1093/infdis/jiy029.

Catto, B.A., and Ottesen, E.A. (1979). Serotonin uptake in schistosomules of *Schistosoma mansoni*. *Comp Biochem Physiol C Comp Pharmacol* 63(2), 235-242. doi: 10.1016/0306-4492(79)90067-4.

Chase, D.L., and Koelle, M.R. (2007). Biogenic amine neurotransmitters in *C. elegans*. *WormBook*. doi:10.1895/wormbook.1.132.1.

Chen, L.L., Rekosh, D.M., and LoVerde, P.T. (1992). *Schistosoma mansoni* p48 eggshell protein gene: characterization, developmentally regulated expression and comparison to the p14 eggshell protein gene. *Mol Biochem Parasitol* 52(1), 39-52. doi: 10.1016/0166-6851(92)90034-h.

Chen, R., Wang, J., Gradinaru, I., Vu, H.S., Geboers, S., Naidoo, J., et al. (2022). A male-derived nonribosomal peptide pheromone controls female schistosome development. *Cell* 185(9), 1506-1520.e17. doi: 10.1016/j.cell.2022.03.017.

Cioli, D., Pica-Mattoccia, L., and Archer, S. (1995). Antischistosomal drugs: Past, present … and future? *Pharmacol Ther* 68(1), 35-85. doi: 10.1016/0163-7258(95)00026-7.

Cioli, D., Pica-Mattoccia, L., Basso, A., and Guidi, A. (2014). Schistosomiasis control: praziquantel forever? *Mol Biochem Parasitol* 195(1), 23-29. doi: https://doi.org/10.1016/j.molbiopara.2014.06.002.

Clough E. R. (1981). Morphology and reproductive organs and oogenesis in bisexual and unisexual transplants of mature *Schistosoma mansoni* females. *Int J Parasitol* 67(4), 535-539. doi: https://pubmed.ncbi.nlm.nih.gov/7264839/.

Cogswell, A.A., Collins, J.J., Newmark, P.A., and Williams, D.L. (2011). Whole mount *in situ* hybridization methodology for *Schistosoma mansoni*. *Mol Biochem Parasitol* 178(1), 46-50. doi: 10.1016/j.molbiopara.2011.03.001.

Collins, J.J., 3rd, Wang, B., Lambrus, B.G., Tharp, M.E., Iyer, H., and Newmark, P.A. (2013). Adult somatic stem cells in the human parasite *Schistosoma mansoni*. *Nature* 494(7438),

476-479. doi: 10.1038/nature11924.

Collins, J.J., Hou, X., Romanova, E.V., Lambrus, B.G., Miller, C.M., Saberi, A., et al. (2010). Genome-wide analyses reveal a role for peptide hormones in planarian germline development. *PLoS Biol* 8(10), e1000509. doi: 10.1371/journal.pbio.1000509.

Cooper, D.M., Mons, N., and Karpen, J.W. (1995). Adenylyl cyclases and the interaction between calcium and cAMP signaling. *Nature* 374(6521), 421-424. doi: 10.1038/374421a0.

Da Silva, L.C., Chieffi, P.P., and Carrilho, F.J. (2005). Schistosomiasis *mansoni* -- clinical features. *Gastroenterol Hepatol* 28(1), 30-39. doi: 10.1157/13070382.

De Bont, J., and Vercruysse, J. (1997). The epidemiology and control of cattle schistosomiasis. *Parasitol Today* 13(7), 255-262. doi: 10.1016/s0169-4758(97)01057-0.

De Luca, M., Roshina, N.V., Geiger-Thornsberry, G.L., Lyman, R.F., Pasyukova, E.G., and Mackay, T.F. (2003). Dopa decarboxylase (Ddc) affects variation in *Drosophila* longevity. *Nat Genet* 34(4), 429-433. doi: 10.1038/ng1218.

Den Hollander, J.E., and Erasmus, D.A. (1985). *Schistosoma mansoni*: male stimulation and DNA synthesis by the female. *Parasitology* 91 (Pt 3), 449-457. doi: 10.1017/s0031182000062697.

Dettman, C.D., Higgins-Opitz, S.B., and Saikoolal, A. (1989). Enhanced efficacy of the paddling method for schistosome infection of rodents by a four-step pre-soaking procedure. *Parasitol Res* 76(2), 183-184. doi: 10.1007/BF00930846.

deWalick, S., Tielens, A.G.M., and van Hellemond, J.J. (2012). *Schistosoma mansoni*: The egg, biosynthesis of the shell and interaction with the host. *Exp Parasitol* 132(1), 7-13. doi: 10.1016/j.exppara.2011.07.018.

Dias, L.C., and Olivier, C.E. (1986). Failure at inducing resistance to schistosomicidal drugs in a Brazilian human strain of *Schistosoma mansoni*. *Rev Inst Med Trop Sao Paulo* 28(5), 352-357. doi: 10.1590/s0036-46651986000500010.

Diaz Soria, C.L., Lee, J., Chong, T., Coghlan, A., Tracey, A., Young, M.D., et al. (2020). Single-cell atlas of the first intra-mammalian developmental stage of the human parasite *Schistosoma mansoni*. *Nat Commun* 11(1), 6411. doi: 10.1038/s41467-020-20092-5.

Dorak, M. (Ed.). (2006). Real-time PCR. *Taylor & Francis*. doi: https://doi.org/10.4324/9780203967317.

Duckert, P., Brunak, S., and Blom, N. (2004). Prediction of proprotein convertase cleavage sites. *Protein Eng Des Sel* 17(1), 107-112. doi: 10.1093/protein/gzh013.

Duvall, R.H., and DeWitt, W.B. (1967). An improved perfusion technique for recovering adult schistosomes from laboratory animals. *Am J Trop Med Hyg* 16(4), 483-486. doi: 10.4269/ajtmh.1967.16.483.

El-Sakkary, N., Chen, S., Arkin, M.R., Caffrey, C.R., and Ribeiro, P. (2018). Octopamine signaling in the metazoan pathogen *Schistosoma mansoni*: localization, small-molecule screening and opportunities for drug development. *Dis Model Mech* 11(7). doi: 10.1242/dmm.033563.

El-Shehabi, F., and Ribeiro, P. (2010). Histamine signaling in *Schistosoma mansoni*: immunolocalisation and characterisation of a new histamine-responsive receptor (*Sm*GPR-2). *Int J Parasitol* 40(12), 1395-1406. doi: 10.1016/j.ijpara.2010.04.006.

El-Shehabi, F., Taman, A., Moali, L.S., El-Sakkary, N., and Ribeiro, P. (2012). A novel G protein-coupled receptor of *Schistosoma mansoni* (*Sm*GPR-3) is activated by dopamine and is widely expressed in the nervous system. *PLoS Negl Trop Dis* 6(2), e1523. doi: 10.1371/journal.pntd.0001523.

El-Shehabi, F., Vermeire, J.J., Yoshino, T.P., and Ribeiro, P. (2009). Developmental expression analysis and immunolocalization of a biogenic amine receptor in *Schistosoma mansoni*. *Exp Parasitol* 122(1), 17-27. doi: 10.1016/j.exppara.2009.01.001.

Fitzpatrick, J.M., Hirai, Y., Hirai, H., and Hoffmann, K.F. (2007). Schistosome egg production is dependent upon the activities of two developmentally regulated tyrosinases. *FASEB J* 21(3), 823-835. doi: 10.1096/fj.06-7314com.

Fitzpatrick, J.M., and Hoffmann, K.F. (2006). Dioecious *Schistosoma mansoni* express divergent gene repertoires regulated by pairing. *Int J Parasitol* 36(10-11), 1081-1089. doi: 10.1016/j.ijpara.2006.06.007.

Foskett. J.K., White. C., Cheung. K.H., and Mak, D.O. (2007). Inositol trisphosphate receptor $Ca2^{+}$ release channels. *Physiol Rev* 87(2), 593-658. doi: 10.1152/physrev.00035.2006.

Ford, C. E., Skiba, N. P., Bae, H., Daaka, Y., Reuveny, E., Shekter, L. R., Rosal, R., Weng, G., Yang, C. S., Iyengar, R., Miller, R. J., Jan, L. Y., Lefkowitz, R. J., and Hamm, H.E. (1998). Molecular basis for interactions of G protein betagamma subunits with effectors. *Science* 280(5367), 1271-1274. doi: 10.1126/science.280.5367.1271.

Fraguas, S., Barberán, S., Ibarra, B., Stöger, L., and Cebrià, F. (2012). Regeneration of neuronal cell types in *Schmidtea mediterranea*: an immunohistochemical and expression study. *Int J Dev Biol* 56(1-3), 143-153. doi: 10.1387/ijdb.113428sf.

Fredriksson, R., Lagerström, M.C., Lundin, L.G., and Schiöth, H.B. (2003). The G-protein-coupled receptors in the human genome form five main families. Phylogenetic analysis, paralogon groups, and fingerprints. *Mol Pharmacol* 63(6), 1256-1272. doi: 10.1124/mol.63.6.1256.

Fridovich, I. (1975). Superoxide dismutases. *Annu Rev Biochem* 44, 147-159. doi: 10.1146/annurev.bi.44.070175.001051.

Galanti, S.E., Huang, S.C.C., and Pearce, E.J. (2012). Cell death and reproductive regression in female *Schistosoma mansoni*. *PLoS Negl Trop Dis* 6(2), e1509. doi: 10.1371/journal.pntd.0001509.

Gasser, R.B., Morahan, G., and Mitchell, G.F. (1991). Sexing single larval stages of *Schistosoma mansoni* by polymerase chain reaction. *Mol Biochem Parasitol* 47(2), 255-258. doi: 10.1016/0166-6851(91)90187-b.

Geary T.G., and Maule A.G. (2010). Neuropeptide systems as targets for parasite and pest control. Preface. *Adv Exp Med Biol* 692:v-vi. doi: https://pubmed.ncbi.nlm.nih.gov/21189670/.

Gilman, A.G. (1987). G proteins: transducers of receptor-generated signals. *Annu Rev Biochem* 56, 615-649. doi: 10.1146/annurev.bi.56.070187.003151.

Gonnert, R. (1955a). Schistosomiasis studies. II. Oogenesis of *Schistosoma mansoni* and the development of the eggs in the host organism. *Z Tropenmed Parasitol* 6(1), 33-52. doi: https://pubmed.ncbi.nlm.nih.gov/14387065/.

Gonnert, R. (1955b). Schistosomiasis studies. I. Contributions to the anatomy and histology of *Schistosoma mansoni*. *Z Tropenmed Parasitol* 6(1), 18-33. doi: https://pubmed.ncbi.nlm.nih.gov/14387064/.

Gray, D.J., McManus, D.P., Li, Y., Williams, G.M., Bergquist, R., and Ross, A.G. (2010). Schistosomiasis elimination: lessons from the past guide the future. *Lancet Infect Dis* 10(10), 733-736. doi: 10.1016/S1473-3099(10)70099-2.

Grevelding, C.G. (1995). The female-specific W1 sequence of the Puerto Rican strain of *Schistosoma mansoni* occurs in both genders of a Liberian strain. *Mol Biochem Parasitol* 71(2), 269-272. doi: 10.1016/0166-6851(94)00058-u.

Grevelding, C.G., Sommer, G., and Kunz, W. (1997). Female-specific gene expression in *Schistosoma mansoni* is regulated by pairing. *Parasitology* 115(6), 635-640. doi: 10.1017/S0031182097001728.

Grevelding, C. G. (2004). *Schistosoma*. *Curr Biol* 14(14), R545. doi: 10.1016/j.cub.2004.07.006.

Guidi, A., Mansour, N.R., Paveley, R.A., Carruthers, I.M., Besnard, J., Hopkins, A.L., et al. (2015). Application of RNAi to genomic drug target validation in schistosomes. *PLoS Negl Trop Dis* 9(5), e0003801. doi: 10.1371/journal.pntd.0003801.

Gupta B.C., and Basch P.F. (1987). Evidence for transfer of a glycoprotein from male to female *Schistosoma mansoni* during pairing. *J Parasitol* 73(3), 674-675. doi: https://pubmed.ncbi.nlm.nih.gov/3298604/.

Gustafsson, M.K. (1987). Immunocytochemical demonstration of neuropeptides and serotonin in the nervous systems of adult *Schistosoma mansoni*. *Parasitol Res* 74(2), 168-174. doi: 10.1007/bf00536029.

Haeberlein, S., Angrisano, A., Quack, T., Lu, Z., Kellershohn, J., Blohm, A., et al. (2019). Identification of a new panel of reference genes to study pairing-dependent gene expression in *Schistosoma mansoni*. *Int J Parasitol* 49(8), 615-624. doi: 10.1016/j.ijpara.2019.01.006.

Hahnel, S., Quack, T., Parker-Manuel, S.J., Lu, Z., Vanderstraete, M., Morel, M., et al. (2014). Gonad RNA-specific RT-qPCR analyses identify genes with potential functions in

schistosome reproduction such as *Sm*Fz1 and *Sm*FGFRs. *Front Genet* 5, 170. doi: 10.3389/fgene.2014.00170.

Hahnel, S., Wheeler, N., Lu, Z., Wangwiwatsin, A., McVeigh, P., Maule, A., et al. (2018). Tissue-specific transcriptome analyses provide new insights into GPCR signaling in adult *Schistosoma mansoni*. *PLoS Pathog* 14(1), e1006718. doi: 10.1371/journal.ppat.1006718.

Hallgren, J., Tsirigos, K.D., Pedersen, M.D., Almagro Armenteros, J.J., Marcatili, P., Nielsen, H., et al. (2022). DeepTMHMM predicts alpha and beta transmembrane proteins using deep neural networks. *bioRxiv*, 2022.2004.2008.487609. doi: 10.1101/2022.04.08.487609.

Halton, D.W., and Maule, A.G. (2004). Flatworm nerve–muscle: structural and functional analysis. *Can J Zool* 82(2), 316-333. doi: 10.1139/z03-221.

Hamdan, F.F., Abramovitz, M., Mousa, A., Xie, J., Durocher, Y., and Ribeiro, P. (2002). A novel *Schistosoma mansoni* G protein-coupled receptor is responsive to histamine. *Mol Biochem Parasitol* 119(1), 75-86. doi: 10.1016/s0166-6851(01)00400-5.

Hauser, A.S., Attwood, M.M., Rask-Andersen, M., Schiöth, H.B., and Gloriam, D.E. (2017). Trends in GPCR drug discovery: new agents, targets and indications. *Nat Rev Drug Discov* 16(12), 829-842. doi: 10.1038/nrd.2017.178.

Hoffmann, K.F., Davis, E.M., Fischer, E.R., and Wynn, T.A. (2001). The guanine protein coupled receptor rhodopsin is developmentally regulated in the free-living stages of *Schistosoma mansoni*. *Mol Biochem Parasitol* 112(1), 113-123. doi: 10.1016/s0166-6851(00)00352-2.

Hofmann, L., and Palczewski, K. (2015). The G protein-coupled receptor rhodopsin: a historical perspective. *Methods Mol Biol* 1271, 3-18. doi: 10.1007/978-1-4939-2330-4_1.

Holden-Dye, L., and Walker, R.J. (2007). Anthelmintic drugs. *WormBook*, 1-13. doi: 10.1895/wormbook.1.143.1.

Holtfreter, M., Moné, H., Müller-Stöver, I., Mouahid, G., and Richter, J. (2014). *Schistosoma haematobium* infections acquired in Corsica, France, August 2013. *Euro Surveill* 19(22). doi: 10.2807/1560-7917.es2014.19.22.20821.

Honeycutt, J., Hammam, O., Fu, C.L., and Hsieh, M.H. (2014). Controversies and challenges in research on urogenital schistosomiasis-associated bladder cancer. *Trends Parasitol* 30(7), 324-332. doi: 10.1016/j.pt.2014.05.004.

Hook, V., Funkelstein, L., Lu, D., Bark, S., Wegrzyn, J., and Hwang, S.R. (2008). Proteases for processing proneuropeptides into peptide neurotransmitters and hormones. *Annu Rev Pharmacol Toxicol* 48, 393-423. doi: 10.1146/annurev.pharmtox.48.113006.094812.

Hotez, P. (2008). Hookworm and poverty. *Ann N Y Acad Sci* 1136, 38-44. doi: 10.1196/annals.1425.000.

Huang, C. L., Slesinger, P. A., Casey, P. J., Jan, Y. N., and Jan, L. Y. (1995). Evidence that direct binding of G beta gamma to the GIRK1 G protein-gated inwardly rectifying K^+ channel is important for channel activation. *Neuron* 15(5), 1133-1143. doi: 10.1016/0896-6273(95)90101-9.

Houhou, H., Puckelwaldt, O., Strube, C., and Haeberlein, S. (2019). Reference gene analysis and its use for kinase expression profiling in *Fasciola hepatica*. *Sci Rep* 9(1), 15867. doi: 10.1038/s41598-019-52416-x.

Howe, K.L., Bolt, B.J., Shafie, M., Kersey, P., and Berriman, M. (2017). WormBase ParaSite - a comprehensive resource for helminth genomics. *Mol Biochem Parasitol* 215, 2-10. doi: 10.1016/j.molbiopara.2016.11.005.

Humphries, J.E., Kimber, M.J., Barton, Y.W., Hsu, W., Marks, N.J., Greer, B., et al. (2004). Structure and bioactivity of neuropeptide F from the human *parasites Schistosoma mansoni* and *Schistosoma japonicum*. *J Biol Chem* 279(38), 39880-39885. doi: 10.1074/jbc.M405624200.

Jiang, Y., Ma, W., Wan, Y., Kozasa, T., Hattori, S., and Huang, X.Y. (1998). The G protein Gα12 stimulates Bruton's tyrosine kinase and a rasGAP through a conserved PH/BM domain. *Nature* 395(6704), 808-813. doi: 10.1038/27454.

Kakkar, R., Raju, R.V.S., and Sharma, R.K. (1999). Calmodulin-dependent cyclic nucleotide phosphodiesterase (PDE1). *Cell Mol Life Sci* 55(8), 1164-1186. doi: 10.1007/s000180050364.

Kamara, I. K., Thao, J. T., Kaur, K., Wheeler, N. J., and Chan, J. D. (2023). Annotation of G-Protein Coupled Receptors in the Genomes of Parasitic Blood Flukes. *Micro Publ Biol* 2023. doi: 10.17912/micropub.biology.000704.

Katz, N., Dias, E., Araújo, N., and Souza, C. (1973). Estudo de uma cepa humana de *Schistosoma mansoni* resistente a agentes esquistossomicidas. *Rev Soc Bras Med Trop* 7, 381-387. doi: 10.1590/S0037-86821973000600008.

Kenne, E., Rasmuson, J., Renné, T., Vieira, M.L., Müller-Esterl, W., Herwald, H., et al. (2019). Neutrophils engage the kallikrein-kinin system to open up the endothelial barrier in acute inflammation. *Faseb j* 33(2), 2599-2609. doi: 10.1096/fj.201801329R.

Knobloch, J., Kunz, W., and Grevelding, C. G. (2002). Quantification of DNA synthesis in multicellular organisms by a combined DAPI and BrdU technique. *Dev Growth Differ* 44(6), 559-563. doi: 10.1046/j.1440-169x.2002.00667.x.

Koslow, S.H., and Butler, I.J. (1977). Biogenic amine synthesis defect in dihydropteridine reductase deficiency. *Science* 198(4316), 522-523. doi:10.1126/science.20665.

Kouadio, J.N., Giovanoli Evack, J., Achi, L.Y., Fritsche, D., Ouattara, M., Silué, K.D., et al. (2020). Prevalence and distribution of livestock schistosomiasis and fascioliasis in Côte d'Ivoire: results from a cross-sectional survey. *BMC Vet Res* 16(1), 446. doi: 10.1186/s12917-020-02667-y.

Koziol, U., Koziol, M., Preza, M., Costábile, A., Brehm, K., and Castillo, E. (2016). De novo discovery of neuropeptides in the genomes of parasitic flatworms using a novel comparative approach. *Int J Parasitol* 46(11), 709-721. doi: 10.1016/j.ijpara.2016.05.007.

Krautz-Peterson, G., Radwanska, M., Ndegwa, D., Shoemaker, C.B., and Skelly, P.J. (2007). Optimizing gene suppression in schistosomes using RNA interference. *Mol Biochem Parasitol* 153(2), 194-202. doi: 10.1016/j.molbiopara.2007.03.006.

Krishnan, A., Almén, M.S., Fredriksson, R., and Schiöth, H.B. (2012). The origin of GPCRs: identification of mammalian like Rhodopsin, Adhesion, Glutamate and Frizzled GPCRs in fungi. *PLoS One* 7(1), e29817. doi: 10.1371/journal.pone.0029817.

Kumari, N., Reabroi, S., and North, B.J. (2021). Unraveling the molecular nexus between GPCRs, ERS, and EMT. *Mediators Inflamm* 2021, 6655417. doi: 10.1155/2021/6655417.

Kunz, W. (2001). Schistosome male-female interaction: induction of germ-cell differentiation. *Trends Parasitol* 17(5), 227-231. doi: 10.1016/s1471-4922(01)01893-1.

Lange, A.B. (2009). Tyramine: from octopamine precursor to neuroactive chemical in insects. *Gen Comp Endocrinol* 162(1), 18-26. doi: 10.1016/j.ygcen.2008.05.021.

Larhammar, D., Blomqvist, A.G., and Wahlestedt, C. (1993). The receptor revolution--multiplicity of G-protein-coupled receptors. *Drug Des Discov* 9(3-4), 179-188. doi: https://pubmed.ncbi.nlm.nih.gov/8400001/.

Lecová, L., Stuchlíková, L., Prchal, L., and Skálová, L. (2014). Monepantel: the most studied new anthelmintic drug of recent years. *Parasitology* 141(13), 1686-1698. doi: 10.1017/s0031182014001401.

Lefkowitz, R.J., Rockman, H.A., and Koch, W.J. (2000). Catecholamines, cardiac β-adrenergic receptors, and heart failure. *Circulation* 101(14), 1634-1637. doi: doi:10.1161/01.CIR.101.14.1634.

Leutner, S., Oliveira, K.C., Rotter, B., Beckmann, S., Buro, C., Hahnel, S., et al. (2013). Combinatory microarray and SuperSAGE analyses identify pairing-dependently transcribed genes in *Schistosoma mansoni* males, including follistatin. *PLoS Negl Trop Dis* 7(11), e2532. doi: 10.1371/journal.pntd.0002532.

Li, C. (2005). The ever-expanding neuropeptide gene families in the nematode *Caenorhabditis elegans*. *Parasitology* 131(S1), S109-S127. doi: 10.1017/S0031182005009376.

Li, C., and Kim, K. (2008). Neuropeptides. *WormBook*, 1-36. doi: 10.1895/wormbook.1.142.1.

Li, C., Nelson, L.S., Kim, K., Nathoo, A., and Hart, A.C. (1999). Neuropeptide gene families in the nematode *Caenorhabditis elegans*. *Ann N Y Acad Sci* 897, 239-252. doi: 10.1111/j.1749-6632.1999.tb07895.x.

Li, H., Liang, Y., Dai, J., Wang, W., Qu, G., Li, Y., et al. (2011). Studies on resistance of *Schistosoma* to praziquantel XIV experimental comparison of susceptibility to praziquantel between PZQ-resistant isolates and PZQ-susceptible isolates of

Schistosoma japonicum in stages of adult worms, miracidia and cercariae. *Zhongguo Xue Xi Chong Bing Fang Zhi Za Zhi* 23(6), 611-619. doi: http://www.zgxfzz.com/EN/Y2011/V23/I6/611.

Li, J., Gao, J., Han, L., Zhang, Y., Guan, W., Zhou, L., et al. (2016). Development of a membrane-anchored ligand and receptor yeast two-hybrid system for ligand-receptor interaction identification. *Sci Rep* 6(1), 35631. doi: 10.1038/srep35631.

Li, P., Nanes Sarfati, D., Xue, Y., Yu, X., Tarashansky, A.J., Quake, S.R., et al. (2021). Single-cell analysis of *Schistosoma mansoni* identifies a conserved genetic program controlling germline stem cell fate. *Nat Commun* 12(1), 485. doi: 10.1038/s41467-020-20794-w.

Li, W., Kennedy, S.G., and Ruvkun, G. (2003). daf-28 encodes a *C. elegans* insulin superfamily member that is regulated by environmental cues and acts in the DAF-2 signaling pathway. *Genes Dev* 17(7), 844-858. doi: 10.1101/gad.1066503.

Li, X., Weth, O., Haeberlein, S., and Grevelding, C.G. (2023). Molecular characterization of *Smtdc-1* and *Smddc-1* discloses roles as male-competence factors for the sexual maturation of *Schistosoma mansoni* females. *Front Cell Infect Microbiol* 13. doi: 10.3389/fcimb.2023.1173557.

Liu, N., Li, T., Wang, Y., and Liu, S. (2021). G-protein coupled receptors (GPCRs) in insects-a potential target for new insecticide development. *Molecules* 26(10). doi: 10.3390/molecules26102993.

Livak, K. J., and Schmittgen, T. D. (2001). Analysis of relative gene expression data using real-time quantitative PCR and the 2(-Delta Delta C(T)) Method. *Methods* 25(4), 402-408. doi: 10.1006/meth.2001.1262.

LoVerde, P.T. (2019). Schistosomiasis. *Adv Exp Med Biol* 1154, 45-70. doi: 10.1007/978-3-030-18616-6_3.

LoVerde, P.T., Niles, E.G., Osman, A., and Wu, W. (2004). *Schistosoma mansoni* male-female interactions. *Can J Zool* 82(2), 357-374. doi: 10.1139/z03-217.

Lu, Z., Sessler, F., Holroyd, N., Hahnel, S., Quack, T., Berriman, M., et al. (2016). Schistosome sex matters: a deep view into gonad-specific and pairing-dependent transcriptomes reveals a complex gender interplay. *Sci Rep* 6, 31150. doi: 10.1038/srep31150.

Lu, Z., Spänig, S., Weth, O., and Grevelding, C.G. (2019). Males, the wrongly neglected partners of the biologically unprecedented male-female interaction of schistosomes. *Front Genet* 10, 796. doi: 10.3389/fgene.2019.00796.

Lu, Z., Zhang, Y., and Berriman, M. (2018). A web portal for gene expression across all life stages of *Schistosoma mansoni*. *bioRxiv*, 308213. doi: https://doi.org/10.1101/308213.

Luttrell, L.M. (2008). Reviews in molecular biology and biotechnology: transmembrane signaling by G protein-coupled receptors. *Mol Biotechnol* 39(3), 239-264. doi: 10.1007/s12033-008-9031-1.

MacDonald, K., Kimber, M.J., Day, T.A., and Ribeiro, P. (2015). A constitutively active G protein-coupled acetylcholine receptor regulates motility of larval *Schistosoma mansoni*. *Mol Biochem Parasitol* 202(1), 29-37. doi: 10.1016/j.molbiopara.2015.09.001.

Magee, R.M., Fairweather, I., Johnston, C.F., Halton, D.W., and Shaw, C. (1989). Immunocytochemical demonstration of neuropeptides in the nervous system of the liver fluke, *Fasciola hepatica* (Trematoda, Digenea). *Parasitology* 98(2), 227-238. doi: 10.1017/S0031182000062132.

Maule, A., and Day, T. A. (2005). Parasite neuromusculature and its utility as a drug target. *Cambridge University Press*. doi: https://www.cambridge.org/is/universitypress/subjects/life-sciences/zoology/parasite-neuromusculature-and-its-utility-drug-target.

McKellar, Q.A., and Jackson, F. (2004). Veterinary anthelmintics: old and new. *Trends Parasitol* 20(10), 456-461. doi: 10.1016/j.pt.2004.08.002.

McKnight, G.S. (1991). Cyclic AMP second messenger systems. *Curr Opin Cell Biol* 3(2), 213-217. doi: 10.1016/0955-0674(91)90141-k.

McManus, D.P., Bergquist, R., Cai, P., Ranasinghe, S., Tebeje, B.M., and You, H. (2020). Schistosomiasis-from immunopathology to vaccines. *Semin Immunopathol* 42(3), 355-371. doi: 10.1007/s00281-020-00789-x.

McManus, D.P., Dunne, D.W., Sacko, M., Utzinger, J., Vennervald, B.J., and Zhou, X.N. (2018). Schistosomiasis. *Nat Rev Dis Primers* 4(1), 13. doi: 10.1038/s41572-018-0013-8.

McManus, D.P., and Loukas, A. (2008). Current status of vaccines for schistosomiasis. *Clin Microbiol Rev* 21(1), 225-242. doi: 10.1128/CMR.00046-07.

McVeigh, P., Leech, S., Marks, N. J., Geary, T. G., and Maule, A. G. (2006). Gene expression and pharmacology of nematode NLP-12 neuropeptides. *Int J Parasitol* 36(6), 633-640. doi: 10.1016/j.ijpara.2006.01.009.

McVeigh, P., Mair, G.R., Atkinson, L., Ladurner, P., Zamanian, M., Novozhilova, E., et al. (2009). Discovery of multiple neuropeptide families in the phylum Platyhelminthes. *Int J Parasitol* 39(11), 1243-1252. doi: 10.1016/j.ijpara.2009.03.005.

Mellin, T. N., Busch, R. D., Wang, C. C., and Kath, G. (1983). Neuropharmacology of the parasitic trematode, *Schistosoma mansoni*. *Am J Trop Med Hyg* 32(1), 83-93. doi: 10.4269/ajtmh.1983.32.83.

Meng, J., Glick, J.L., Polakis, P., and Casey, P.J. (1999). Functional interaction between Galpha(z) and Rap1GAP suggests a novel form of cellular cross-talk. *J Biol Chem* 274(51), 36663-36669. doi: 10.1074/jbc.274.51.36663.

Miao, Y., and McCammon, J. A. (2016). G-protein coupled receptors: advances in simulation and drug discovery. *Curr Opin Struct Biol* 41, 83-89. doi: 10.1016/j.sbi.2016.06.008.

Midway, S., Robertson, M., Flinn, S., and Kaller, M. (2020). Comparing multiple comparisons: practical guidance for choosing the best multiple comparisons test. *PeerJ* 8, e10387. doi: 10.7717/peerj.10387.

Milligan, G., and Kostenis, E. (2006). Heterotrimeric G-proteins: a short history. *Br J Pharmacol* 147(S1), S46-S55. doi: 10.1038/sj.bjp.0706405.

Moczon, T., Swiderski, Z., and Huggel, H. (1992). *Schistosoma mansoni*: the chemical nature of the secretions produced by the Mehlis' gland and ootype as revealed by cytochemical studies. *Int J Parasitol* 22(1), 65-73. doi: 10.1016/0020-7519(92)90081-u.

Modena, C.M., Lima, W.d.S., and Coelho, P.M.Z. (2008). Wild and domesticated animals as reservoirs of *Schistosomiasis mansoni* in Brazil. *Acta Tropica* 108(2), 242-244. doi: 10.1016/j.actatropica.2008.07.004.

Montazeri, M., Fakhar, M., and Keighobadi, M. (2022). The potential role of the serotonin transporter as a drug target against parasitic infections: A scoping review of the

literature. *Recent Adv Antiinfect Drug Discov* 17(1), 23-33. doi: 10.2174/1574891x16666220304232301.

Naghshineh, S., Noguchi, M., Huang, K. P., and Londos, C. (1986). Activation of adipocyte adenylate cyclase by protein kinase C. *J Biol Chem* 261(31), 14534-14538. doi: https://pubmed.ncbi.nlm.nih.gov/3771540/.

Nathoo, A.N., Moeller, R.A., Westlund, B.A., and Hart, A.C. (2001). Identification of neuropeptide-like protein gene families in *Caenorhabditis elegans* and other species. *Proc Natl Acad Sci U S A* 98(24), 14000-14005. doi: 10.1073/pnas.241231298.

Neves, R.H., de Lamare Biolchini, C., Machado-Silva, J.R., Carvalho, J.J., Branquinho, T.B., Lenzi, H.L., et al. (2005). A new description of the reproductive system of *Schistosoma mansoni* (Trematoda: Schistosomatidae) analyzed by confocal laser scanning microscopy. *Parasitol Res* 95(1), 43-49. doi: 10.1007/s00436-004-1241-2.

Odoemelam, C.S., Percival, B., Wallis, H., Chang, M.W., Ahmad, Z., Scholey, D., et al. (2020). G-Protein coupled receptors: structure and function in drug discovery. *RSC Adv* 10(60), 36337-36348. doi: 10.1039/d0ra08003a.

Oleaga, A., Rey, O., Polack, B., Grech-Angelini, S., Quilichini, Y., Pérez-Sánchez, R., et al. (2019). Epidemiological surveillance of schistosomiasis outbreak in Corsica (France): Are animal reservoir hosts implicated in local transmission? *PLoS Negl Trop Dis* 13(6), e0007543. doi: 10.1371/journal.pntd.0007543.

Olveda, D.U., Olveda, R.M., McManus, D.P., Cai, P., Chau, T.N., Lam, A.K., et al. (2014). The chronic enteropathogenic disease schistosomiasis. *Int J Infect Dis* 28, 193-203. doi: 10.1016/j.ijid.2014.07.009.

Orr-Burks, N., Murray, J., Todd, K.V., Bakre, A., and Tripp, R.A. (2021). G-protein-coupled receptor and ion channel genes used by influenza virus for replication. *J Virol* 95(9). doi: 10.1128/jvi.02410-20.

Overington, J. P., Al-Lazikani, B., and Hopkins, A. L. (2006). How many drug targets are there? *Nat Rev Drug Discov* 5(12), 993-996. doi: 10.1038/nrd2199.

Park, S.K., Gunaratne, G.S., Chulkov, E.G., Moehring, F., McCusker, P., Dosa, P.I., et al. (2019). The anthelmintic drug praziquantel activates a schistosome transient receptor potential channel. *J Biol Chem* 294(49), 18873-18880. doi: 10.1074/jbc.AC119.011093.

Park, S.K., and Marchant, J.S. (2020). The journey to discovering a flatworm target of praziquantel: A long TRP. *Trends Parasitol* 36(2), 182-194. doi: 10.1016/j.pt.2019.11.002.

Patocka, N., and Ribeiro, P. (2013). The functional role of a serotonin transporter in *Schistosoma mansoni* elucidated through immunolocalization and RNA interference (RNAi). *Mol Biochem Parasitol* 187(1), 32-42. doi: 10.1016/j.molbiopara.2012.11.008.

Patocka, N., Sharma, N., Rashid, M., and Ribeiro, P. (2014). Serotonin signaling in *Schistosoma mansoni*: a serotonin-activated G protein-coupled receptor controls parasite movement. *PLoS Pathog* 10(1), e1003878. doi: 10.1371/journal.ppat.1003878.

Pax, R.A., Siefker, C., and Bennett, J.L. (1984). *Schistosoma mansoni*: differences in acetylcholine, dopamine, and serotonin control of circular and longitudinal parasite muscles. *Exp Parasitol* 58(3), 314-324. doi: 10.1016/0014-4894(84)90048-1.

Pfaffl, M.W. (2001). A new mathematical model for relative quantification in real-time RT-PCR. *Nucleic Acids Res* 29(9), e45. doi: 10.1093/nar/29.9.e45.

Pica-Mattoccia, L., Orsini, T., Basso, A., Festucci, A., Liberti, P., Guidi, A., et al. (2008). *Schistosoma mansoni*: Lack of correlation between praziquantel-induced intra-worm calcium influx and parasite death. *Exp Parasitol* 119(3), 332-335. doi: 10.1016/j.exppara.2008.03.012.

Pierce, K.L., Premont, R.T., and Lefkowitz, R.J. (2002). Seven-transmembrane receptors. *Nat Rev Mol Cell Biol* 3(9), 639-650. doi: 10.1038/nrm908.

Pierce, S.B., Costa, M., Wisotzkey, R., Devadhar, S., Homburger, S.A., Buchman, A.R., et al. (2001). Regulation of DAF-2 receptor signaling by human insulin and ins-1, a member of the unusually large and diverse *C. elegans* insulin gene family. *Genes Dev* 15(6), 672-686. doi: 10.1101/gad.867301.

Popiel, I., and Basch, P.F. (1984). Reproductive development of female *Schistosoma mansoni* (Digenea: Schistosomatidae) following bisexual pairing of worms and worm segments. *J Exp Zool* 232(1), 141-150. doi: 10.1002/jez.1402320117.

Protasio, A.V., Tsai, I.J., Babbage, A., Nichol, S., Hunt, M., Aslett, M.A., et al. (2012). A systematically improved high quality genome and transcriptome of the human blood fluke *Schistosoma mansoni*. *PLoS Negl Trop Dis* 6(1), e1455. doi: 10.1371/journal.pntd.0001455.

Quack, T., Beckmann, S., and Grevelding, C.G. (2006). Schistosomiasis and the molecular biology of the male-female interaction of *S. mansoni*. *Berl Munch Tierarztl Wochenschr* 119(9-10), 365-372. doi: https://pubmed.ncbi.nlm.nih.gov/17007463/.

Ramalli, L., Mulero, S., Noël, H., Chiappini, J. D., Vincent, J., Barré-Cardi, H., et al. (2018). Persistence of schistosomal transmission linked to the Cavu river in southern Corsica since 2013. *Euro Surveill* 23(4), 18-00017. doi: 10.2807/1560-7917.ES.2018.23.4.18-00017.

Ramírez-Zacarías, J.L., Castro-Muñozledo, F., and Kuri-Harcuch, W. (1992). Quantitation of adipose conversion and triglycerides by staining intracytoplasmic lipids with Oil red O. *Histochemistry* 97(6), 493-497. doi: 10.1007/bf00316069.

Raso, G., N'Goran, E.K., Toty, A., Luginbühl, A., Adjoua, C.A., Tian-Bi, N.T., et al. (2004). Efficacy and side effects of praziquantel against *Schistosoma mansoni* in a community of western Côte d'Ivoire. *Trans R Soc Trop Med Hyg* 98(1), 18-27. doi: 10.1016/s0035-9203(03)00003-8.

Reinitz, C. A., Herfel, H. G., Messinger, L. A., and Stretton, A. O. (2000). Changes in locomotory behavior and cAMP produced in *Ascaris suum* by neuropeptides from *Ascaris suum* or *Caenorhabditis elegans*. *Mol Biochem Parasitol* 111(1), 185-197. doi: 10.1016/s0166-6851(00)00317-0.

Reis, M.G., Kuhns, J., Blanton, R., and Davis, A.H. (1989). Localization and pattern of expression of a female specific mRNA in *Schistosoma mansoni*. *Mol Biochem Parasitol* 32(2-3), 113-119. doi: 10.1016/0166-6851(89)90062-5.

Ribeiro, P., Gupta, V., and El-Sakkary, N. (2012). Biogenic amines and the control of neuromuscular signaling in schistosomes. *Invert Neurosci* 12(1), 13-28. doi: 10.1007/s10158-012-0132-y.

Richter, D., Reynolds, S.R., and Harn, D.A. (1993). Candidate vaccine antigens that stimulate the cellular immune response of mice vaccinated with irradiated cercariae of *Schistosoma mansoni*. *J Immunol* 151(1), 256-265. doi: https://pubmed.ncbi.nlm.nih.gov/8326127/.

Riobo, N.A., and Manning, D.R. (2005). Receptors coupled to heterotrimeric G proteins of the G12 family. *Trends Pharmacol Sci* 26(3), 146-154. doi: 10.1016/j.tips.2005.01.007.

Riveau, G., Deplanque, D., Remoué, F., Schacht, A.-M., Vodougnon, H., Capron, M., et al. (2012). Safety and immunogenicity of r*Sh*28GST antigen in humans: phase 1 randomized clinical study of a vaccine candidate against urinary schistosomiasis. *PLoS Negl Trop Dis* 6(7), e1704. doi: 10.1371/journal.pntd.0001704.

Riveau, G., Schacht, A.-M., Dompnier, J.-P., Deplanque, D., Seck, M., Waucquier, N., et al. (2018). Safety and efficacy of the r*Sh*28GST urinary schistosomiasis vaccine: A phase 3 randomized, controlled trial in Senegalese children. *PLoS Negl Trop Dis* 12(12), e0006968. doi: 10.1371/journal.pntd.0006968.

Robb, E., McCammick, E.M., Wells, D., McVeigh, P., Gardiner, E., Armstrong, R., et al. (2022). Transcriptomic analysis supports a role for the nervous system in regulating growth and development of *Fasciola hepatica* juveniles. *PLoS Negl Trop Dis* 16(11), e0010854. doi: 10.1371/journal.pntd.0010854.

Roditi, I. (2016). The languages of parasite communication. *Mol Biochem Parasitol* 208(1), 16-22. doi: 10.1016/j.molbiopara.2016.05.008.

Ross, E.M., and Gilman, A.G. (1977a). Reconstitution of catecholamine-sensitive adenylate cyclase activity: interactions of solubilized components with receptor-replete membranes. *Proc Natl Acad Sci U S A* 74(9), 3715-3719. doi: 10.1073/pnas.74.9.3715.

Ross, E.M., and Gilman, A.G. (1977b). Resolution of some components of adenylate cyclase necessary for catalytic activity. *J Biol Chem* 252(20), 6966-6969. doi: https://pubmed.ncbi.nlm.nih.gov/903346/.

Ross, E.M., Howlett, A.C., Ferguson, K.M., and Gilman, A.G. (1978). Reconstitution of hormone-sensitive adenylate cyclase activity with resolved components of the enzyme. *J Biol Chem* 253(18), 6401-6412. doi: https://pubmed.ncbi.nlm.nih.gov/210183/.

Saberi, A., Jamal, A., Beets, I., Schoofs, L., and Newmark, P.A. (2016). GPCRs direct germline development and somatic gonad function in planarians. *PLoS Biol* 14(5), e1002457. doi: 10.1371/journal.pbio.1002457.

Sainio, E.L., Pulkki, K., and Young, S.N. (1996). L-tryptophan: Biochemical, nutritional and pharmacological aspects. *Amino Acids* 10(1), 21-47. doi: 10.1007/BF00806091.

Salas-Coronas, J., Bargues, M.D., Lozano-Serrano, A.B., Artigas, P., Martínez-Ortí, A., Mas-Coma, S., et al. (2021). Evidence of autochthonous transmission of urinary schistosomiasis in Almeria (southeast Spain): An outbreak analysis. *Travel Med Infect Dis* 44, 102165. doi: 10.1016/j.tmaid.2021.102165.

Santini-Oliveira, M., Coler, R.N., Parra, J., Veloso, V., Jayashankar, L., Pinto, P.M., et al. (2016). Schistosomiasis vaccine candidate *Sm*14/GLA-SE: Phase 1 safety and immunogenicity clinical trial in healthy, male adults. *Vaccine* 34(4), 586-594. doi: 10.1016/j.vaccine.2015.10.027.

Schayer, R.W. (1960). Relationship of induced histidine decarboxylase activity and histamine synthesis to shock from stress and from endotoxin. *Am J Physiol* 198(6), 1187-1192. doi: 10.1152/ajplegacy.1960.198.6.1187.

Schiöth, H.B., and Fredriksson, R. (2005). The GRAFS classification system of G-protein coupled receptors in comparative perspective. *Gen Comp Endocrinol* 142(1-2), 94-101. doi: 10.1016/j.ygcen.2004.12.018.

Seubert, J., Pohlke, R., and Loebich, F. (1977). Synthesis and properties of praziquantel, a novel broad spectrum anthelmintic with excellent activity against Schistosomes and Cestodes. *Experientia* 33(8), 1036-1037. doi: 10.1007/bf01945954.

Severinghaus, A.E. (1928). Memoirs: Sex Studies on *Schistosoma japonicum*. *J Cell Sci* s2-71 (284): 653–702. doi: https://doi.org/10.1242/jcs.s2-71.284.653.

Shariatgorji, M., Svenningsson, P., and Andrén, P. E. (2014). Mass spectrometry imaging, an emerging technology in neuropsychopharmacology. *Neuropsychopharmacology* 39(1), 34-49. doi: 10.1038/npp.2013.215.

Shinn, G.L. (1993). Formation of egg capsules by flatworms (phylum Platyhelminthes). *Trans Am Microsc Soc* 112(1), 18-34. doi: 10.2307/3226779.

Sibomana, J.P., Campeche, A., Carvalho-Filho, R.J., Correa, R.A., Duani, H., Pacheco Guimaraes, V., et al. (2020). Schistosomiasis pulmonary arterial hypertension. *Front Immunol* 11, 608883. doi: 10.3389/fimmu.2020.608883.

Sievers, F., Wilm, A., Dineen, D., Gibson, T.J., Karplus, K., Li, W., et al. (2011). Fast, scalable generation of high-quality protein multiple sequence alignments using Clustal Omega. *Mol Syst Biol* 7, 539. doi: 10.1038/msb.2011.75.

Skuce, P.J., Johnston, C.F., Fairweather, I., Halton, D.W., Shaw, C., and Buchanan, K.D. (1990). Immunoreactivity to the pancreatic polypeptide family in the nervous system of the adult human blood fluke, *Schistosoma mansoni. Cell Tissue Res* 261(3), 573-581. doi: 10.1007/bf00313537.

Smith, K. A., Komuniecki, R. W., Ghedin, E., Spiro, D., and Gray, J. (2007). Genes encoding putative biogenic amine receptors in the parasitic nematode *Brugia malayi*. *Invert Neurosci* 7(4), 227-244. doi: 10.1007/s10158-007-0058-y.

Smyth, J.D., and Clegg, J.A. (1959). Egg-shell formation in trematodes and cestodes. *Exp Parasitol* 8(3), 286-323. doi: 10.1016/0014-4894(59)90027-x.

Southey, B.R., Amare, A., Zimmerman, T.A., Rodriguez-Zas, S.L., and Sweedler, J.V. (2006). NeuroPred: a tool to predict cleavage sites in neuropeptide precursors and provide the masses of the resulting peptides. *Nucleic Acids Res* 34(Web Server issue), W267-272. doi: 10.1093/nar/gkl161.

Spence, I.M., and Silk, M.H. (1971a). Ultrastructural studies of the blood fluke--*Schistosoma mansoni*. V. The female reproductive system--a preliminary report. *S Afr J Med Sci* 36(3), 41-50. doi: https://pubmed.ncbi.nlm.nih.gov/5154347/.

Spence, I.M., and Silk, M.H. (1971b). Ultrastructural studies of the blood fluke--*Schistosoma mansoni*. VI. The mehlis gland. *S Afr J Med Sci* 36(3), 69-76. doi: https://pubmed.ncbi.nlm.nih.gov/5154349/.

Standley, C.J., Dobson, A.P., and Stothard, J.R. (2012). Out of animals and back again: schistosomiasis as a zoonosis in Africa. *Schistosomiasis. InTech* 209-230. doi:10.5772/25567.

Stephens, L., Smrcka, A., Cooke, F.T., Jackson, T.R., Sternweis, P.C., and Hawkins, P.T. (1994). A novel phosphoinositide 3 kinase activity in myeloid-derived cells is activated by G protein beta gamma subunits. *Cell* 77(1), 83-93. doi: 10.1016/0092-8674(94)90237-2.

Stunkard, H.W. (1951). The invertebrates: platyhelminthes and rhynchocoela. The acoelomate bilateria. Vol. II. *Q Rev Biol* 26(4), 403-403. doi: 10.1086/398483.

Taman, A., and Ribeiro, P. (2009). Investigation of a dopamine receptor in *Schistosoma mansoni*: Functional studies and immunolocalization. *Mol Biochem Parasitol* 168(1), 24-33. doi: 10.1016/j.molbiopara.2009.06.003.

Taman, A., and Ribeiro, P. (2011). Glutamate-mediated signaling in *Schistosoma mansoni*: A novel glutamate receptor is expressed in neurons and the female reproductive tract. *Mol Biochem Parasitol* 176(1), 42-50. doi: 10.1016/j.molbiopara.2010.12.001.

Tamura, K., Stecher, G., and Kumar, S. (2021). MEGA11: Molecular evolutionary genetics analysis version 11. *Mol Biol Evol* 38(7), 3022-3027. doi: 10.1093/molbev/msab120.

Tang, W.J., and Gilman, A.G. (1991). Type-specific regulation of adenylyl cyclase by G protein beta gamma subunits. *Science* 254(5037), 1500-1503. doi: 10.1126/science.1962211.

Tennakoon, M., Senarath, K., Kankanamge, D., Ratnayake, K., Wijayaratna, D., Olupothage, K., Ubeysinghe, S., Martins-Cannavino, K., Hébert, T. E., and Karunarathne, A. (2021). Subtype-dependent regulation of Gβγ signaling. *Cell Signal* 82, 109947. doi: 10.1016/j.cellsig.2021.109947.

Tran, M.H., Freitas, T.C., Cooper, L., Gaze, S., Gatton, M.L., Jones, M.K., et al. (2010). Suppression of mRNAs encoding tegument tetraspanins from *Schistosoma mansoni*

results in impaired tegument turnover. *PLoS Pathog* 6(4), e1000840. doi: 10.1371/journal.ppat.1000840.

Tran, M.H., Pearson, M.S., Bethony, J.M., Smyth, D.J., Jones, M.K., Duke, M., et al. (2006). Tetraspanins on the surface of *Schistosoma mansoni* are protective antigens against schistosomiasis. *Nat Med* 12(7), 835-840. doi: 10.1038/nm1430.

Tusnády, G.E., and Simon, I. (2001). The HMMTOP transmembrane topology prediction server. *Bioinformatics* 17(9), 849-850. doi: 10.1093/bioinformatics/17.9.849.

Vale, N., Gouveia, M.J., Rinaldi, G., Brindley, P.J., Gärtner, F., and Correia da Costa, J.M. (2017). Praziquantel for schistosomiasis: single-drug metabolism revisited, mode of action, and resistance. *Antimicrob Agents Chemother* 61(5). doi: 10.1128/aac.02582-16.

van Biesen, T., Luttrell, L.M., Hawes, B.E., and Lefkowitz, R.J. (1996). Mitogenic signaling via G protein-coupled receptors. *Endocr Rev* 17(6), 698-714. doi: 10.1210/edrv-17-6-698.

van Keulen, H., Mertz, P. M., LoVerde, P. T., Shi, H., and Rekosh, D. M. (1991). Characterization of a 54-nucleotide gap region in the 28S rRNA gene of *Schistosoma mansoni*. *Mol Biochem Parasitol* 45(2), 205-214. doi: 10.1016/0166-6851(91)90087-m.

von Bülow, V., Lichtenberger, J., Grevelding, C. G., Falcone, F. H., Roeb, E., and Roderfeld, M. (2021). Does *Schistosoma mansoni* facilitate carcinogenesis? *Cells* 10(8), 1982. doi: 10.3390/cells10081982.

Wang, B., Lee, J., Li, P., Saberi, A., Yang, H., Liu, C., et al. (2018). Stem cell heterogeneity drives the parasitic life cycle of *Schistosoma mansoni*. *Elife* 7, e35449. doi: 10.7554/eLife.35449.

Wang, J., Chen, R., and Collins, J.J. (2019). Systematically improved *in vitro* culture conditions reveal new insights into the reproductive biology of the human parasite *Schistosoma mansoni*. *PLoS Biol* 17(5), e3000254-. doi: 10.1371/journal.pbio.3000254.

Wang, J., Hua, T., and Liu, Z. (2020a). Structural features of activated GPCR signaling complexes. *Curr Opin Struct Biol* 63, 82-89. doi: 10.1016/j.sbi.2020.04.008.

Wang, J., Paz, C., Padalino, G., Coghlan, A., Lu, Z., Gradinaru, I., et al. (2020b). Large-scale RNAi screening uncovers therapeutic targets in the parasite *Schistosoma mansoni*. *Science* 369(6511), 1649-1653. doi: 10.1126/science.abb7699.

Wang, J., Yu, Y., Shen, H., Qing, T., Zheng, Y., Li, Q., et al. (2017). Dynamic transcriptomes identify biogenic amines and insect-like hormonal regulation for mediating reproduction *in Schistosoma japonicum*. *Nat Commun* 8, 14693. doi: 10.1038/ncomms14693.

Wang, S., Luo, X., Zhang, S., Yin, C., Dou, Y., and Cai, X. (2014). Identification of putative insulin-like peptides and components of insulin signaling pathways in parasitic platyhelminths by the use of genome-wide screening. *FEBS J* 281(3), 877-893. doi: 10.1111/febs.12655.

Wang, Y., Zayas, R.M., Guo, T., and Newmark, P.A. (2007). Nanos function is essential for development and regeneration of planarian germ cells. *Proc Natl Acad Sci U S A* 104(14), 5901-5906. doi: 10.1073/pnas.0609708104.

Webster, P., Mansour, T.E., and Bieber, D. (1989). Isolation of a female-specific, highly repeated *Schistosoma mansoni* DNA probe and its use in an assay of cercarial sex. *Mol Biochem Parasitol* 36(3), 217-222. doi: 10.1016/0166-6851(89)90169-2.

Wendt, G., Zhao, L., Chen, R., Liu, C., O'Donoghue, A.J., Caffrey, C.R., et al. (2020). A single-cell RNA-seq atlas of *Schistosoma mansoni* identifies a key regulator of blood feeding. *Science* 369(6511), 1644-1649. doi: 10.1126/science.abb7709.

Weth, O., Haeberlein, S., Haimann, M., Zhang, Y., and Grevelding, C.G. (2019). Towards deorphanizing G protein-coupled receptors of *Schistosoma mansoni* using the MALAR yeast two-hybrid system. *Parasitology* 147(8), 1-21. doi: 10.1017/S0031182019001756.

Wheeler, N.J., Hallem, E.A., and Zamanian, M. (2022). Making sense of sensory behaviors in vector-borne helminths. *Trends Parasitol* 38(10), 841-853. doi: 10.1016/j.pt.2022.07.003.

Will, R. G., Hull, E. M., and Dominguez, J. M. (2014). Influences of dopamine and glutamate in the medial preoptic area on male sexual behavior. *Pharmacol Biochem Behav* 121, 115-123. doi: 10.1016/j.pbb.2014.02.005.

World Health Organization. 2023. Fact sheets, Schistosomiasis. https://www.who.int/news-room/fact-sheets/detail/schistosomiasis.

Worzfeld, T., Wettschureck, N., and Offermanns, S. (2008). G12/G13-mediated signaling in mammalian physiology and disease. *Trends Pharmacol Sci* 29(11), 582-589. doi: 10.1016/j.tips.2008.08.002.

You, H., Cai, P., Tebeje, B.M., Li, Y., and McManus, D.P. (2018). Schistosome vaccines for domestic animals. *Trop Med Infect Dis* 3(2), 68. doi: 10.3390/tropicalmed3020068.

You, H., and McManus, D.P. (2015). Vaccines and diagnostics for zoonotic schistosomiasis japonica. *Parasitology* 142(2), 271-289. doi: 10.1017/S0031182014001310.

Zamanian, M., Kimber, M.J., McVeigh, P., Carlson, S.A., Maule, A.G., and Day, T.A. (2011). The repertoire of G protein-coupled receptors in the human parasite *Schistosoma mansoni* and the model organism *Schmidtea mediterranea*. *BMC Genomics* 12, 596. doi: 10.1186/1471-2164-12-596.

Zamponi, G., Bourinet, E., Nelson, D. et al. (1997). Crosstalk between G proteins and protein kinase C mediated by the calcium channel α1 subunit. *Nature* 385, 442-446. doi: 10.1038/385442a0.

Zhang, W., Molehin, A.J., Rojo, J.U., Sudduth, J., Ganapathy, P.K., Kim, E., et al. (2018). *Sm*-p80-based schistosomiasis vaccine: double-blind preclinical trial in baboons demonstrates comprehensive prophylactic and parasite transmission-blocking efficacy. *Ann N Y Acad Sci* 1425(1), 38-51. doi: 10.1111/nyas.13942.

Zimmermann, G., and Taussig, R. (1996). Protein kinase C alters the responsiveness of adenylyl cyclases to G protein alpha and betagamma subunits. *J Biol Chem* 271(43), 27161-27166. doi: 10.1074/jbc.271.43.27161.

Zimmermann, G., Zhou, D., and Taussig, R. (1999). Activating mutation of adenylyl cyclase reverses its inhibition by G proteins. *Mol Pharmacol* 56(5), 895-901. doi: 10.1124/mol.56.5.895.

Zipper, H., Brunner, H., Bernhagen, J., and Vitzthum, F. (2004). Investigations on DNA intercalation and surface binding by SYBR Green I, its structure determination and methodological implications. *Nucleic Acids Res* 32(12), e103. doi: 10.1093/nar/gnh101.

8. Supplementary data

Supplementary Figure 1

Sequences and accession numbers used for the phylogenetic analyses of the *S. mansoni* GPCR Smp_084270

Species include: schistosomes (*Schistosoma japonicum* (A0A4Z2CQX1), *S. mansoni* (Smp_084270 (A0A3Q0KIK8)), *S. haematobium* (A0A095C4R8), and *Trichobilharzia regent* (A0A183WMW7)); other trematodes (*Clonorchis sinensis* (H2KRY6) and *Fasciola gigantica* (A0A504Z2P0)); cestoda (*Echinococcus granulosus* (U6J3B5) and *Taenia asiatica* (A0A0R3W0W9)); monogenea (*Protopolystoma xenopodis* (A0A3S5CMM6)); turbellaria (*Schmidtea mediterranea* (A0A193KU74)); nematodes (*Caenorhabditis elegans* (G5EDR2)); molluscs (*Pomacea canaliculate* (A0A2T7PVN7) and *Biomphalaria glabrata* (A0A2C9LEA4)); arthropods (*Apis mellifera* (Q9NG02) and *Daphnia pulex* (E9G3B6)); amphibians (*Xenopus laevis* (B7ZRQ1)); mammals (*Homo sapiens* (Q14439)).

>tr|A0A3S5CMM6|A0A3S5CMM6_9PLAT G_PROTEIN_RECEP_F1_2 domain-containing protein OS=Protopolystoma xenopodis OX=117903 GN=PXEA_LOCUS26816 PE=4 SV=1

MANEDPQWPYLDSPWDLLRDCFHIRKLENEHTDWTACILSRILGVLSAYIFPVIGLLGLLVNCLTAFI
FLRCFRTPTRQMIYLACLAVSDGLTILLFGWLWVFPAKGIPYATDGKTYFFTFYSGWTECRIHRWAYS
FTSCLGNNIFLLTTLDRCMSIYLPLKFSRLPQKRAWQMLLAITLVSGVMMLPFGISTGLYPTQGNKVI
CWLTEDQTFLQLYHVLFANAGFLQTVLIIAFNLALLIRLRQNALLRKQLTCKFTTGRKEVSASILLLL
LSTIVVICALPQTVAYMFAFIYQTALPHDTGSMLTRLAYNISDIGWNLLFLQYTANFFLYLSRMPNFR
LATLRLITCRCGQALQRRLEEHYYSSRPAGKTQTTNMFQVGSKRALVVRSLTEQVKRCQHGRYSQNGP
GRICYQDETMVDVWPASPRFHNGPTSLPTHSFFSHSPSPAISLPQSSPSPPPSSPHLPPPPSLMRISA
SPPALSSPSSLPSPSPLMKLQLRLQLPPLSLTAQSSSSPVPTPQLMKLPRYPPSPPTIGHSLSTYSHS
PRSFGGSIDKTQPHWGNRKTSNSQQHVVTFSPPTSRGTRVGESLPDDEVTRF

>tr|A0A3Q0KIK8|A0A3Q0KIK8_SCHMA Rhodopsin-like orphan GPCR, putative OS=Schistosoma mansoni OX=6183 PE=4 SV=1

MISMNSSELIFTERPQRIFQDCILLVQNYSYIQELKCLSSKVIGTIVGYLIPIFSIPCIIINLFIAIN
VIMKGKKASRQLIYISGICLSSAIANIMFIWLWQYPSYGLPYTTNGTQFFSFLNISITACRFHRFMYS
FSATFMCNMRVCASSDRCLAVWKPIMLRKFRHHYAWYVYGVVIFISALLMLPFAIEVNWIPTKYGLQC
WVQSANVYIQIHHAFLSNLGPVQTMILIIIDITFAFKFRQQLKKNKTDGIDVTSSKQMHRYLLLFISA
ASYNVLAATQCTFLLLARLGSVSFIKFESGLAYNISDILWYINSLREVLDFVIYHRCFHVFSGITSRI
SKMFYYTSKKTISVSRDISKISVVSGHNY

>tr|A0A193KU74|A0A193KU74_SCHMD GCR027 OS=Schmidtea mediterranea OX=79327 GN=gcr027 PE=2 SV=1

MDNGTFPIFNMSFHSRYNWAYVGLFIIPMLSMWGNSLVCISVWVEVGLRKRFNYFLVSLAMSDFLCAI
LVMPISAWKMIDNYYLETINHQWCLIWYSLDVFFTASTIIHLCTISIDRYNALKNPLKIHGQKRYRSL
VVQLVCAWIIPFSIACPLFLFALELDKTREHSSFKGCGPQNAYFILIATIVTFFIPLIIMTVTYVLTV
KILYVQRKEAEANLYSNAVASLVFKPKLSSSLAKFTRTPSTKVMSEKKLNGKNENSSAMHRRSISTSC
LVNSLDSEFKETENHNHFEMTPLLAKTTRNNFVENTSMNLCGSDNLKPPLQEDQYKQTLPQRQVSFRE
QQKTKNHYWKSNTVCTVLENPLALLSHQRSFKMSNKTKTDEYSAFYTKKKETEKQLKQINRSRKAVQT
LGILFLLFVICYLPFFVAYLVDFFFKICSVSSTAEKMLTFLEWMGYSGSMFNPIVYHFFNPIFRHTYQ
RLMKCQCYRVFIRHASSSQR

>tr|A0A095C4R8|A0A095C4R8_SCHHA Putative rhodopsin-like orphan GPCR OS=Schistosoma haematobium OX=6185 GN=MS3_0016311 PE=4 SV=1

MNSSELIFIERPQRIFQDCMLLVQNYTYIQELKCLSSKTIGTIVGYLIPIFSIPCIMINLFIAINVMM
KGKKASRQLIYIAGICLSSAIANIMFIWLWQYPSYGLPYTTNGTKFFSFLNISITSCRFHRFMYSFSA
TLMCNMRVCASFDRCLAIWKPIKLRKFRHHYAWYVYGVVIFISAVLMIPFATEVNWIPTKYGLQCWVL
STNVYIQIHHAFLSNLGPVQTMILIVIDITFAFKFRQQLKKHRTDGIDVTSSKQMHRYLLLFISAVSY
NILAATQCIFLLLARLGTVSFIKFESGLAYNISDILWYLNSLREVLDFVIYHRCFHVFSGITSRISKM
FPYKSKETISISRDISKISIASAYNY

>tr|A0A4Z2CQX1|A0A4Z2CQX1_SCHJA Rhodopsin-like orphan GPCR OS=Schistosoma japonicum OX=6182 GN=EWB00_008264 PE=4 SV=1

MNSSELIFSERPQRIFQECLLLEQNDSYMQQLKCLSSRIIGTLVGYFIPVVSIPCITINLFIAIIVII
NAKKASRQLIYISGICMSSGLANIIFTWLWQYPSYGLPYITNGAKFFSFLNISPEACRFHRFMYSFSA
TFMCNMRVCASVDRCLAIWKPLLLRKFRPHYAWYVYGAFIVISALLMLPFATEVNWIPSRYGLQCWVK
FTDVYIQIHHAFLSNLGPIQTTLLIIIDITFAIKFRQQLKKHKSDKIDTTYSKLMRRYLLLFLSAITY
NILAATQCTFLLLARLSSVGLIKFDSGLAYNISDILWYLNSFREILDFIIYHKCFHVFHIITSRLSKA
FVNIKNSVSTSRSLSTTTVGSVNNY

>tr|A0A183WMW7|A0A183WMW7_TRIRE G_PROTEIN_RECEP_F1_2 domain-containing protein OS=Trichobilharzia regenti OX=157069 GN=TRE_LOCUS13470 PE=4 SV=1

MNSQEINFAETPKNILFQCQLLKQNYSYIQNLRCLSSSVIGVIVGYLLPVCSIPCILTNLFIAITVMF
KWRTAARQLIYISGICLSSATADVFFIWLWQYPAYGLPYTTNGAKFFTFLNVSPTACRFHRFVYSSSA
TLMCNMRICSSLDRCLAIYVPIKLKKFHHKYAWFVYGATACFSALLMLPLATEMDWIPSKYGVQCWFR
NANTHPNANNSTNIYLQLHHAFLSNLGPVQTILLIIIDLAFVVKFRRHLNKHKRHNTTTTDTKKETKT
FNRYRLLFISAVSYTLLATVQCIFLALARLSSVEIISFETTLAYNMSDILWYLNILREVLDFVIYQKC
FRIFNIIVVKVSVICCRPTLSTRSGNLFTRTEMTTE

>sp|Q14439|GP176_HUMAN G-protein coupled receptor 176 OS=Homo sapiens OX=9606 GN=GPR176 PE=2 SV=1

MGHNGSWISPNASEPHNASGAEAAGVNRSALGEFGEAQLYRQFTTTVQVVIFIGSLLGNFMVLWSTCR
TTVFKSVTNRFIKNLACSGICASLVCVPFDIILSTSPHCCWWIYTMLFCKVVKFLHKVFCSVTILSFP
AIALDRYYSVLYPLERKISDAKSRELVMYIWAHAVVASVPVFAVTNVADIYATSTCTEVWSNSLGHLV
YVLVYNITTVIVPVVVVFLFLILIRRALSASQKKKVIIAALRTPQNTISIPYASQREAELHATLLSMV
MVFILCSVPYATLVVYQTVLNVPDTSVFLLLTAVWLPKVSLLANPVLFLTVNKSVRKCLIGTLVQLHH
RYSRRNVVSTGSGMAEASLEPSIRSGSQLLEMFHIGQQQIFKPTEDEEESEAKYIGSADFQAKEIFST
CLEGEQGPQFAPSAPPLSTVDSVSQVAPAAPVEPETFPDKYSLQFGFGPFELPPQWLSETRNSKKRLL
PPLGNTPEELIQTKVPKVGRVERKMSRNNKVSIFPKVDS

>tr|U6J3B5|U6J3B5_ECHGR Rhodopsin orphan GPCR OS=Echinococcus granulosus OX=6210 GN=EGR_02845 PE=4 SV=1

MLFAENSRSILPEDPNWPYLDSPWDLLRDCQDYNSDAPNASTLLSACVLSHMLGFVSAYIFPIVGLFG
VVSNLFITYIFLFVFRKPSRQMIYLACVAAADVITIILFGWIWMFPAKGLPYATGARVYFFIFNVNNY
SCKVMRYLYSFSSCLSSSLFLLTAFDRCLCIYFPLKFARISRRRAWEAVGVITLFSALVMLPFGLLVE
HGFSNGKIICWVQVEPNTLQIYHVLLANSSLLQTVLVIIINIALLIRLRQSAVLRETMSKCTSANREI
AASMLLVILSTIVVICALPQSIAYIFSTILSQMLNGEAGRMAVRIAYNISDLGWQLLFFQQASNWVLY
MKRMKNFRRATLRLLRCHCSMGRGMVDDAFGSIHYLSTKARNLTSELRFTRADASKVNGIRFPTTKKG
GISDLWKMKYSGGVIGTSFGSSRHQDRRGDNSNYNISEICRYTYRGSMRHTTTMSTITPGTVYADVDT
PTKPTPDPGRSFTRF

>tr|G5EDR2|G5EDR2_CAEEL G_PROTEIN_RECEP_F1_2 domain-containing protein OS=Caenorhabditis elegans OX=6239 GN=srw-33 PE=4 SV=1

MNSSNDLYPGFSDEDIKFWTEIDELLAVLSILFNMLSFLISIIGILPTIFHIIVLSRKSMRTLTINAF
LLGIGICDLARMMFIIMVLGPLYTEHFSHLEHPECMSPNYYSTILFALISGFTGKLVEYLSIWLAVAM
AIIRSLVIKYPLNSRISDLIESKYGIRVLFLITLPIIILSIPKYFRYSIQPFGSLWVPPQNCTDFPKN
YFQIQYTYVETHIFEKSTDFLTGMEGVLYVIIPSILLPISTLILIFQLRISRKKSEALRHTSNSGGDR
TTKLVTFMTISFTISTAPFGILHLVKVIVSEAIGSEGMNLIVDRIASLFPLIITINGAIHFFLCYFLS
SQYRDAVREMFGRNKKSKNSISLQHPAMSTVSTFVKVE

>tr|A0A504Z2P0|A0A504Z2P0_FASGI G_PROTEIN_RECEP_F1_2 domain-containing protein OS=Fasciola gigantica OX=46835 GN=FGIG_07041 PE=4 SV=1

MWHFVDSPLDLIWQCRALEEGGNNVTKVDCVMSTVLGITSAYILPFICGFSLVGTVFFMTVVVVTKNL
ISRQFIYLFCMFASNAATSVLFGWLWIFLAKGLPFATNGRVYFFTFYSSPTACSVHRFAYSFTSTLSC
NVLLVASVDRLLCVYFPMEFSNIPKRYGWYVIVITVIVSVFLLVPMAGLMIWTSVGDKIICWFPDKYQ

YMEYYHTLISNGGVIQPLAIFVINVIFFVRVRKYAQQLGRVEVLNAQAKHNIQACVTLLIFSLIFVIC
ALPQSIAYICAYTIIRTNPALTTQIRLAYNVADLFWNLYFIRDVIYLILMFRLTGICRWFFQFLRGKK
HRNKFIISGTFWGQDQMIIVE

>tr|B7ZRQ1|B7ZRQ1_XENLA G_PROTEIN_RECEP_F1_2 domain-containing protein OS=Xenopus laevis OX=8355 PE=2 SV=1

MGDGWGPMECRNRSGTPTTVPSPMHPLPELTHQWTVGMTMFMAAIILLIVMGNIMVIVAIGRNQRLQT
LTNVFITSLACADLIMGLFVVPLGATLVVSGKWLYGSIFCEFWTSVDVLCVTASIETLCVISIDRYIA
ITSPFRYQSLLTKGRAKGIVCSVWGISALVSFLPIMMHWWRDTGDPLAMKCYEDPGCCDFVTNRAYAI
ASSIISFYVPLIVMIFVYIRVFKEAQKQMKKIDKCEGRFSHSHVLSHGRSSRRILSKILVAKEQKALK
TLGIIMGTFTLCWLPFFLANVVNVCYRNLIPDKLFLFLNWLGYANSAFNPIIYCRSPDFRKAFKRLLC
CPKKADWHLQTTGELSRTSGGFVNSLDTNALGTCSECNGVRTSLD

>tr|A0A0R3W0W9|A0A0R3W0W9_TAEAS G_PROTEIN_RECEP_F1_2 domain-containing protein OS=Taenia asiatica OX=60517 GN=TASK_LOCUS3344 PE=4 SV=1

MRFVGSSRTILPEDPNWPYLDSPWDLLRDCHDYNSDAYNTSSHLSACILSHMLGFVSAYIFPFVGLFG
VVSNIFVTYIFLFVFRKPSRQMIYLACVAAADVITIVLFGWIWMFPAKGLPYATGARVYFFILNVNTY
SCKIMRYLYSFSSCLSSSLFLLTAFDRCLCVYFPLKFARISRRRAWEAVGVITLFSALSMLPFGVLVG
HGLSNGKIICWVQVGPNALQIYHVLLANSSLLQTILVIIINIALLIRLRQSAVLRETMSKCTSANREI
AASMLLVILSTIVVICTLPQSIAYIFSTILAQVLDGDTGRTAVRIAYNISDLGWQLLFIQQASNWALY
MKRMKNFRRATLRLLRCHCNTGRGWVDDAFGSLHYLSTKARNFTSELRFTRADTSKTYGIRFPTTKKS
GVSDFWKMKYSGGVIRTSFGNFRYQGKSGNNSINNKSEVCRYTYRGSMRHTTTMSTITPATVYADIDT
PTEPALESGRVLTRF

>tr|H2KRY6|H2KRY6_CLOSI Rhodopsin-like orphan GPCR OS=Clonorchis sinensis OX=79923 GN=CLF_107485 PE=4 SV=1

MSRYLELQKNYSFYDTPYDMLVQCEEVRQGLPGASMANCVSSTILGIYSGYILPFVCTFGFLANVWTA
VLFLLGFRRQTRQLVYLAFLAIANAAIHVLWGWLWLFPAKGLPFMTGARVYYFTFSQSQEACRLHRFA
YSFGSTLSANLLLLAASDRFMCTYWPTKMLRFQRRHAYYAVIAVTVLSIVMMLPLGICIEWVTIGEKV
WCWIDSVYTGVDVYHALFSNACVIQPLCTGVLNICFLVKIRQLLHKRAQLSSSIGSSGRREVAASETL
LVITLVTLCTALPQSAAYNAAFVLSRRPNTQEQTSLAFNISDIMWCVMLTQTACNIIVYLVRMSAFRK
MSLSVIKCQGFRRRVIEGTKDQDKTLQVNMTTQRSNTENMTTAGAATFRIGSD

>tr|A0A2T7PVN7|A0A2T7PVN7_POMCA G_PROTEIN_RECEP_F1_2 domain-containing protein OS=Pomacea canaliculata OX=400727 GN=C0Q70_00037 PE=3 SV=1

MTTALATTTEMVSNTTHIYDTYDLFIHPHWKQFPLIPEAWHYAIGVYITIVGISGVFGNLLVIYIFGT
TKSLRTPSNMFIVNLALSDLTFSAVNGFPLLTISAFNKRWFFGKVACEFYGLIGGIFGLMSIDTMAVI

AIDRYNVIARPLKASRSLGYRKAFIMIVMVWVWSLIWTLPPLFGWGAYIPEGFQTSCTFDYLTRTDYF
RSYIMCLYICGFAMPLGIIMFCYFFIYRAVAKHEKEMGKMAKKLNAEIRQGAAAQGSEIKTAKIAMTI
ITTYLISWLPYATIALIAQFGPAEYVTPYLSELPVMFAKASAMHNPIIYALSHPKFREVLDTRFPWLL
CCCRFSQKEKDAAANTKSQMTRADSVNSNVVGGNYSNMSR

>tr|A0A2C9LEA4|A0A2C9LEA4_BIOGL G_PROTEIN_RECEP_F1_2 domain-containing protein OS=Biomphalaria glabrata OX=6526 GN=106056607 PE=3 SV=1

MTLLQSKAAGGPRSVLTDATTIGSVVTTDMLADNATEGRHFIPLSDAGFTFIACMLGFTFVVGSFSNG
LCLFVFIRNRRLRSPTNVFVMALNLVDFLMCFTGIPMAMTSAWNHKWIWGDAMCDFEAFLVYFLGMAS
MYVLMAIAFDRYIAISKPLLGTKITKSIAYVSCVIWAIPPAFGWNEFGLEGAGISCSVVWENPDPLYM
SYIWAIFFFCFIIPLGIMVYSYWGVLATLRNLNKNSVWDMNSRVARKNLAIEKKMFKTAVLIVASYWI
CWMPYTIVSFISAFIGSEIIPPLFATIPPVIAKCQGIFNPLILVTRHKAFQKAFFATFVVQRKRKQRT
DYSMRVIEVRRTDVLSSCVLS

>tr|Q9NG02|Q9NG02_APIME G-protein coupled receptor OS=Apis mellifera OX=7460 GN=tyr1 PE=2 SV=1

MNSSGESGGTMTEDYDMTGCGPPEEETGSNLPVWEAAAASLTLGFLVLATVLGNALVILSVFTYRPLR
IVQNFFIVSLAVADLAVAILVMPFNVAYLLLGKWIFGIHLCKLWLTCDVLCCTASILNLCAIALDRYW
AITDPINYAQKRTLKRVLATIAGVWILSGAISSPPLAGWNDWPEELEPGTPCQLTRRQGYVIYSSLGS
FFIPLLLMSLVYLEIYLATRRRLRERARQSRINAVQSTRHREADDAEESVSSETNHNERSTPRSHAKP
SLIDDEPTEVTIGGGGTTSSRRTTGSRAAATTTTVYQFIEERQRISLSKERRAARTLGVIMGVFVVCW
LPFFLMYVIVPFCPDCCPSDRMVYFITWLGYVNSALNPLIYTIFNLDYRRAFRRLLRIR

>tr|E9G3B6|E9G3B6_DAPPU G_PROTEIN_RECEP_F1_2 domain-containing protein OS=Daphnia pulex OX=6669 GN=DOP-R PE=3 SV=1

MEIVVVPTLLNVTRWDEGNLTSENATVLVEEKDWDDGNPILALVLFSFCLATVLGNALVIAAVTRERY
LHTVTNYFIMSLAVADCLVGSIVMPFSAAVEMQSDRRWLFGRDLCDVWHSFDVLASTASILNLCVISM
DRYWAITDPFTYPSRMTPKRAACFIALVWVCSSLISFPAIAWWRAVARIHPLPEHCVFTDDIGYLVFS
STVSFYGPLSVMVFTYYRIYRAAVAQSRSLRLGIKQVVMASTGEMGKGTGGGSGSGSGGSGSAETVEL
LTLRIHRGGRVASDNRRCAAAAALLTYQAANRHQLAIDPSSTRKLAKIAKERKAAKTLGIVMGVFIAC
WLPFFVTNLLSAFCQSCIHNPERVVTVVTWLGWINSGMNPVIYACWSRDFRRAFARILCGCCPRLFHR
WKRHSGKSGTNNPMNVSSRVDQIFIATSKFGD

>sp|P35359|OPSD_DANRE Rhodopsin OS=Danio rerio OX=7955 GN=rho PE=1 SV=2

MNGTEGPAFYVPMSNATGVVRSPYEYPQYYLVAPWAYGLLAAYMFFLIITGFPVNFLTLYVTIEHKKL
RTPLNYILLNLAIADLFMVFGGFTTTMYTSLHGYFVFGRLGCNLEGFFATLGGEMGLWSLVVLAIERW
MVVCKPVSNFRFGENHAIMGVAFTWVMACSCAVPPLVGWSRYIPEGMQCSCGVDYYTRTPGVNNESFV

IYMFIVHFFIPLIVIFFCYGRLVCTVKEAAAQQQESETTQRAEREVTRMVIIMVIAFLICWLPYAGVA
WYIFTHQGSEFGPVFMTLPAFFAKTSAVYNPCIYICMNKQFRHCMITTLCCGKNPFEEEEGASTTASK
TEASSVSSSSVSPA

Supplementary Figure 2

Supplementary Figure 2: As negative controls for WISH (see **Figure 3.8** and main text), sense probes of genes were used that showed no signals in male and female worms upon hybridization. Scale-bars: 200 µm.

Supplementary Figure 3

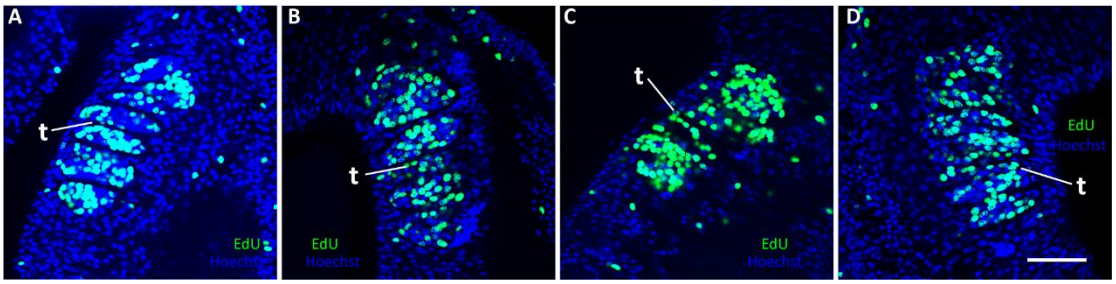

Supplementary Figure 3: Results of the EdU-staining of male gonadal stem-cells upon dsRNA treatment. Shown are representative images of testes from the control (**D**, untreated) and dsRNA combinations of *Smgpcr20* and *Smnpp26* (**A**), *Smgpcr20* and *Smnpp40* dsRNA (**B**), or all three specific

dsRNAs (**C**) males showing no differences of stem-cell proliferation following treatment. Cells were labelled by Hoechst 33342 (blue); EdU-stained cells were colored in green; t: teste. Scale bar: 50 µm.

Supplementary Figure 4

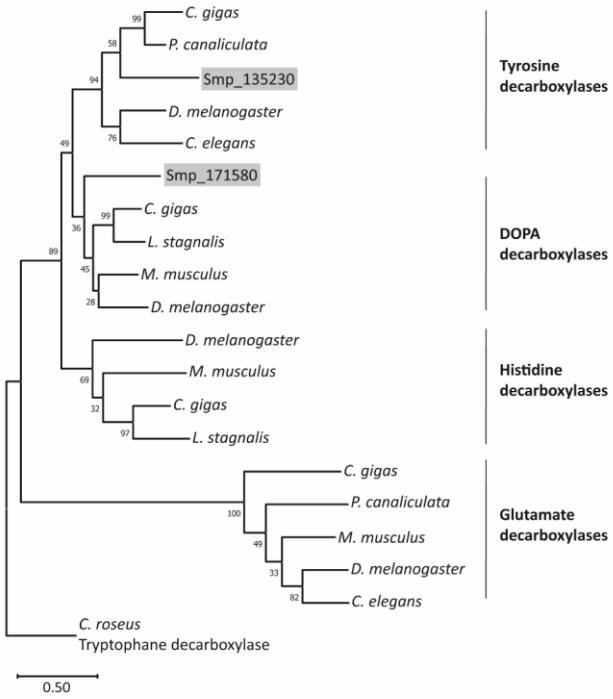

Supplementary Figure 4: Phylogenetic analysis grouped *Sm*TDC-1 and *Sm*DDC-1 of *S. mansoni* in different clades of decarboxylase genes. Shown is the results of a maximum-likelihood phylogram including aa sequences of decarboxylase genes of selected animals in relation to *Sm*TDC-1 (Smp_135230) and *Sm*DDC-1 (Smp_171580). The identified gene families of DOPA-, histidine-, tyrosine-, and glutamate-decarboxylases are marked. Bootstrap values are shown at each node; scale bar = the average number of substitutions per site along each branch. Species included *Mus musculus* (mouse), *Drosophila melanogaster* (fly), *Crassostrea gigas* (oyster), *Pomacea canaliculata* (snail), *Lymnaea stagnalis* (snail), *Caenorhabditis elegans* (nematode). *Catharanthus roseus* (periwinkle plant) was used as outgroup.

Supplementary Figure 5
Cell atlas data

A

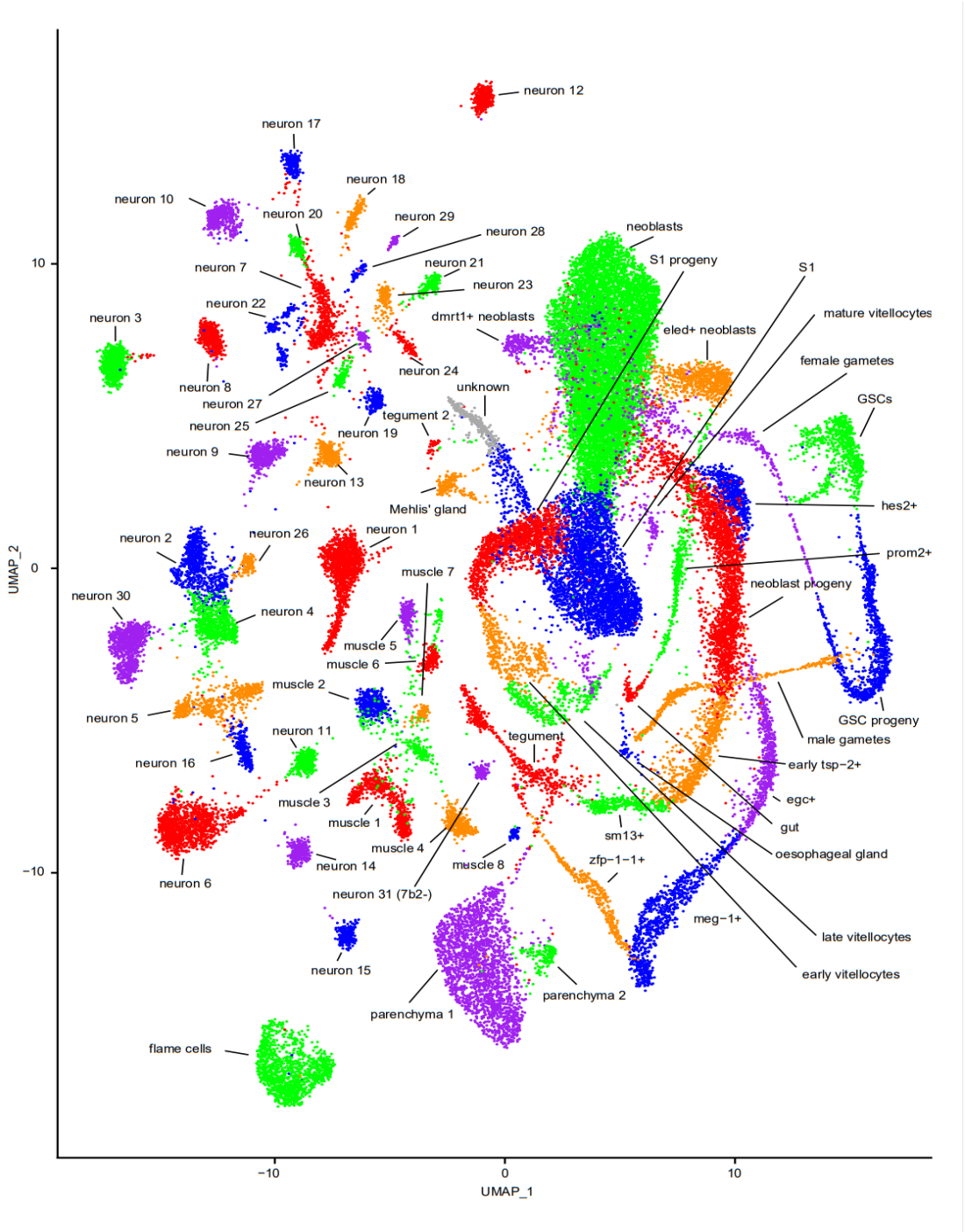

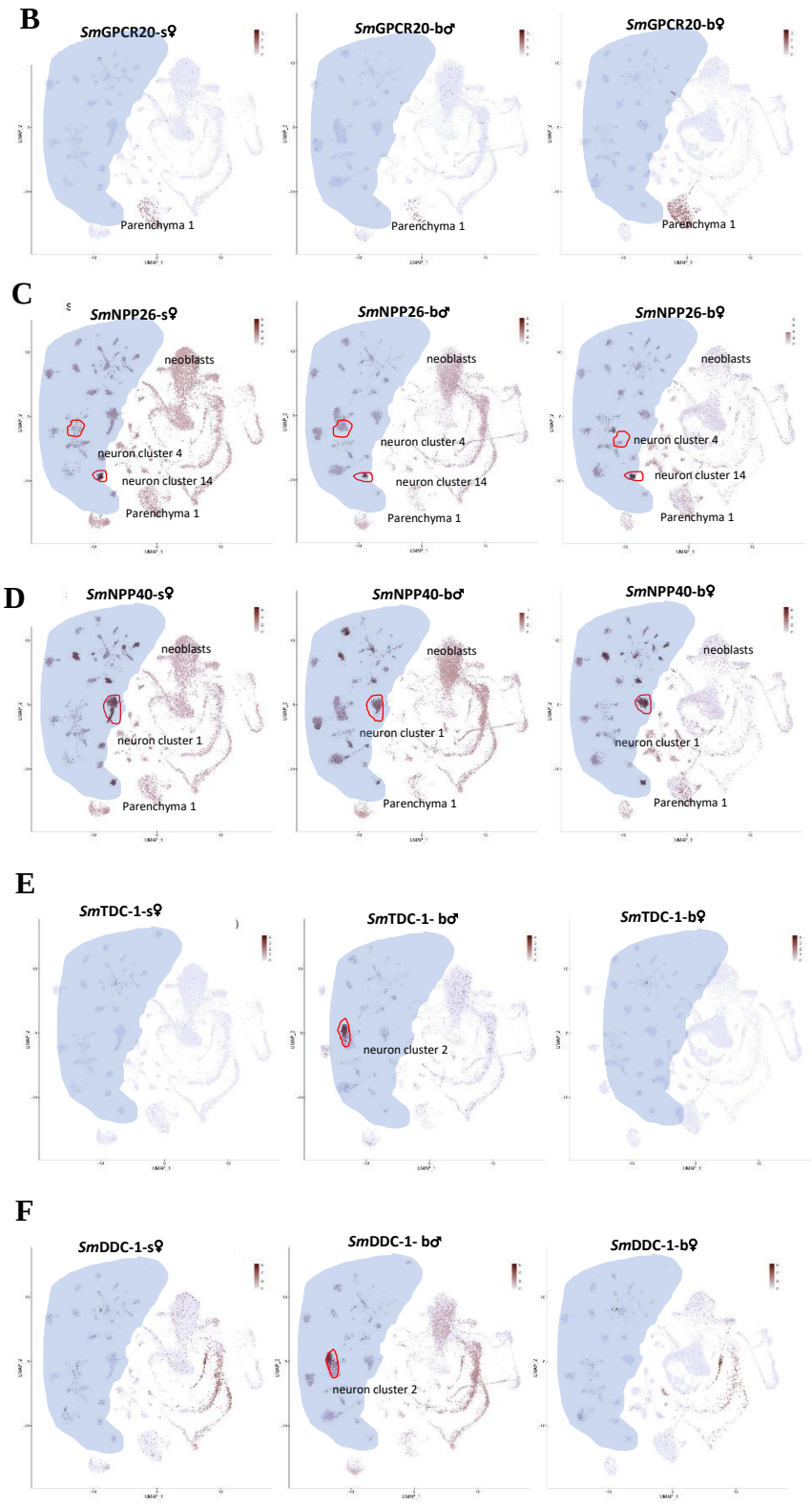

Supplementary Figure 5: The represented cell atlas data were obtained by single-cell RNA-seq analysis. (**A**) The overview shows cell clusters assigned to various tissues of *S. mansoni*. (**B**) *Sm*GPCR20 was found to be preferentially transcribed in the parenchyma and weakly in some neuronal clusters - such as 1, 2 and 4. *Sm*NPP26 (**C**) and *Sm*NPP40 (**D**) showed widespread distribution in different cell

clusters, especially in neurons and neoblast cells, as indicated, *Smtdc-1* (**E**) and *Smddc-1* (**F**) are preferentially transcribed in neuron 2 cells (Red circle), and weakly also in other neuronal cells, neoblasts, and tegumental cells. Neuronal clusters are highlighted in light blue.

Supplementary Figure 6

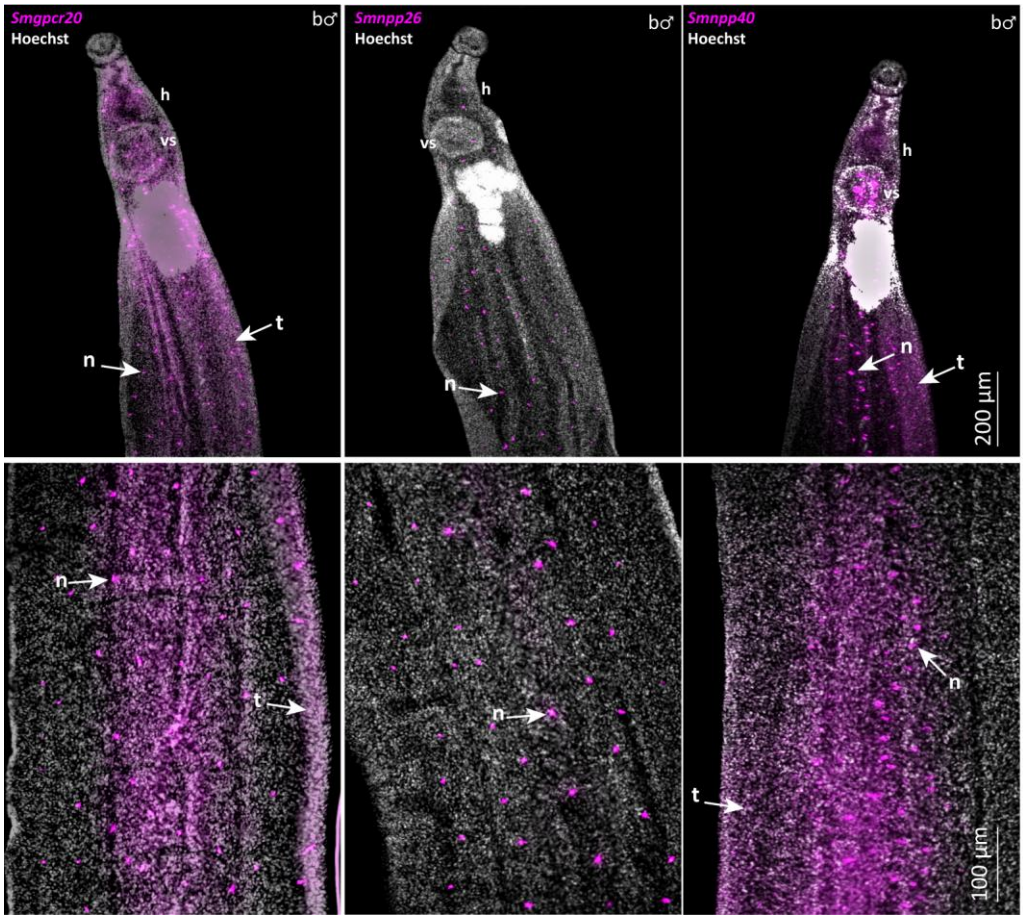

Supplementary Figure 6: FISH analyses revealed localization of *Smgpcr20, Smnpp26,* and *Smnpp40* in bM. Collection of FISH results showing the expression of *Smgpcr20*, *Smnpp26*, and *Smnpp40* in different cells in bM, DIG-labelled *Smgpcr20, Smnpp26*, and *Smnpp40* are shown in magenta. For counter staining, cells were labelled by Hoechst 33342 (white). bM = pairing-experienced males, h = head, vs = ventral sucker, n = neuronal cells, t = tegument area. Scale bars: up: 200 µm, down: 100 µm.

Supplementary Figure 7

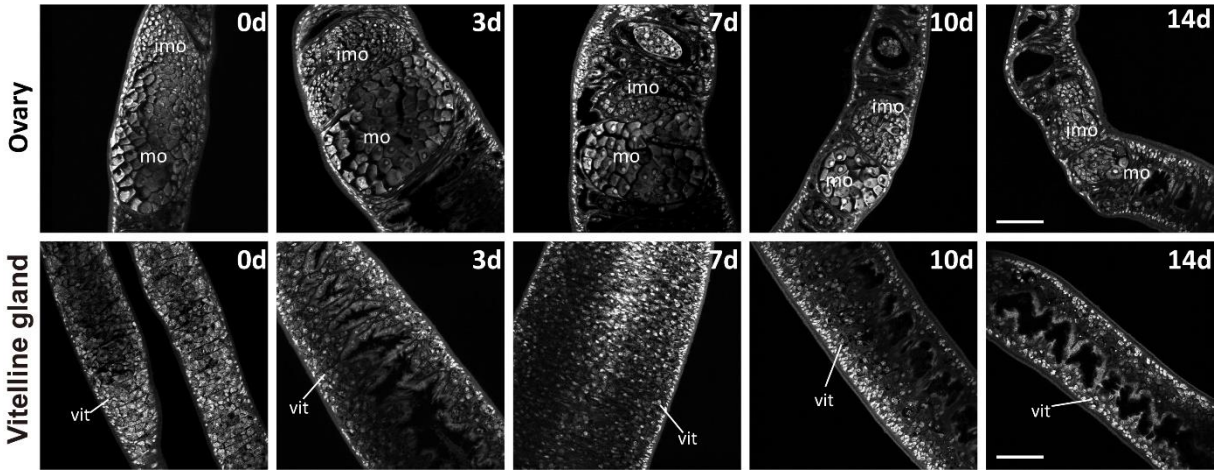

Supplementary Figure 7: Gonad dedifferentiation of pairing-experienced females in the absence of male worms during *in vitro* culture. CLSM analysis showing the dedifferentiation of the female ovary (upper row) and vitellarium (bottom row) during 14 d of culture in M199 3+ medium. Representative images from 3 biological replicates with n > 10 parasites are shown. imo = immature oocytes; mo = mature oocytes; vit = vitelline cells. Scale bars: 50 µm.

LIST OF FIGURES

LIST OF TABLES

9. Acknowledgments

No matter how tightly I hold my hand, I can’t grasp the time that flows away like water. This thesis is the culmination of a long and arduous journey-one that I have only been able to make as a result of the dedicated support I have received from so many people along the way. My story here began in the fall of 2019 and ended in the fall of 2023, is just like this thesis, with a shy beginning, a bumpy process, a rich storyline, and an impressive ending. It is not only full of difficulties and tribulations but joy and hope. What's past is prologues, I believe that graduation is not the end but the beginning of a new life.

First and foremost, the deepest and sincerest gratitude goes to my supervisor Prof. Dr. Christoph Grevelding for his continuous and valuable guidance throughout my PhD studies. It is a great honor and privilege that I was given the opportunity to work under his supervision. I would like to thank him for his patience, support, empathy, and great sense of humor. I consider myself one of the luckiest people who benefitted from Professor Christoph Grevelding´s knowledge and character. I thank him for giving me continuous encouragement and valuable suggestions to me, to this thesis, to improve my skills in English speaking and writing, and also to my life.

Furthermore, I’d like to give special thanks to my colleagues and closest buddies in Gevelding’s lab as well as the other groups of the parasitology institute, a group of lovely and like-minded people is the key to a colorful life. I am very grateful to meet all of them, thanks for their technical guidance and needful assistance during my study period: Dr. Oliver Weth, PD. Dr. Simone Häberlein, Dr. Thomas Quack, Hicham Houhou, Mughal Mudassar, Max Möscheid, Oliver Puckelwaldt, Monique Überall, Sophie Welsch, Martin Haimann. Especially, I would like to thank Dr. Oliver Weth for assisting me with the lab equipment and guiding me into this project, in the first year of my study. It is my pleasure acknowledging excellent work of Christina Scheld, Bianca Kulik and Geogette Stovall for maintaining schistosome life cycle. I would also express my gratitude to colleagues and friends: Hicham Houhou, Mughal, Mudassar, Monique Überall, Sophie Welsch, Max Möscheid, Oliver Puckelwaldt, for their scholarly criticism, important suggestions and absolute friendly atmosphere during this period, and for all the fun we have had in the last four years.

Furthermore, I would like to give special thanks to all the friends in Giessen, Wenjie, Chaoyu, and Yuxi. Thank you for sharing your time, all the food healing and outing made me

fascinate with every frame of my campus life. It was such an unforgettable and memory that I will forever cherish it.

Many thanks to the Giessen Graduate Centre for the Life Sciences (GGL), which organized diverse courses and conferences, and which broadened my view in different fields.

I also thank the China Scholarship Council (CSC) for giving me financial support for pursuing the doctorate degree for three years.

Finally, I would like to thank my boyfriend Yongle. He has been urging me to finish my studies and to write my thesis, and he encouraged me when I experienced setbacks. Putting him into my thesis is not only to thank him, but also let my love be included in this arduous journey. Last but not the least, I would like to thank my mother, father, and all family members, who have given their support to me during my studies.

10. Declaration

I declare that this thesis is my original work and other sources of information have been properly quoted. This work has not been previously presented to obtain any other degree from any other university.

Ich erkläre: Ich habe die vorgelegte Dissertation selbständig und ohne unerlaubte fremde Hilfe und nur mit den Hilfen angefertigt, die ich in der Dissertation angegeben habe. Alle Textstellen, die wörtlich oder sinngemäß aus veröffentlichten oder nicht veröffentlichten Schriften entnommen sind, und alle Angaben, die auf mündlichen Auskünften beruhen, sind als solche kenntlich gemacht. Bei den von mir durchgeführten und in der Dissertation erwähnten Untersuchungen habe ich die Grundsätze guter wissenschaftlicher Praxis, wie sie in der "Satzung der Justus-Liebig-Universität Gießen zur Sicherung guter wissenschaftlicher Praxis" niedergelegt sind, eingehalten.

Signed: _____

Date: _____